

STEVE  
REYNOLDS



The Arizona Geological Society and the University of Arizona

1981 Symposium on

**"RELATIONS OF TECTONICS TO ORE DEPOSITS  
IN THE SOUTHERN CORDILLERA"**

AGS/UA Mine Tour and Field Trip data for:

**TRIP #7**

**"South Mountain-Vulture-Harquahala-  
Little Harquahala Mountains"**

**March 21-22**

**Leaders: S. Keith (AZ BGMT),**

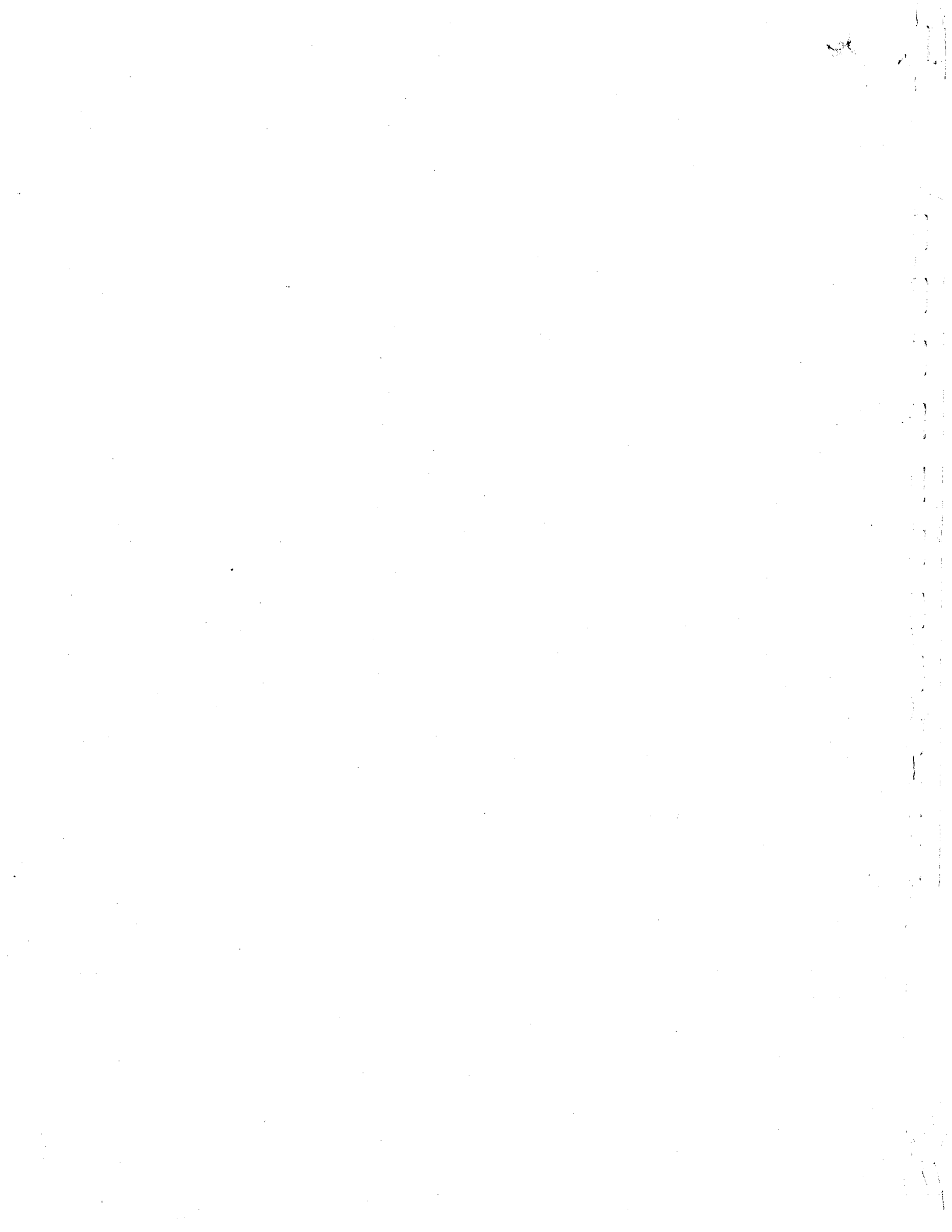
**S. Reynolds (U of A),**

**W. Rehrig (Conoco).**

STATE OF ARIZONA  
BUREAU OF GEOLOGY  
AND MINERAL TECHNOLOGY  
OPEN-FILE REPORT

**81-2**

Field Trip Coordinator: Parry Willard (GMRC).



LOW-ANGLE TECTONIC PHENOMENA  
BETWEEN TUCSON AND SALOME, ARIZONA

ROAD LOGS AND DISCUSSIONS

by

Stanley B. Keith<sup>1</sup>, Stephen J. Reynolds<sup>1</sup>,  
William A. Rehrig<sup>2</sup> and Stephen M. Richard<sup>3</sup>

<sup>1</sup> Arizona Bureau of Geology and Mineral Technology, 845 N. Park Avenue,  
Tucson, Arizona, 85719

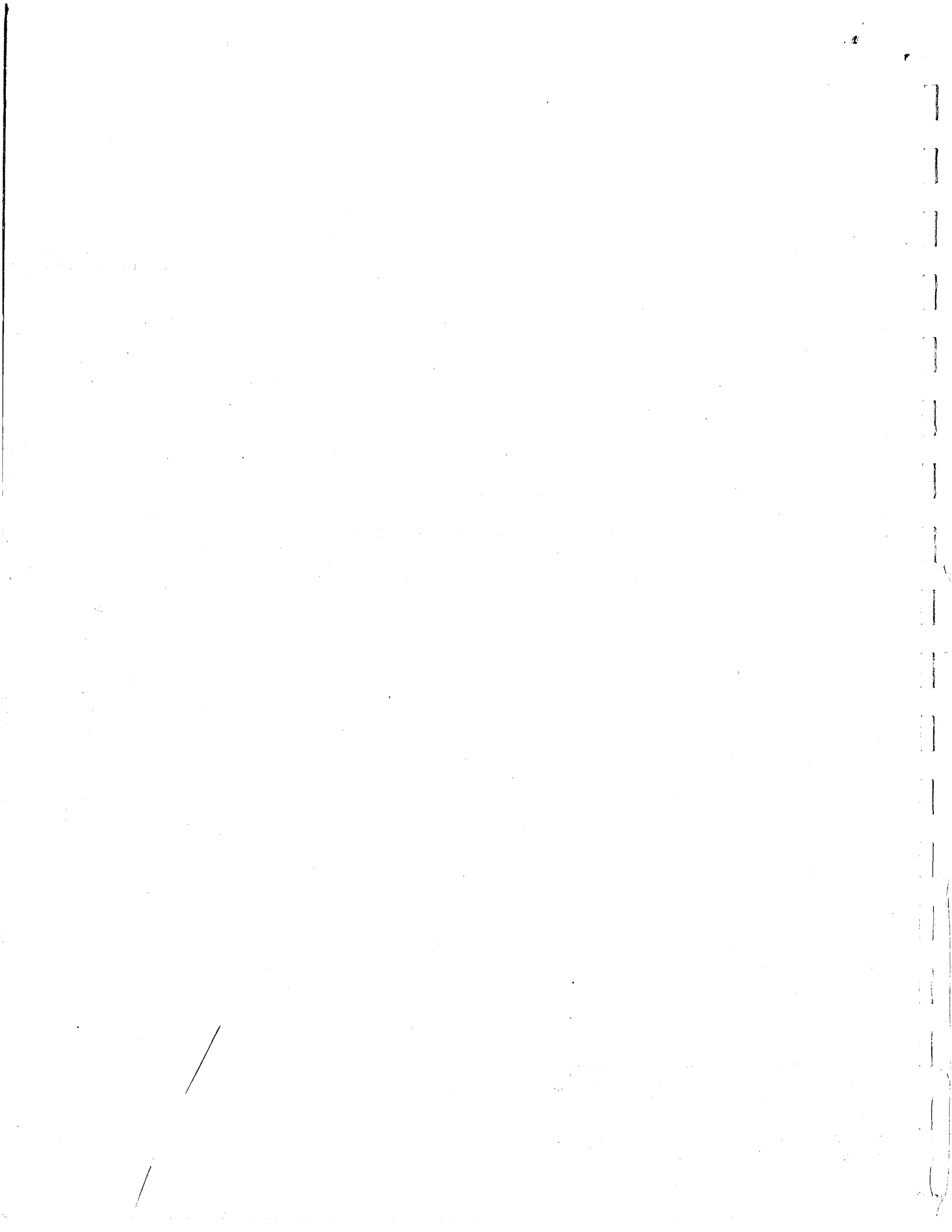
<sup>2</sup> CONOCO INC., Geologic Studies Group, 555 17th Street, Denver, Colorado 80202

<sup>3</sup> Department of Geosciences, University of Arizona, AZ 85721

STATE OF ARIZONA  
BUREAU OF GEOLOGY  
AND MINERAL TECHNOLOGY  
OPEN - FILE REPORT

81-2

This report is preliminary and has not been edited or reviewed for conformity with Arizona Bureau of Geology and Mineral Technology standards. The observations contained herein are those of the author(s) and not necessarily endorsed by the Arizona Bureau of Geology and Mineral Technology.



## INTRODUCTION

It is becoming increasingly clear that Arizona's Basin and Range Province contains an abundance of low-angle tectonic phenomena that are diverse in space, time and tectonic significance. It is the purpose of this field trip to examine a representative sample of these tectonic phenomena, emphasizing their geometry, timing, kinematics and regional significance to Arizona's tectonic and mineral-deposit framework (Figure 1). With this goal in mind we will discuss from a distance the complex low-angle fault, mylonitic, and plutonic terranes in the eastern Tortolita, Santa Catalina, and Picacho Mountains (DAY 1: STOPS 1 AND 2). These Mountains contain Laramide through mid-Tertiary mylonitic phenomena that geologists have variously related to early Laramide northeast-vergent thrusting, late Laramide southwest-vergent thrusting and two-mica granite magmatism, mid-Tertiary regional crustal extension. These stops will be primarily lead by Stan Keith.

We will next visit South Mountains (STOPS 3, 4 AND 5), where Steve Reynolds will show us a comparatively simple assemblage of Precambrian amphibolite grade gneissic rocks overprinted by chiefly late Oligocene mylonitization and plutonism. We will also see how this mylonitic assemblage has in turn been overprinted by the recently much discussed and debated chloritic breccia phenomena and accompanying dislocation tectonics. Then it is off to the Vulture Mountains (STOP 6) where Bill Rehrig will lead us through an impressive array of low-angle normal faults that have effected wholesale block rotations of mid-Miocene volcanic rocks and an underlying crystalline complex consisting of a Laramide granodioritic pluton that has intruded Precambrian plutonic and amphibolite-grade metamorphic rocks.

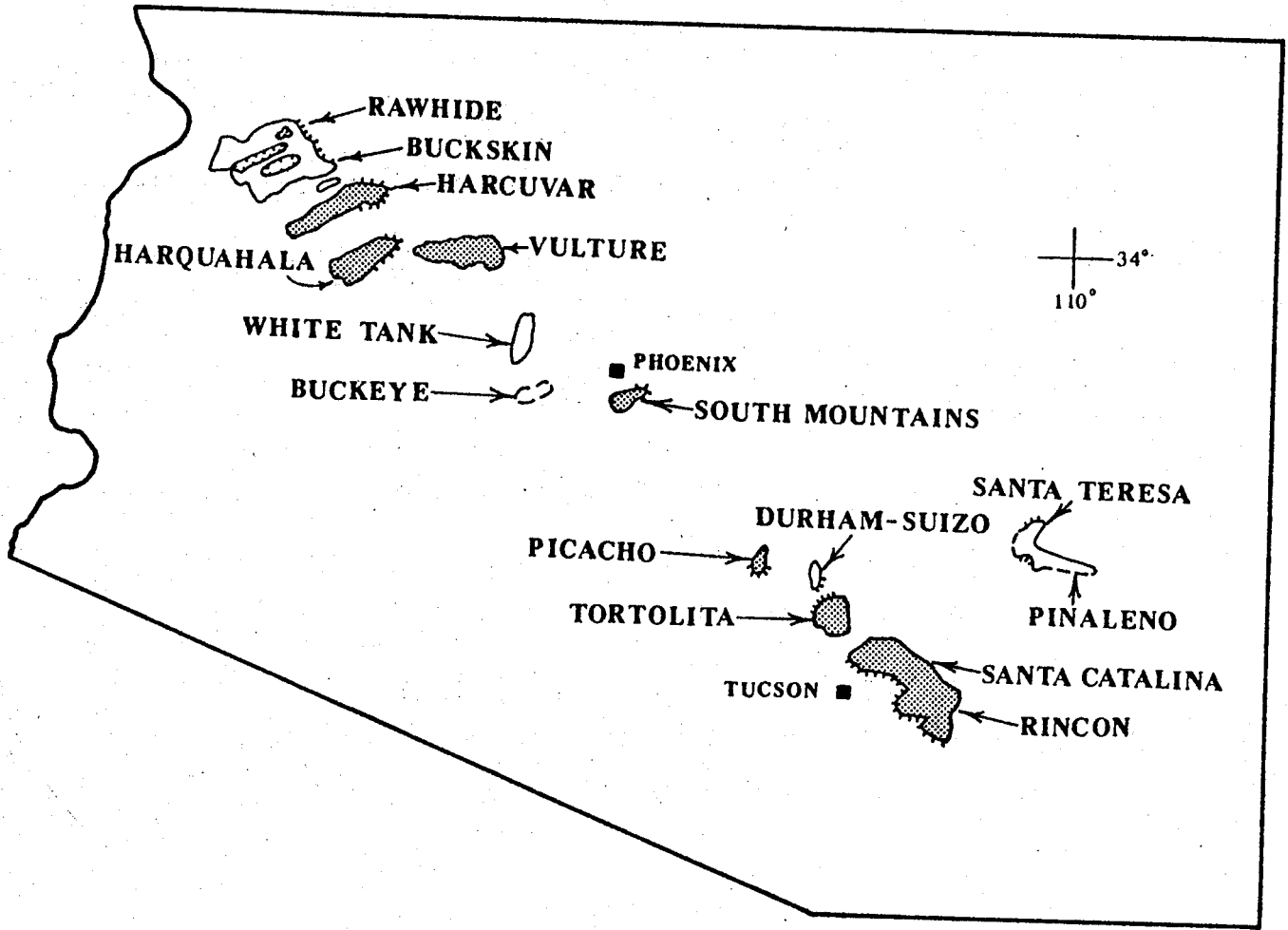


Figure 1. Map of southern Arizona showing location of selected mountain ranges with low-angle tectonic phenomena. Dot pattern shows mountain ranges that will be examined or discussed on this field trip.

Day 2 will carry us further west to the Harquahala Mountains where we will use another assemblage of mylonitic gneisses separated from a Miocene volcanic cover by another dislocational zone (STOP 1). Then we will structurally descend into the intriguing Laramide thrust fault geology that prevades the "crystalline core" of the Haruahala Mountains. We will investigate a series of stacked overthrusts that are beautifully exposed at the White Marble Mine (STOP 2) and look at the basal (?) thrust of the region at "S" Mountain (STOP 3). Finally, we will show how the Laramide thrust fault system has localized probably Miocene copper-gold mineralization in the Little Harquahala Mountains (STOP 4).

During the trip it will become very obvious that the field trip leaders have many differences (as well as some agreements) about the timing, kinematics, and regional significance of the various low-angle tectonic phenomena. This was done intentionally so that the participants will get as fair an insight as possible into what we know and don't know about these important, provocative and complex phenomena. We also strongly urge as much participant participation as possible, for there is a lot your leaders don't know! The participant will notice that the road logs contain a series of mini-papers spliced into them, each with its own set of figures and author(s). This was done to give each author a forum to air his own observations and opinions. We hope you find this format useful, diverting and stimulating.

FIRST DAY

ROAD LOG FROM TUCSON TO WICKENBURG VIA SOUTH MOUNTAINS.

Leaders: Stanley B. Keith, Stephen J. Reynolds and William A. Rehrig.

Saturday, March 21, 1981.

Assembly

Point: In front of Student Union Building, University of Arizona campus.

Time: 6:30 a.m.

Stops: 6

Distance: Approximately 200 miles.



## MilePost

- 257 Begin road log at mile post 255 on I-10 Interstate freeway after entering I-10 northwest bound for Phoenix at the Speedway onramp. Cumulative mileage will only be used for roads that lack mileposts; all other entries will be keyed to mileposts. The clock system will be used for geographic referencing. Unless otherwise indicated, 12:00 is defined as the direction of travel, with 3:00 to the traveler's right and 9:00 to his left.  
1.0
- 256 Grant Road bridge.  
1.0
- 255 Central Tucson Mountains at 9:00. Wasson Peak (el. 4687) is the highest point in the Tucson Mountains. A Mountain capped by late Oligocene volcanics is at 7:30. About 40 percent of the rocks cropping out in the Tucson Mountains are reddish brown cliffs and slopes of steeply dipping Cat Mountain (8:00) Rhyolite a new northeast tilted ignimbrite dated at 70 m.y. (Bikerman, 1962; Bikerman and Damon, 1966) that comprises the main ridgeline of The Tucson Mountains at 9:00. The eastern foothills (8:00 to 10:00) consist of 70 to 56 m.y. rhyolitic ash-flow tuffs that unconformably overlie the earlier Laramide Cat Mountain rhyolite sequence. Chemical analyses (Dewhurst, 1976) of the two groups indicate the post-Cat Mountain volcanics rocks are more calcic. The Laramide volcanic interval is in turn angularly truncated and overlain by relatively flat-lying late Oligocene-early Miocene volcanics at A-Mountain (7:30) and Safford Peak (11:00).  
2.0
- 253 Santa Catalina Mountains at 3:00; Tortolita Mountains comprise the low-relief Mountains with accordant summits at 1:00.  
3.0
- 250 Bridge over Orange Grove Road. Safford Peak now is at 10:30. From the work of Lonswiler (1959) and Bikerman and Damon (1966), Safford Peak is a 25 m.y. old dacite neck intruded into a sequence of andesitic flows and rhyolitic tuffs and tuff breccia dated by the K-Ar method as 39 to 26 m.y. old.  
3.0
- 247 Cortaro Road exit. Bear right onto off ramp and proceed to Cortaro Road intersection. Turn right and then left onto frontage road and continue northbound.  
2.7  
Pull off to left for STOP 1.

## STOP 1

### OVERVIEW OF PLUTONIC GEOLOGY AND LOW-ANGLE MYLONITIC PHENOMENA IN THE CRYSTALLINE CORES OF THE SANTA CATALINA AND TORTOLITA CRYSTALLINE COMPLEXES.

by Stanley B. Keith

#### Orientation:

Define 12:00 as the frontage road northwest bound. Tortolita Mountains are low range of accordant peaks and summits at 1:00 to 3:00. Santa Catalina Mountains comprise the high range in distance at 2:30 to 3:30. The main feature of the Santa Catalina Mountains in view is the Pusch Ridge segment of the Santa Catalina forerange. Peaks on Pusch R. are Mt. Kimball and Cathedral Peak. The city of Tucson is now at 3:00 to 6:00. Tucson Mountains are now at 9:00 to 6:30.

#### General Geology of the Santa Catalina-Rincon-Tortolita Crystalline Complex (from Keith and others, 1980).

General geology of the Santa Catalina-Rincon-Tortolita crystalline complex is presented in simplified map form in Figure 1 and depicted diagrammatically in four cross sections (Figs. 2, 3, 4 and 5). Readers are directed to discussions and references cited in Creasey and others (1977), Budden (1975), Shakel (1974, 1978), Davis (1975, 1977a, 1977b, 1978 and 1980), Drewes (1977), Thorman and Drewes (1978), Thorman (1977), Davis and Coney (1979), and Banks (1980) for other recent perspectives.

In a general way, the Santa Catalina-Rincon-Tortolita complex is composed of a crystalline core that is dominated by Phanerozoic plutonic rocks (~75% of outcrop). The remainder of the crystalline core consists of middle Proterozoic plutonic rocks (~20% of outcrop) and subordinate amounts of middle Proterozoic and Phanerozoic metasedimentary rocks. The crystalline core is mostly fault-bounded, except for segments of its north and northeast margins which are intrusive in nature.

The Phanerozoic plutonic rocks form a large composite batholith within which at least 10 and possibly 12 or more individual plutons (Fig. 1) have been delineated (see App. 1 for discussion of nomenclature of these bodies). Individual plutons are generally compositionally zoned and commonly have asymmetric laccolithic shapes. The tops of many of the laccolithic bodies and sills occur just below or at the Precambrian Apache Group unconformity with older Precambrian rocks or within the Apache Group (Figs. 3, 4). The asymmetric laccolithic geometry is spectacularly

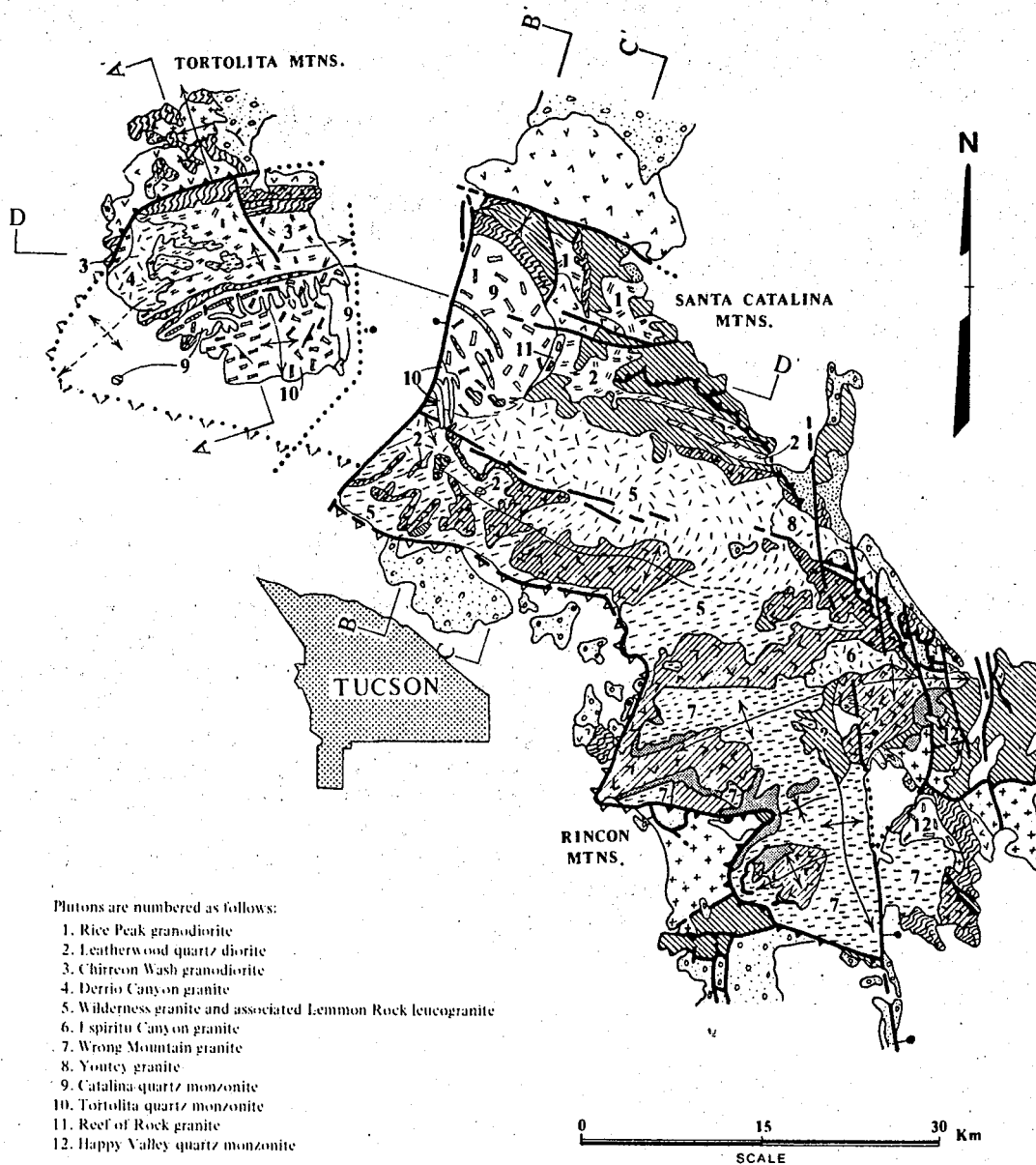
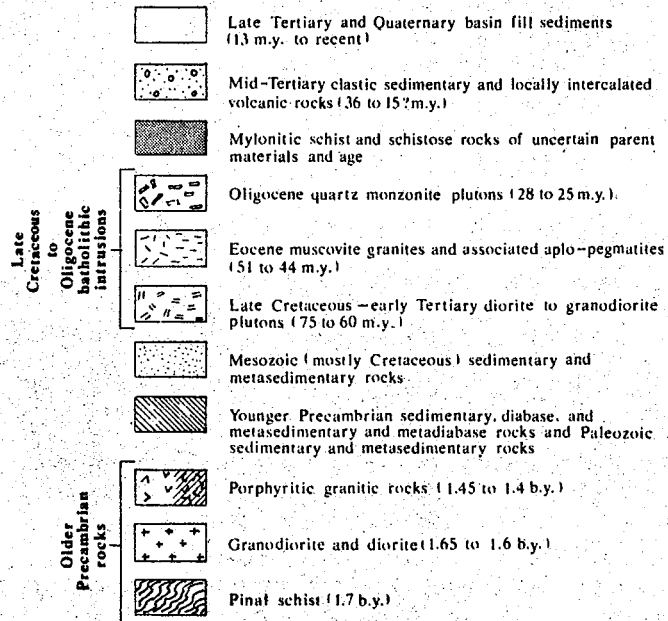


**Figure 1.** Generalized geologic map of Santa Catalina-Rincon-Tortolita crystalline complex showing locations of cross sections and plutons discussed in text. Sources of map data are as follows: for Tortolita Mountains—Budden (1975), Banks and others (1977), and Keith (unpub. mapping); for Santa Catalina Mountains—Tolman (1914, unpub. mapping as presented in Wilson and others, 1969), Creasey (1967), Shakel (1974), Creasey and Theodore (1975), Banks (1976), Hoelle (1976), Suemnicht (1977), Wilson (1977), and Keith (unpub. mapping); for Rincon Mountains—Drewes (1974, 1977) and Thorman and Drewes (1978). Aligned patterns in Late Cretaceous through Oligocene intrusions show deformed areas of mylonitic gneiss, and random patterns show undeformed areas. East-northeast-trending ruled lines show areas of mylonitically deformed porphyritic mesocratic gneiss believed to have been previously undeformed 1,400- to 1,450-m.y.-old biotite granitic rocks (shown by random pattern). Barbed heavy lines are low-angle faults with barbs in upper plate. Heavy lines are high-angle normal faults with bar and ball on downthrown side.

## EXPLANATION



displayed in the western end of the Santa Catalina Mountains (Fig. 6) where a batholithic sill of Wilderness granite extends southward into the Catalina forerange from its root zone in Cargodera Canyon. The asymmetric, flat-lying parts of the various intrusions occupy large areas throughout the complex and, together with their host rocks, have been affected by a conspicuous mylonitization which has imposed on the rocks a penetrative, gently inclined mylonitic foliation. Although all three ranges of the complex have these general attributes in common, enough differences exist to merit brief discussions of the geology of each range.

#### Plutonic Geology of the Tortolita Mountains (from Keith and others, 1980).

The northern part of the crystalline core in the Tortolita Mountains consists of the Chirreon Wash granodiorite, an east-northeast-to-due-east-trending composite pluton with quartz diorite, granodiorite, and quartz monzonite phases (Fig. 2). Intruding the granodiorite in its western exposures are abundant tabular bodies of granite, pegmatites, and alaskite herein referred to as Derrio Canyon granite. These plutons are locally mylonitic and bordered by east-trending schistose bands on both the north and south. To the north, the schistose rocks are in contact with mylonitized Oracle Granite. Farther to the northwest, both Oracle Granite and the schistose rocks are chloritized, brecciated, and overlain by a dislocation surface (Guild Wash fault). The schistose band that borders the Chirreon Wash pluton on the south is intruded on its south side by an east-northeast-trending mass of quartz monzonite which is lithologically similar to and correlated by us with the Catalina quartz monzonite of the northwest Santa Catalina Mountains. The Catalina quartz monzonite locally contains large quartz diorite inclusions of presumed Chirreon Wash granodiorite and truncates pegmatite apophyses of Derrio Canyon granite in the east-central Tortolita Mountains. In turn, the Catalina quartz monzonite is intruded by numerous apophyses of the Tortolita quartz monzonite pluton that crops out to the south-southeast. Both the Catalina and Tortolita intrusions locally contain a low-angle mylonitic foliation. The mylonitic foliation in all plutons is crosscut by northwest-striking, high-angle normal faults and shears that in many places are intruded by northwest-striking, undeformed to locally foliated granodiorite, quartz monzonite, and quartz latite dikes.

#### Plutonic Geology of the Santa Catalina Mountains (from Keith and Reynolds, 1980).

The plutonic geology of much of the Santa Catalina Mountains can be viewed in terms of a stacked sill complex that consists of five major lithologic pseudo-stratigraphic assemblages which have gently inclined tabular forms and boundaries, (see Figure 7). The five assemblages are described below from structurally lowest to highest levels.

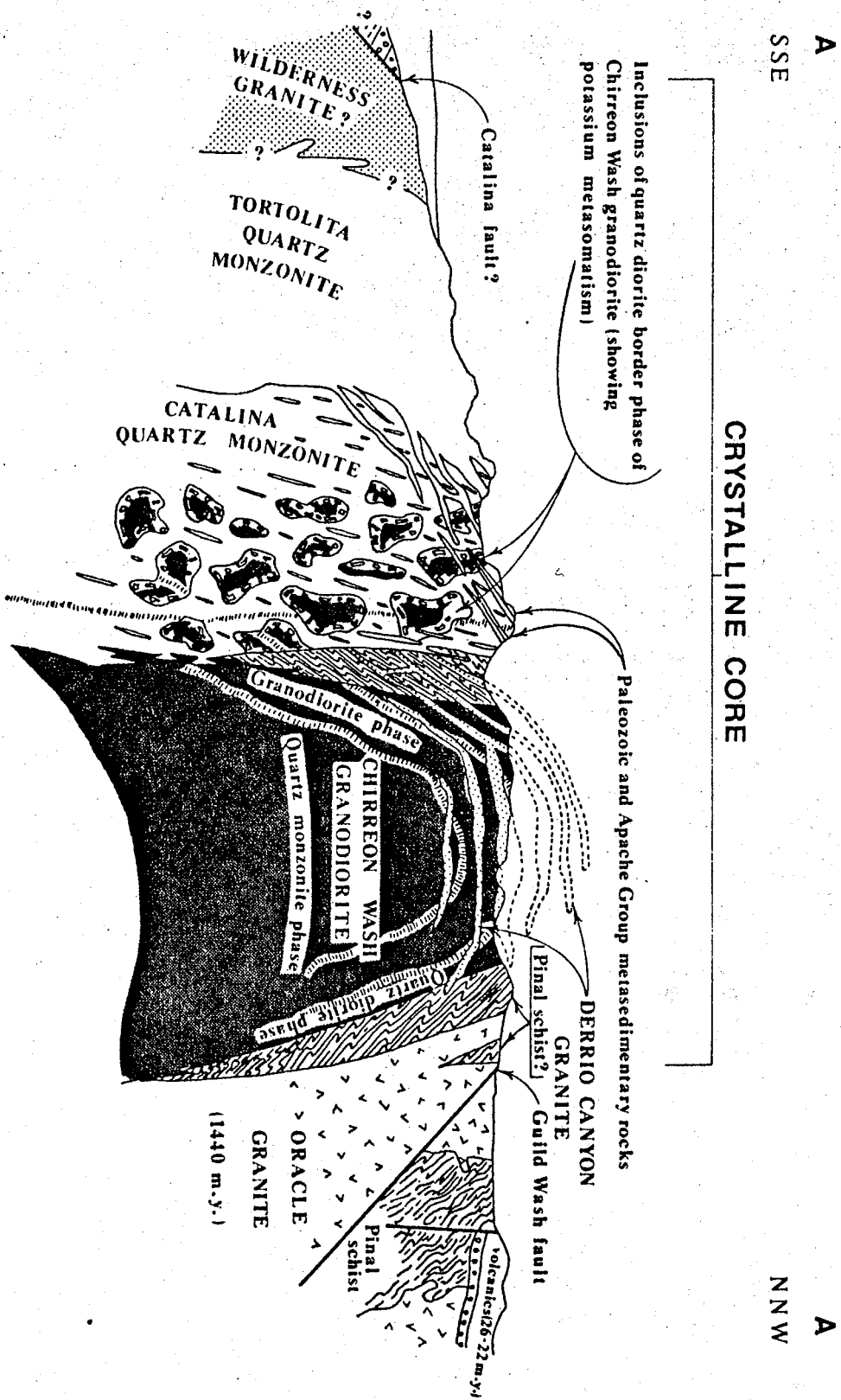


Figure 2. Diagrammatic cross section A-A through Tortolita Mountains. Location of section shown in Figure 1.

B  
SSW

CRYSTALLINE CORE

B  
NNE

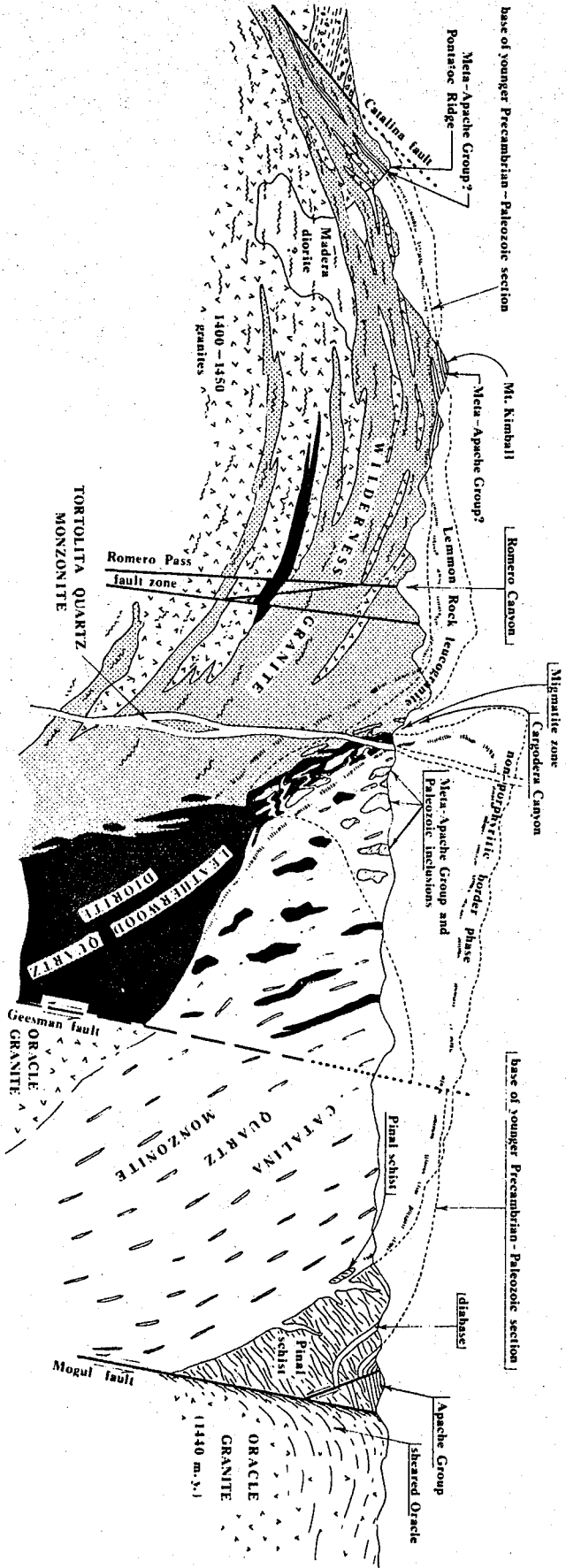


Figure 3. Diagrammatic cross section B-B' through western Santa Catalina Mountains. Location of section shown in Figure 1. Mylonitic rocks shown by wavy lines.

C  
SSW

C  
NNE

CRYSTALLINE CORE

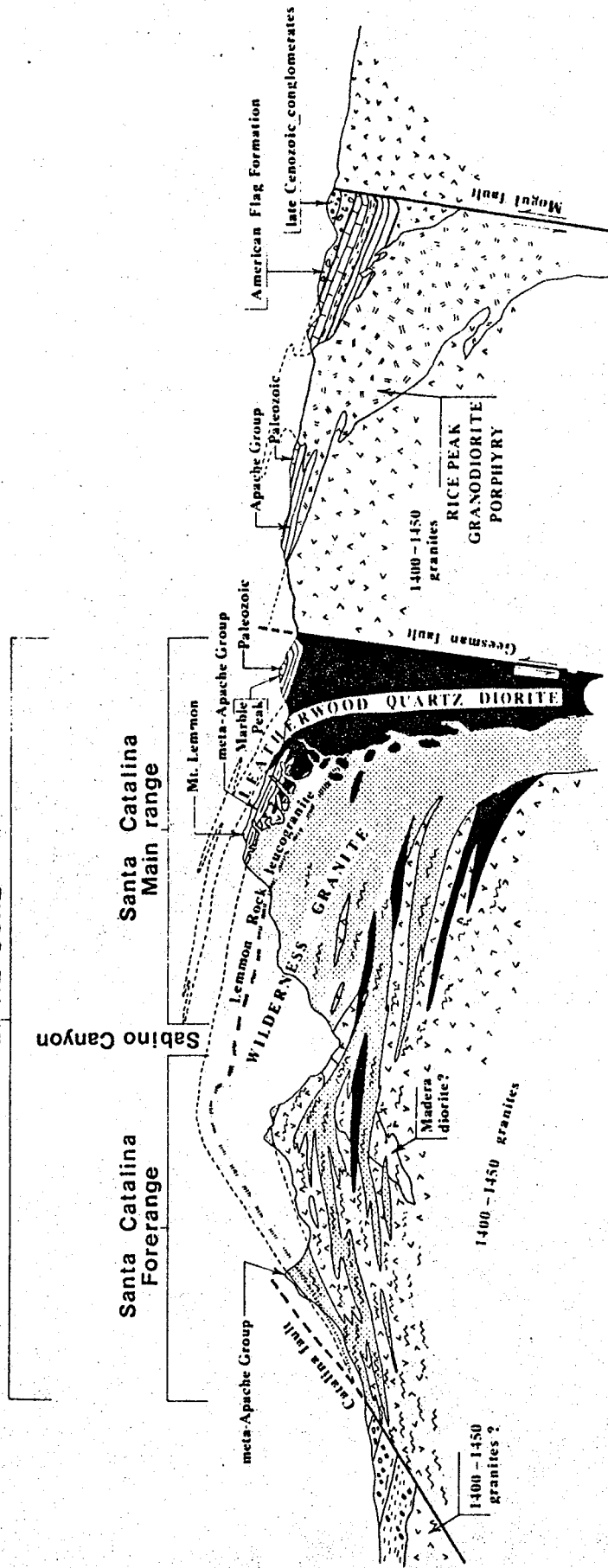


Figure 4: Diagrammatic cross section C-C' through central Santa Catalina Mountains. Location of section shown in Figure 1. Mylonitic rocks shown by wavy lines.



D'  
ESE

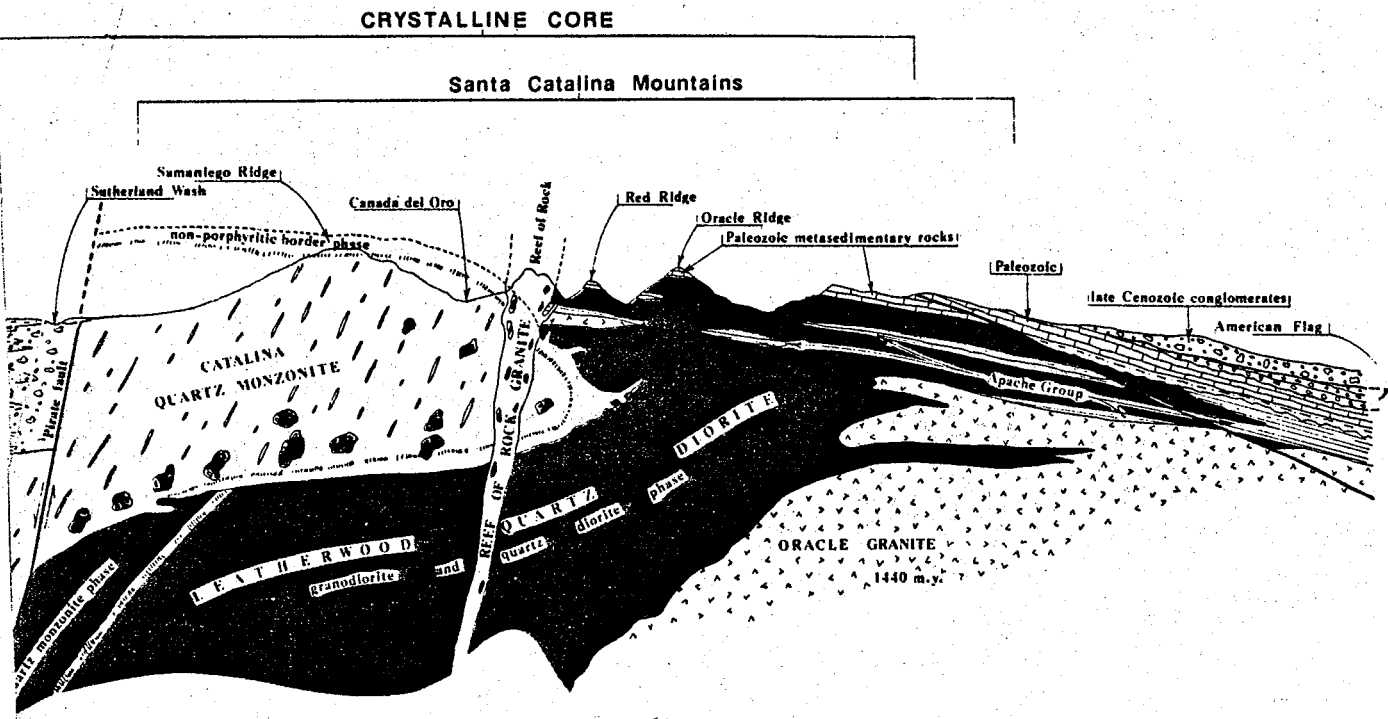


Figure 5 (facing pages). Diagrammatic cross section D-D' through central Tortolita Mountains and northern Santa Catalina Mountains.

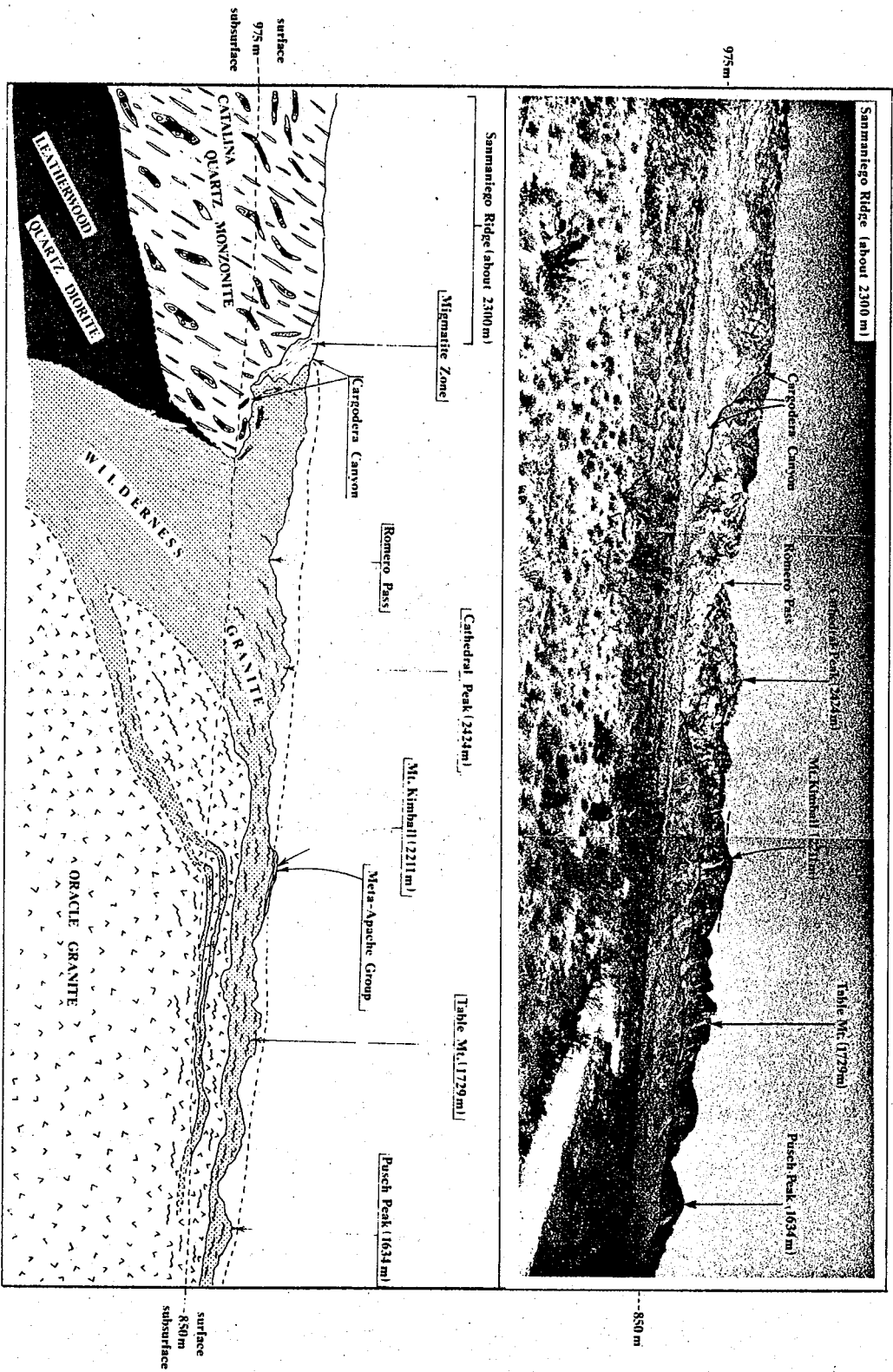


Figure 6. Panorama of the western Santa Catalina Mountains looking southeast. Photo and interpretative diagram show the asymmetric laccolithic geometry of the Wilderness granite batholith and, with less certainty, the inferred laccolithic geometry of the Catalina quartz monzonite intrusion. Mylonitic rocks are shown by wavy lines. Field of view is 25 km wide.



TABLE 1  
 AVERAGE CHEMICAL COMPOSITION OF COMPONENTS  
 WITHIN THE WILDERNESS GRANITE STACKED STILL COMPLEX

MAIN RANGE STILL

Increasing structural level →

Element <sup>3</sup> or Element Oxide	Seven Falls Foliated granite		Lower Portion Foliated biotite granite		Upper Portion Two-mica granite		Lemmon Rock Leucogranite		Garnet schlieren	
	n	n	n	n	n	n	n			
SiO <sub>2</sub>	64.88	1	70.6	1	74.06	13	75.2	2	70.63	1
Al <sub>2</sub> O <sub>3</sub>	16.6	1	14.5	1	14.67	13	13.1	2	13.5	1
Fe <sub>2</sub> O <sub>3</sub>	.81	1	1.01 <sup>2</sup>	1	.50	10	.29	4	1.51	1
FeO	1.42	1	.68 <sup>2</sup>	1	.39	10	.195	4	1.39	1
MgO	.59	1	.32	1	.19	13	.06	2	.17	1
CaO	3.14	1	1.81	1	1.3	13	.44	5	.25	1
Na <sub>2</sub> O	5.61	1	3.51	1	3.92	13	4.04	2	2.08	1
K <sub>2</sub> O	2.09	1	4.23	1	3.62	13	4.48	5	1.92	1
P <sub>2</sub> O <sub>5</sub>	.14	1	.10	2	.041	13	.09	2	.03	1
U	.90	1	.90	2	1.37	14	3.5	2	28.5	1
Th	6	1	6.5	2	<4.8	14	<2.5	2	50	1
Sc	4	1	5	2	3.3	14	<5.0	2	9	1
Ti	2200	1	2050	2	770	15	110	4	280	1
Mn	350	1	345	2	470	15	1980	5	34,000	1
Y	10	1	11.5	2	7.6	14	8.5	2	270	1
Ce	76	1	52	2	<37	14	<25	2	53	1
Nb	<4	1	4	2	<8.5	14	<72	2	24	1
Ba	1100	1	2050	2	1375	15	482	2	21	1
L1	27	1	14.5	2	26	14	128	2	32	1
V	35	1	21.5	2	7.	14	2	1	<2	1
Cu	7	1	9	2	15.	15	19.5	2	4	1
Zn	72	1	81.5	2	65.	15	155.	5	260	1
Cr	6	1	6.5	2	7.	14	19.5	2	5	1
Ni	4	1	6	2	<4.5	14	12	2	<4	1
Be	2	1	1	2	2.1	14	7.5	2	2	1
Rb			70	1	121	12	378	7		
Sr	760	1	490	2	320	25	28.3	7	10	1

Notes: 1) n= number of samples  
 2) Less than sign (<) indicates some samples for the element  
 in question were below the detection limit for that element.  
 3) Element analytical values are in ppm.  
 4) Element oxide values are in weight percent.

TABLE 2. MODAL MINERALOGY OF WILDERNESS GRANITE

	Quartz	Plagioclase	K-Feldspar*	Biotite	Muscovite	Opaque grains	Garnet	Others	Reference
Marshall Gulch pegmatite (part of Lemmon Rock leucogranite)	25	35 (An <sub>7-12</sub> )	37 (m)	Minor	Minor	Minor	Minor	Minor	Matter (1969)
Control Road pegmatite (part of Lemmon Rock leucogranite)	35	31 (An <sub>7-12</sub> )	29 (m)	Minor	More than above	Minor	Minor	Minor	Matter (1969)
Caseco pegmatite—about 30 m below upper contact between Wilderness Granite and metamorphosed Apache Groups	20	42 (An <sub>7-13</sub> )	27	Trace	6	..	4	..	Matter (1969)
Aplite—same location as above	19	32 (An <sub>7-13</sub> )	43	Minor	4	..	1	..	Matter (1969)
Wilderness Granite—various locations within upper half of main sill; average of 10 analyses	28	29 (An <sub>20-25</sub> )	27 (m)	4	7	1 (magnetite)	1-2 <sup>†</sup>	..	Pilkington (1962)
East Fork gneiss#—layer just below base of main Wilderness Granite sill; average of 7 analyses	31.3	26.6 (An <sub>20-25</sub> ) <sup>‡</sup>	29.7 (o)	7.4	4.5	0.2	..	0.4	Sherwonit (1974)
Thimble Peak gneiss#—average of 16 analyses	32.9	33.6 (An <sub>20-25</sub> ) <sup>‡</sup>	26.6	4.1	2.4	0.2	..	0.2	Sherwonit (1974)
Sabino Narrows gneiss#—light bands; average of 8 analyses	31.6	36.8 (An <sub>20-25</sub> ) <sup>‡</sup>	28.2	1.7	1.6	0.1	..	..	Sherwonit (1974)
Gibbons Mountain gneiss#—average of 7 analyses	29.9	35.5 (An <sub>20-25</sub> ) <sup>‡</sup>	26.0	7.7	0.3	0.4	..	0.2	Sherwonit (1974)
Soldier Canyon gneiss#—light bands; average of 15 analyses	30.4	37.8 (An <sub>25-30</sub> ) <sup>‡</sup>	25.7	4.2	0.6	0.3	..	0.2	Sherwonit (1974)
Seven Falls gneiss#—average of 7 analyses	29.1	41.3 (An <sub>25-30</sub> ) <sup>‡</sup>	21.8	7.2	0.1	0.3	..	0.3	Sherwonit (1974)

\*Microcline = m; orthoclase = o.

<sup>†</sup>Included under "others" by Pilkington (1962).<sup>‡</sup>These An values are from Peterson (1968).

#Terminology for gneiss units in Santa Catalina forerange is from Peterson (1968). These units are interpreted by us as injection sheets on lower levels of the Wilderness sill complex.

Seven Falls Foliated Biotite Granite. A leucocratic foliated biotite granite named the Seven Falls Gneiss by Petersen (1968) is exposed at the lowest structural level of the Wilderness stacked sill complex. We hereafter refer to this unit as the Seven Falls foliated granite. Chemical analyses and model data for the Seven Falls foliated granite are presented in Tables 1 and 2 respectively.

Forerange banded gneiss complex (north facing slope former below cliffs on Pusch Ridge). A banded gneiss complex overlies the Seven Falls foliated granite throughout the Santa Catalina forerange. This gneiss complex consists of alternating light- and dark-colored lithologies which are interlayered on a wide variety of scales. The dark components are rich in biotite (20%) and are predominantly composed of mylonitically deformed Oracle Granite (1.45 b.y. B.P. emplacement age). Keith and others (1980) have interpreted most of the light-colored components of the gneiss complex as sills of Eocene Wilderness that were injected in lit-par-lit fashion into darker phases of 1.45 b.y. B.P. Oracle Granite. Petrographic data (Sherwonit, 1974; see Table 1) indicate that Wilderness equigranular biotite granite sills which are structurally low in the banded gneiss complex are more biotite-rich than those higher in the banded gneiss complex.

Pegmatitic Wilderness phases contain muscovite only in the upper two-thirds of the banded gneiss complex and are more biotite-rich in the lower third. We believe the forerange banded gneiss complex extends northward beneath a large higher-level sill of Wilderness granite in the Santa Catalina main range as a large, tabular, highly injected sheet (refer to Figure 7).

Main Range Wilderness Granite Sill. (Cliff former that caps Pusch Ridge). A batholithic, laccolithic sill of Eocene wilderness granite overlies the banded gneiss complex. This 2.5 km-thick intrusion exhibits an asymmetrical laccolithic geometry. The Wilderness laccolithic sill is composed of equigranular granite and interlayered pegmatite, aplite, and alaskite. Throughout most of the laccolithic sill, the equigranular granite contains biotite, muscovite, and garnet. However, near the base of the laccolith, the equigranular granite contains biotite and sparse garnet, but no muscovite. We refer to the gradational zone between the main two-mica phase and the structurally lower, biotite-only phase as the "muscovite-in boundary". Pegmatites, aplite, and alaskite within the Wilderness main range laccolith generally contain muscovite and garnet. Modal analyses and average chemical data for the main range laccolithic sill are presented in Tables 1 and 2 respectively.

Lemmon Rock Leucogranite. (just below top of Mt. Kimball). Late-stage pegmatite, aplites, and leucogranites are especially abundant near the top of the main range Wilderness laccolith. In many places, alasko-pegmatitic rocks form a leucogranite "cap" named Lemmon Rock leucogranite by Shake1 (1978). This "cap" grades downward into the main range laccolithic sill of equigranular two-mica granite and intrudes upward into the late Cretaceous Leatherwood quartz diorite and younger Precambrian Apache Group. Garnet is locally abundant and in places forms spectacular "railroad track" bands of garnet schlieren. Representative modes and chemical analyses of the Lemmon Rock leucogranite and the lithologically unusual garnet schlieren leucogranite are presented in Tables 5-4 and 5-5 respectively.

Sedimentary "cover" and Leatherwood Quartz Diorite. (top of Mt. Kimball). The uppermost of the five major pseudostratigraphic assemblages is composed of Precambrian Apache Group sedimentary rocks, Precambrian diabase, Paleozoic sedimentary rocks, and sill-like apophyses of Late Cretaceous Leatherwood quartz diorite which have chiefly intruded between the Apache Group and Paleozoic sedimentary rocks. The sedimentary rocks are highly metamorphosed directly above their contact with the underlying Wilderness granite laccolith and adjacent to the quartz diorite sills; they are less metamorphosed up structural section to the north.

#### Geochronology of the plutonic rocks

Geochronology of the complex has been a lively topic of debate. My present interpretation of that geochronology follows Keith and others (1980) who presented an extensive discussion and review of the available geochronologic data. Participants should refer to that paper for a more in-depth discussion of the geochronology which is only summarized below. According to Keith and others (1980):

Recent field work and accumulated Rb-Sr studies, when combined with previous U-Th-Pb and K-Ar investigations, allow a new synthesis of the crystalline terrane within the Santa Catalina-Rincon-Tortolita crystalline complex. When all the available data are integrated, it is apparent that the crystalline core is mainly a composite batholith that has been deformed by variable amounts of cataclasis. The batholith was formed by three episodes of geologically, mineralogically, geochemically, and geochronologically distinct plutons. The first episode (75 to 60 m.y. B.P.) consisted of at least two (and probably three) calc-alkalic, epidote-bearing biotite granodiorite plutons (Leatherwood suite). The Leatherwood suite is intruded by distinctive leucocratic muscovite-bearing peraluminous granite plutons (Wilderness suite), which are 44 to 50 m.y. old. At least three Wilderness suite plutons are known, and their origin has been much debated. Leatherwood and Wilderness plutons are intruded by a third suite of four biotite quartz monzonite to granite plutons (Catalina suite) that mark the final consolidation of the batholith 29 to 25 m.y. ago.

## Mylonitization of the plutonic rocks

Description. The following is a description from Keith and Reynolds (1980) of mylonitic rocks from within the Wilderness stacked sill complex outlined previously.

Rocks in five major pseudostratigraphic assemblages locally exhibit a gently inclined mylonitic foliation. The banded gneiss complex of the forerange, and the lower half of the Wilderness granite laccolith are generally mylonitic; rocks higher in the mountain range are generally not mylonitic (see Figure 7). In the context of this project, James DuBois has examined many thin-sections of mylonitic and undeformed phases of Wilderness granite, and has established the following generalized deformation sequence in muscovite-bearing, equigranular phases of the Wilderness pluton:

- (1) quartz recrystallizes, becoming amoeboid;
- (2) quartz becomes finer-grained and feldspars become somewhat rounded;
- (3) quartz forms streaked lenses, and coarse green muscovite begins to break down to fine-grained, white muscovite; fine-grained biotite also develops; feldspars become cracked both parallel to and perpendicular to the foliation with quartz filling the fractures;
- (4) biotite forms foliated laminae through the rock which are wrapped around feldspar grains; feldspars become more rounded; pressure solution deposits of quartz form adjacent to feldspars, forming small augen; and
- (5) total rounding of feldspars takes place; biotite becomes millimeter-scale bands through the rock; magnetite and sphene appear intergrown with the biotite; chlorite develops on the biotite.

This general sequence mainly applies to the muscovite-stable, equigranular phases of Wilderness granite above the "muscovite-in" boundary in Figure 7.

Mylonitically deformed Oracle Granite in the Santa Catalina forerange banded gneiss complex comprises the distinctive mesocratic augen gneisses (informally referred to as 'dark bands'). Where the coarse-grained augen gneiss is concordantly inter-layered with the Wilderness leucocratic component, contacts are commonly marked by a zone of mylonite schist. Some of the leucocratic sills or light bands are completely encased in a sheath of mylonitic schist. Zones of mylonitic schist may vary from one to several meters in thickness; away from the contact, they progressively grade into coarse-grained augen gneiss. In thicker exposures of augen gneiss, there are comparatively non-rounded, rectangular 'box car' crystals of potassium feldspar; these are typical of undeformed Oracle Granite. Biotite is the only mica present in the dark component of the forerange banded gneiss. However, muscovite becomes common and locally is the

dominant mica in areas of mylonitic Oracle Granite that are intruded by equigranular muscovite-bearing Wilderness phases, K-feldspar augen in the deformed Oracle Granite are enveloped by a fine-grained matrix of feldspar and quartz. Foliation surfaces are undulatory and contain aligned aggregates of biotite and recrystallized quartz. Elongate aggregates of quartz with sutured boundaries or with ribbon textures are common within the plane of foliation and are expressed as a rod-like lineation which resembles "hot" slickensides.

Relationship of low-angle mylonitization to the plutonic episodes (from Keith and others, 1980). Within the batholithic complex of the Santa Catalina-Rincon-Tortolita crystalline complex. Plutons of *each* suite have been deformed to varying degrees by distinctive, gently inclined mylonitic foliation with conspicuous lineation that plunges east-northeast and west-southwest. At least three episodes or events of mylonitization (and probably more) are recorded in relationships where undeformed parts of younger plutons cut deformed parts of older plutons.

The oldest mylonitic event is post-75 m.y. B.P. because it deforms Leatherwood quartz diorite. This fabric must be pre-50 m.y. because mylonitic foliation in Leatherwood is intruded in many places by dated 44- to 50-m.y. old undeformed muscovite pegmatites east of Mount Lemmon (Hanson, 1966). In a well-exposed roadcut along the new paved-highway access to the Mount Lemmon ski area 2.5 km east-northeast of Mount Lemmon, several instructive relationships may be observed between mylonitic events in the Leatherwood quartz diorite and muscovite pegmatites of the Lemmon Rock leucogranite. Here, an older, coarser-grained mylonitic foliation is cut at a low angle by a younger, fine-grained, more intense mylonitic foliation. Two generations of pegmatites are present. The older generation consists of shallowly inclined sheets about 0.1 to 0.2 m thick which cut the older, coarser-grained mylonitic foliation but are conspicuously boudined where they cross the younger, fine-grained mylonitic foliation. The two foliation events and the shallowly inclined pegmatites are clearly crosscut by large, steeply inclined, undeformed pegmatite dikes that constitute 90% of the pegmatite exposed in the roadcut.

Similar relationships occur 20 km to the east-southeast of Mount Lemmon (Wilson, 1977; Ted Theodore, 1979, oral commun.) where undeformed pegmatite apophyses of the Wilderness pluton discordantly cut mylonite schist derived from Leatherwood. In addition, equigranular main-phase Wilderness granite may intrude mylonitic Leatherwood quartz diorite east of Green Mountain, about 12 km east-southeast of Mount Lemmon (Pilkington, 1962). The southern part of the Leatherwood pluton is continuously deformed along its east-southeast-trending margin for more than 20 km. As

such, mylonitic fabric in the Leatherwood constitutes a major pre-50 m.y. B.P. and post-75 m.y. B.P. mylonitic event in the Santa Catalina-Rincon-Tortolita crystalline complex.

Orientation of mineral lineation in mylonitic Leatherwood quartz diorite is distinct from that in main-range-exposures of mylonitic Wilderness granite. Based on 116 measurements mean lineation in Leatherwood quartz diorite exposures along the Oracle road 3 to 6 km northeast of Mount Lemmon is  $16^{\circ}$   $N85^{\circ}E$  (Tom Heidrick, 1979, written commun). Lineation on low-angle mylonitic surfaces in the deformed Wilderness intrusion in the Windy Point and Spencer Peak areas about 5 and 15 km., respectively, southeast of Mount Lemmon is more northeasterly (about  $N35^{\circ}E$  to  $N65^{\circ}E$ ). The difference in lineation orientation suggests that mylonitic foliation in the Leatherwood and Wilderness intrusions may have formed during two distinct episodes of cataclasis.

The next major mylonitic episode deformed the structurally lower parts of the Wilderness granite and its wall rocks in the Santa Catalina forerange. Analogous deformation may be represented by widespread mylonitic fabric in the mineralogically similar Wrong Mountain granite (Drewes, 1977) of the Rincon Mountains. This mylonitization deformed and therefore postdated the 44- to 50-m.y. old muscovite granites but predated their cooling between 31 and 25 m.y. B.P. as defined by K-Ar and fission-track ages. Keith infers that relationships between deformed and undeformed pegmatites in the Santa Catalina forerange suggest that the mylonitic fabric exposed there formed during the emplacement of Wilderness equivalent pegmatites. Mylonitization in the forerange must have been completely over by the time of intrusion of an undeformed 21-m.y. -old trachyte dike (Shakel, 1974; Damon and others, 1981).

One of the above two episodes may be widespread throughout the northwestern Tortolita Mountains where the Chirreon Wash (Leatherwood suite) and Derrio Canyon (Wilderness suite) intrusions are strongly mylonitized - particularly so in the area of the Derrio Canyon granite sill sequence (Figs. 2 and 5). At least part of this deformation predated emplacement of the Catalina pluton as evidenced by large, strongly deformed and lined inclusions of quartzite, Pinal Schist, stretched-pebble metaconglomerate and Oracle Granite in relatively less-deformed Catalina quartz monzonite. Presence of mylonitic inclusions of Leatherwood quartz diorite in Catalina quartz monzonite in the Santa Catalina Mountains (Suemnicht, 1977) also indicates a mylonitic event that predated emplacement of the Catalina quartz monzonite.

In the southwestern Tortolita Mountains the youngest episode of mylonitization clearly affects to varying degrees the Catalina quartz monzonite and the entire western half of the Tortolita quartz monzonite. This episode must postdate the two ~26-m.y. old plutons but predate cooling of the mylonitic rocks between 17 and 20 m.y. B.P. as defined by fission-track apatite ages. An additional minimum age for this episode is provided by a series of northwest-trending dikes which discordantly intrude mylonitic foliation. One of these dikes which cuts mylonitic Chirreon Wash grandiorite has yielded a 24-m.y. K-Ar biotite date. Thus, a significant mylonitic episode is

bracketed very close to 25 m.y. B.P. In the South Mountains near Phoenix, Reynolds and Rehrig ( 1980 ) have documented almost exactly the same age for mylonitic fabric that deforms a pluton which resembles phases of Tortolita quartz monzonite in rock type, texture, and style of mylonitic deformation.

In the Tortolita Mountains, several events of mylonitization are recognizable within the youngest episode of mylonitization. For example, near the mouth of Wild Burro Canyon, strongly mylonitized inclusions of Oracle Granite that were deformed during an earlier episode are included in the coarsely porphyritic phase of Catalina quartz monzonite. This phase in turn contains a younger, much weaker mylonitic foliation. These are both cross-cut by low-dipping sheets of the granitic phase of Tortolita quartz monzonite which has been strongly mylonitized by a still-younger mylonitic event. This youngest mylonitic event may be related to a widespread set of shallow-dipping, relatively wide-spaced shears that cut older, more steeply inclined foliations (some of which are mylonitic) in the Chirreon and Catalina intrusions.

#### Summary and conclusions (from Keith and others, 1980).

Various rocks within the Santa Catalina-Rincon-Tortolita crystalline complex can be correlated with rocks inside and locally outside of the complex by utilizing field relationships and lithologic, trace-element, and isotopic analyses. Deformed Precambrian, Paleozoic, Mesozoic, and Cenozoic rocks all occur within the complex, but its geology is *dominated* by a series of Late Cretaceous(?) through middle Tertiary plutonic and deformational episodes. Major plutonism was apparently episodic and produced three distinct ages and suites of intrusions. The Laramide (75 to 64 m.y. B.P.) quartz diorite and granodiorite (Leatherwood suite) were emplaced earliest. These were followed by Eocene (44 to 50 m.y. B.P.) muscovite granite, pegmatite, and alaskite (Wilderness suite). Finally, quartz monzonites (Catalina suite) were intruded in middle Tertiary time (27 to 25 m.y. B.P.). At least three episodes of mylonitic deformation occurred between 75 and 20 m.y. B.P. Although the plutonism was episodic, it cannot be definitively demonstrated that the mylonitic deformation was also episodic rather than part of a prolonged continuum. However, the close spatial and temporal association of mylonitization with plutonism suggests a genetic relationship between the two, and therefore supports episodicity of mylonitization.

## SOME SPECULATIONS CONCERNING REGIONAL SW-DIRECTED OVERTHRUSTING

by  
Stanley B. Keith

Keith (this conference) has offered a somewhat different view of how the Santa Catalina Mountains fits into the regional tectonic history of southern Arizona. The question has been asked by many geologists in the past as to in what way the drastically different appearing geologies of the Tucson Mountains and Santa-Catalina Mountains are related — in particular — how do the two geologies structurally fit together. My current approach to the problem is to suggest that the geology of the Santa Catalina and Tortolita Mountains may rest tectonically beneath the Tucson Mountains. A low-angle fault similar to the Catalina fault at the southern margin of the Catalina Mountains may separate the two terrains. Kinematic indicators in both upper and lower plates of the Catalina fault in the Santa Catalina and Rincon Mountains indicate a major episode of southwest vergent, low-angle tectonic transport (southwest upper plate motion relative to lower plate motion). I believe much of this transport occurred in the Eocene concurrent with the emplacement of the Wilderness peraluminous muscovite-bearing granitoid suite in the Santa Catalina-Rincon-Tortolita crystalline core.

Evidence for the synkinematic relationship between the peraluminous-muscovite granite and the event of southwest-directed low-angle tectonic transport may be present in Redington Pass, the low swail that separates the Santa Catalina and Rincon massifs. Here, mylonitic foliation probably related to the second mylonitic episode discussed earlier occurs in 1.4 b.y. granitic rocks, contains an anomalous north-northwest trending lineation, and is chiefly truncated at its northern contact by

the undeformed Youtcy pluton (pluton number 8 on Figure 1). However, the first few meters of the Youtcy intrusion at its contact with the mylonitic gneiss contain a mylonitic fabric that is parallel to and carries a northwest-trending lineation like that in the mylonitic 1.4 b.y. granite. To the east, the mylonitically deformed 1.4 b.y. granite is separated from highly deformed, metamorphosed, and tectonically thinned Apache Group and Phanerozoic sedimentary rocks by a northwest-striking northeast-dipping low-angle fault. The metasedimentary rocks also contain a northwest-trending lineation. Lineated foliation in the metasedimentary rocks and the northwest-striking low-angle fault also appear to be truncated by the east-west-striking southern boundary of the Youtcy intrusion. The most accurate map portrayal of these phenomena is that of Thorman and Drewes (1978) who also briefly discuss the above relationships (Drewes and Thorman, 1979). In summary, a major tectonic event which includes formation of mylonitic gniesses pre-dates and/or overlaps with the emplacement of the Youtcy pluton. If the Youtcy pluton is an undeformed eastern extension of the Wilderness intrusion, then the deformational event in eastern Redington Pass is pre- and/or syn- 50 m.y. B.P. It is this event that I believe is related to the SW-vergent transport because folds in the mylonitic 1.4 b.y. granite are SW vergent (Keith and Reynolds, unpublished data).

Overlap of upper and lower plate lithologies in the Rincon Mountains suggests at least 30 miles of SW transport occurred. I believe this transport was the tectonic result of compressively induced SW vergent thrusting related to anomalously low-angle subduction and crustal anatexis in the Tucson area in early Eocene time. It was at this time that the Tucson Mountains became detached from their basement and are now allocthonous.

The current elevational difference between 'upper plate' or structurally higher but elevationally lower Tucson Mountains relative to the Santa Catalina Mountains has been produced by late Oligocene through late Miocene post-mylonite arching around both NW-trending and ENE trending fold axes. In effect, the Santa Catalina, Rincon, Tortolita and Picacho Mountains represent a 'local' uparched structural window into an extensive mylonitized and locally plutonized tectonite basement terrane that may underlie a large portion of southern Arizona's Basin and Range Province.

## 3.6

Tangerine Road bridge and intersection. Return to Interstate 10 Northwest bound.

## 0.5

240 Baboquivari Peak (Jurassic granite) in view at 8:30. Roskruge Mountains are range on low skyline at 9:00. The Kitt Peak Observatory complex built on Jurassic granite (Haxel and others 1980) in the Quinlan Mountains is at 8:45. Safford Peak is now receding to our rear view at 7:00. Notice that Safford Peak appears to sit on a synclinal dish of cliff-forming basaltic andesites.

## 6.5

233.5 Marana overpass. Silver Bell Mountains at 9:30 on skyline with tailings from ASARCO's Silver Bell Mine operations at 9:15 to 9:30. Samaniego Hills at 10-11:00. The prominent peak between the Silver Bell Mountains and Samaniego Hill complex is Ragged Top a quartz latite intrusive complex dated at 25 m.y. (Mauger and others, 1965). The Samaniego Hills consist of a 16 to 26 m.y. volcanic complex that overlays a probably Precambrian 1.4 b.y. old granitoid basement (Eastwood, 1970). Picacho Peak at 11:55 is likely an extension of this geology (SEE STOP 2).

The Samaniego Hills geology is separated from the Silver Bell Mountains block by a major WNW to E-W striking fault named the Ragged Top fault zone by Banks and Dockter (1976). South of the Ragged Top fault, a thick sequence of Laramide volcanics and intrusions with complex cooling ages ranging from 68 m.y. to 19 m.y. (Mauger and others, 1965; Bank and others, 1978) are present. The volcanic section rests directly on a typical SE Arizona Paleozoic section and gives generally younger ages than the plutons which intrude the volcanics. Both intrusions and volcanics have yielded 19 to 22 m.y. fission-track apatite ages. Regional stratigraphic correlations by Dockter (1977) suggest the Laramide volcanic section at Silver Bell correlates with the 75 to 70 m.y. old Laramide volcanic section in the Tucson and Roskruge Mountains. Banks and others (1978) suggest the reduced K-Ar and fission-track ages represent thermal resetting by middle Tertiary batholithic masses in the Tortolita and Picacho Mountains north and east of the Silver Bell Mountains. S. Keith suggests these ages are in some peripheral way related to the reduced radiometric ages in the crystalline cores of the Santa Catalina, Tortolita, and Picacho Mountains. However, because most of the magmatism in these mountains is pre-40 m.y. in age, S. Keith prefers the idea that the reduced Laramide volcanic ages in the Silver Bell represent the termination of a complex thermal history that initiated under this region in Laramide time prior to 40 m.y. ago.

Regardless of their regional significance, the Silver Bell Mountains are the site of one of Arizona's important porphyry copper deposits (the mines are west of the tailings piles at 9:15 to 9:30). The Laramide volcanics in the Silver Bell Mountains have been intruded by an impressive swarm of east-northeast trending dikes and west-northwest elongate plutons (Watson, 1964; 1968). Extensive porphyry copper mineralization documented by Richard and Courtwright (1966) and Galey (1979) is present where the east-northeast-striking dike swarm intersects the west-northwest striking chain of plutons along the southern margin of the range. Several potassium-argon dates on alteration minerals by Mauger and others (1965) indicate the mineralization at Silver Bell is about 65 m.y. old. Cumulative reported production from the Silver Bell district from 1901-1979 is about 1.06 billion pounds of copper, 4.4 million pounds of lead, 40 million pounds of zinc, 4.8 million ounces of silver, and 1900 ounces of gold from 77 million short tons of ore. Also, some 6 million pounds of molybdenum have been produced.

1.5

235 Tortolita Mountains are in view from 3:00 to 5:00. Cochie Canyon (4:00) separates the Laramide part of the Tortolita crystalline core in the northern Tortolita mountains from the mid-Tertiary plutonic portion south of the canyon. The light-colored outcrops in the northwestern Tortolita Mountains (3:00) are of Derrio Canyon granite, one of the muscovite-bearing peraluminous granitoid members of the Eocene aged Wilderness suite according to Keith and others (1980) (REFER TO STOP 1).

2.7

232.3 Pinal County Line.

0.3

232 Marana Air Park Road overpass. The interstate is now crossing the Red Rock basin of Eberly and Stanley (1978), a north trending Basin and Range, graben structure. Drilling (Eloy Dev. #1 state) indicates the central part of the graben south of Interstate 10 is at least 5000 feet deep and contains at least some evaporites. Drilling (Berry Dev. No. 1 Federal) on the west side of the basin south of Interstate 10 encountered a probably mid-Tertiary volcanic section at about 3300 feet. These results suggested to Eberly and Stanley (1978) that the deepest part of the Red Rock graben is about 8 km wide. Recent drilling by the Anschutz-Buckhorn-Phillips consortium off the north end of the Picacho Mountains (1:00) entered Precambrian granite beneath the north end of the basin at about 4000 feet. These results combined with gravity data suggest the Red Rock basin closes about 12 miles north of this point.

231 1.0 Desert Peak (1:00) contains a gneissic quartz diorite (Leatherwood suite?) intruded by abundant pegmatites (Wilderness suite?). Hence, much of the Cenozoic pediment and valley fill alluvium north of interstate 10 between the Tortolita and Picacho Mountains may be underlain by mylonitic granitoid rocks similar to those in the Picacho and Tortolita crystalline complexes.

Owl Head Buttes (3:00) is composed of early Miocene volcanic rocks dated at 26 to 22 m.y. old (Banks and others, 1977, 1978) that rest unconformably on largely non-reset Precambrian crystalline rocks (Banks and others, 1978). This assemblage is juxtaposed against tectonized and plutonized basement in the crystalline core of the northern Tortolita Mountains (3:30) by a low-angle fault named the Guild Wash fault by Banks and others (1977). The Guild Wash fault is probably a Catalina fault analog and points to the regional distribution of these low-angle structures. We will view from a distance another similar structure in the southeast Picacho Mountains ahead (STOP 2).

228 3.0 Newman Peak (12:30) is the highest point in the Picacho Mountains (el. 4508 feet). Picacho Peak looming into view at 11:30.

229.3 1.3 Red Rock exit, Merge right onto off ramp. Turn right at Red Rock Road intersection and make quick left turn onto I-10 frontage road northwest bound.

3.0 The 96 Hills (3:00) are composed of a peraluminous two-mica granite (wilderness equivalent?) that intrudes Precambrian 1.7 b.y. old Pinal Schist and 1.4 b.y. old Oracle Granite. Bradfish (1979) has presented numerous chemical and isotopic data for the two-mica granite which he regarded as a differentiated product of a hornblende granodiorite phase. Both rock are regarded by Cornwall (1975) and Bradfish (1979) as comagmatic phases of a composite pluton named the Teacup granodiorite by Cornwall (1975). A Rb-Sr isochron that includes both phases gives a 70. m.y. isochron with an initial ratio intercept of .7086.

In light of the work by Keith and Reynolds (1980) and Keith and others (1980) in the Santa Catalina and Tortolita Mountains, another interpretation (S. B. Keith's) of Bradfish's data is possible. If the granodiorite point is omitted from the data and only the three muscovite-bearing phases are considered, a 64 m.y. isochron may be constructed. The initial ratio for this isochron is about .7100. If the pegmatite point is omitted, a 43 m.y. two-point isochron may be constructed and the two points plot very near the Keith and others (1980) isochron for the Wilderness Granite. These younger ages are more consistent with other data such as, (1) regional east-west striking dike swarms dated at 62 to 63 m.y. which intrude the hornblende granodiorite phase and may be truncated by the two-mica garnet-bearing phase (2) The fact that the two-mica granite intrudes the hornblende granodiorite phase in several places (Cornwall, 1975; Bradfish, 1979) (3) The chemical and isotopic similarity of the two mica granite phase to Wilderness suite rocks in the Santa Catalina and Tortolita Mountains,

and (4) The chemical and isotopic similarity of the hornblende granodiorite phase to Leatherwood suite plutons in the Santa Catalina and Tortolita Mountains.

In summary, the Teacup pluton is a small composite batholith that consists of two chemically, isotopically, and geologically distinct plutons. One is an older calc-alkalic hornblende granodiorite similar to the Leatherwood suite and other calc-alkalic plutons in the Tortilla and Ray areas, 35 miles northeast of I-10. The other pluton is a younger muscovite-bearing peraluminous granite similar to the Wilderness suite of Keith and others (1980) in the Santa Catalina-Rincon-Tortolita complex. The name "96 Hills granite" is proposed for this granite because of the excellent exposures of this granite in the 96 Hills (the 96 Hills lobe of Bradfish, 1979).

3.5

Pull over to the right, across the road from the BINGO gas station on the left and park for STOP 2.

## STOP 2

### LOW-ANGLE TECTONIC PHENOMENA AND GEOLOGIC OVERVIEW OF THE PICACHO MOUNTAINS.

by Stanley B. Keith

#### Introduction:

Picacho Pass is a familiar landmark in Arizona's cultural history as well as its geologic history. Near here, Arizona's only Civil War Battle was fought in 1862. According to Barnes (1960), the following events took place:

On April 15, 1862, sixteen Confederate cavalymen of Capt. Sherod Hunter's command were with Lt. Jack Swilling when they were overtaken by Lt. James Barrett and a dozen soldiers. During the skirmish, Barrett was killed, as were Pvt. George Johnson and Pvt. William S. Leonard of the Union forces. Two Confederates, whose names are not known, were killed and two others taken prisoner. (Not all accounts agree concerning the Confederates.)

In recent years, major new insights into the geology of the Picacho Mountains have been obtained by a number of workers. On the Arizona State Geologic map (Wilson and others, 1969), the Picacho Mountains (in view to your north) are shown as Precambrian gneisses, whereas Picacho Peak, the prominent Peak to the south of Interstate 10, is depicted as a Cretaceous-Tertiary intrusion. In recent years, work by numerous workers has vastly changed that interpretation. Undoubtedly, that interpretation will continue to evolve significantly.

## Geology: (Refer to Figure 1)

The present geologic interpretation, as I can piece it together, is as follows: The northern Picacho Mountains (north of I-10) is divisible into two major terranes. These terranes are separated by a major WNW-striking fault. The terrane north of this fault (not in view) consists mostly of a schist that strongly resembles Pinal Schist. The schist is intruded to the east by a porphyritic granite that strongly resembles Oracle Granite (Yeend, 1976; Banks, 1980). A more gneissic rock locally occurs between the gneiss and the schist. The above assemblage is cut by a series of WNW-trending shear zones that locally contain dikes of probable Precambrian-aged diabase that are lithologically similar to the well-known younger 1200-1100 m.y. diabase in the Sierra Ancha Mountains thirty-five miles north of Globe, Arizona. The extreme north end of this terrane contains a diorite to granodiorite pluton of early Tertiary age that intrudes the older rocks (Johnson, Masters thesis, in preparation). All of the above rocks are intruded by an impressive NW-striking swarm (especially in western exposures) of intermediate to silicic dikes. The probable age of this dike swarm is middle Tertiary. Copper mineralization at the North Star Mine may be related to this intrusive event. It also may be related to the early Tertiary granodiorite plutons.

South of the WNW-striking fault a much different terrain is present. Several low north-trending and northwest-trending, rounded, low ridges (not viewable from this stop) occur immediately south of the fault. This area of subdued relief is underlain by a granodiorite pluton of middle Tertiary age referred to as the North Star stock. Biotite from the North Star pluton has yielded a K-Ar age of  $24.35 \pm 0.73$  m.y. (Shafiquallah and others, 1978). The North Star intrusion is cut by numerous northwest to west-northwest trending dikes of intermediate composition. These dikes exhibit different lithologies than those that intrude the northern terrane.

About three miles south of the WNW-trending faults, the low-relief topography gives way to a noticeably more rugged, high-relief topography that comprises the main topographic mass of the Picacho Mountains. This is the topography that dominates our view to the north. The high point in this topography is Newman Peak at the 1:00 position (use I-10 NW-bound as the 12:00 reference position). The majority of this high-relief terrane is underlain by a foliated mylonitic, muscovite granite pluton. The mylonitic muscovite granite pluton is intruded by the generally non-foliated, mid-Tertiary Lone Star pluton near the topographic break mentioned above. The light-colored cliffy outcrops and rubble that occupy the exposures to our north are of the muscovite granite. Biotite-rich phases (presumably of the muscovite pluton) are locally observed (for example, the outcrops under the low ledges at 1:30). Their relationship to the main phase must still be rigorously determined and awaits someone's mapping. Muscovite extracted from this pluton has yielded a late Oligocene cooling age (Gary Johnson, Master thesis in preparation). This age is similar to numerous late Oligocene ages reported on the Wilderness Granite in the Santa Catalina Mountains (see Keith et al., 1980, for a review of these apparent ages).

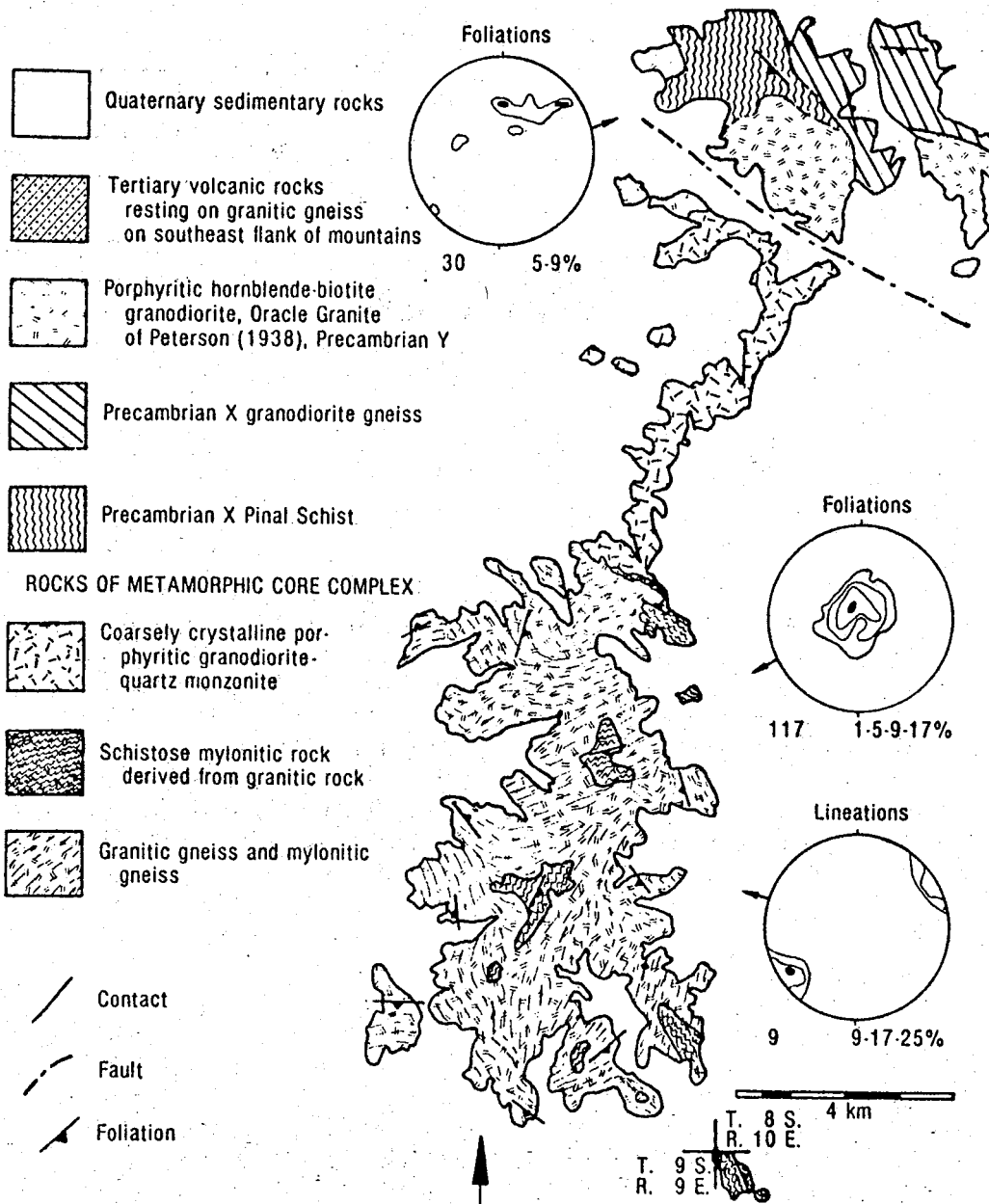


Figure 1. Generalized geologic map of the Picacho Mountains, Arizona (modified from Yeend, 1976), with lower-hemisphere equal-area net projections showing orientation of foliation in the northern Picacho Mountains and foliation and lineation in the southern Picacho Mountains (foliation and lineation data from Yeend, 1976). Contours are percent per one percent area.

From Banks (1980).

The muscovite granite of the Picacho Mountains is presumably a member of Late Cretaceous to Eocene peraluminous granitoid suite that has now been recognized as a major new magma type throughout southern Arizona (Keith and Reynolds, 1981).

Another mylonitic lithology common in the southern part of the main Picacho Mountains (for example, the inselberg outliers at 3:00 and the slopes below the muscovite granite cliffs at 1:00 low) is a porphyritic augen gneiss. This lithology was intruded by the muscovite granite. Yeend (1976) and Banks (1980) believe the protolith for the mylonitic porphyritic augen gneiss is the Oracle Granite dated at about 1400 m.y. I see no reason to doubt this supposition. Nearly all of the mylonitic foliation is low-angle and is responsible for the layered aspect of the rocks. One hundred seventy-one lineations measured by George Davis, all fall in the NE-SW quadrant and average about N 50° E. (Davis, 1980).

Near Newman Peak these mylonitic gneisses are intruded by a non-mylonitic, north-trending dike that resembles the Tortolita quartz monzonite in the Tortolita Mountains to the southeast. A date on this dike could provide a minimum age for the mylonitic deformation.

The mylonitic granitoid rocks are overlain by the curious slope- and ledge-forming mylonitic schist that caps the high ridges of the Picacho Mountains (for example, Newman Peak and the table-like hill @ 1:30). At Newman Peak, the schistose rocks are abundantly intruded by pegmatites and aplites; some of these intrusions are folded. Exposures of the mylonitic schist in the hill at 1:30, and nearby hills, locally contain box-fold structures. Geometric data for 14 box-folds yield an ENE-WSW axis of shortening. These folds fold the older, above-mentioned, lineation. Within the same zone, reverse faults are locally numerous. Geometric data for 25 of these faults yield an average strike of N 37° W at a dip of about 30° SW. Hence, the faults show a marked preference for northeast transport or vergence. The axis of shortening for these faults is S 53° W. These faults are late and cut the mylonitic schist. It is interesting that the axis of shortening for the reverse faults is parallel to lineation phenomena in the same rocks. The data seems to indicate that an event of NE-SW shortening occurred late in the history of, or post-dates the mylonite formation. If the muscovite granite in the Picacho Mountains correlates with similar granitoids in the Tortolita and Santa Catalina Mountains, mylonitic deformation in the Picacho Mountains is syn- to post-middle Eocene and predates emplacement of the 24 m.y. North Star pluton.

Close inspection of the conical hill at 2:00 will reveal a small, dark outcrop that caps the very top of the hill. This outcrop is a volcanic rock that closely resembles the ultrapotassic trachytes in the small outlier at 2:00 and the extensive exposures at Picacho Peak south of I-10. The volcanic rock on this hill rests tectonically on a highly fractured and somewhat chloritic, coarse-grained, biotite granite which in turn rests tectonically on mylonitic schist ledges at the mid-point on the hill. These ledges also contain folds (see previous discussion). The low-angle tectonic contact between the volcanics and the underlying crystalline rocks probably represent a

low-angle normal fault or dislocation surface (in the sense of Rehrig and Reynolds, 1980) of mid-Miocene age. The age of the trachyte is about 22 m.y. (Shafiquallah and others, 1976). The exposure of this fault occurs only on the small hill at 2:00. However, the northeast-dipping volcanic section of Picacho Peak may rest as an allochthon on this low-angle surface. If so, the trace of this fault would pass between the outlier of trachyte at 1:00 low and the crystalline mylonitic rocks underneath Newman Peak at 1:00 high. If the NE dip of the volcanic section is related to movement on this dislocation surface, then the volcanic section at Picacho Peak (which dominates our view from 8:00 to 11:00) was transported SW above this surface. As previously mentioned, Picacho Peak was formerly thought to represent a Tertiary intrusion. Work by Briscoe (1967) and Shafiquallah and others (1976) has shown that Picacho Peak predominantly consists of a 23-21 m.y. pile of northeast-dipping, high-K andesites and ultrapotassic trachytes. The volcanic section is intercalated with conglomeratic clastic rocks (the Wyomola conglomerate of Briscoe, 1967) in the lower part of the section. Base and precious metal mineralization is locally present in northwest-striking fractures that cut this early Miocene section.

#### A SUMMARY OF THE ANSCHUTZ-BUCKHORN-PHILLIPS OIL TEST AND ITS POSSIBLE REGIONAL IMPLICATIONS.

by Stanley B. Keith

The discussion of the Picacho Mountains would be incomplete without some mention of the Anschutz-Buckhorn (formerly Texoma)-Phillips oil test drilled off the northeast end of the Picacho Mountains. On February 14, 1981, Anschutz-Texoma State No. 1-10-2 was plugged and abandoned after reaching a total depth of 18,013 feet, a new Arizona depth record. Recent mud logs received at the Bureau of Geology and Mineral Technology suggest the following lithologies from top to bottom. The lithological interpretations should be considered very preliminary, pending careful perusal of the cuttings.

- 0-2,000 feet: Fine-grained clastics; some gypsiferous muds.
- 2,000 - 4,000: Coarse-grained conglomeratic clastics derived mostly from 1.4 b.y. old Oracle Granite.
- 4,000 - 10,800: Coarse-grained leucocratic to mesocratic biotite quartz monzonite (probably Oracle Granite).
- 10,800 - 12,600: Mostly leucocratic biotite, muscovite granite with intervals of epidote-bearing and locally hornblende-bearing biotite granodiorite.
- 12,600 - 16,300(?): Mostly epidote-bearing and locally hornblende-bearing biotite granodiorite(?).
- 16,300 - 18,013: Mesocratic hornblende, biotite, granitic (?) gneiss

The gneiss in the bottom-hole core contained microdiorite dikes which intruded the gneiss. Also of interest was an interval of copper

mineralization from about 12,600 to 13,100 feet in the biotite granodiorite (?).

Although the hole did not encounter hydrocarbons or a structurally covered mesozoic sedimentary basin as envisioned by Anschutz (see Keith, 1979 and 1980), the lithologies encountered may have some provocative implications for central Arizona geology. One possible scenario (according to S. Keith) is at least consistent with the regional geology. The transition from Oracle granite to muscovite granite at about 10,800 feet is approximately coincident with geophysical estimates of the top of the intriguing "reflectors" in seismic section AZ-18 (see Keith, 1980, Figure 2). Utilizing the northwestern Tortolita Mountains as a model, the Oracle Granite from 4,000 - 10,800 might be part of a relatively non-radiometrically disturbed crystalline plate above a regional detachment plane that separates those crystalline rocks from a tectonized and plutonized basement terrane underneath. The Guild Wash fault in the northwestern Tortolita Mountains similarly may juxtapose non-mylonitic Oracle Granite over mylonitically deformed Derrio Canyon Granite (a muscovite granite of the Wilderness suite) and Chirreon Wash granodiorite (a pluton of the Leatherwood group). The epidote-bearing biotite granodiorite intervals in Anschutz-Texoma State No. 1-10-2 conceivably might be a Leatherwood analog. This would be supported by the above-mentioned copper mineralization. Interleaving of comparatively low density muscovite granite and higher density biotite granodiorite might explain some of the reflectors. Low-angle mylonitic foliation could augment the reflectance effect.

In effect, the Anschutz-Buckhorn-Phillips consortium may have, at about 10,800 feet, drilled into a tectonized and plutonized basement terrane similar to that exposed in the crystalline cores of the Santa Catalina, Tortolita, and Picacho crystalline complexes. If so, then much of the outcrop geology north of the Picacho, Tortolita, and Santa Catalina Mountains may overlie and be detached from a deformed and plutonized basement terrane, i.e. allocthonous. It is interesting that the top of the reflecting zone generally dips northeast in seismic time cross section AZ-18. This suggests that depth to the deformed crystalline tectonite basement increases to the north and east towards the Colorado Plateau and that such a basement might conceivably lie at depth under the plateau. Quien sabe!?

Return to Interstate 10 via the Picacho interchange and continue northwest, bound for Phoenix.

- 1.3
- 219 A good view of the mylonitic foliation may be seen at 1 - 2:00. The inselberg hill at 1:30 is mostly muscovite granite with a southwest-dipping mylonitic foliation.
- 3.0
- 216 A good view of the mylonitic schist intruded abundantly by low-angle pegmatite sheets near the top of Newman Peak is seen at the 3:00 position.

- 0.7  
215.3 Subtle dip in interstate marks the trace of the Picacho fault, one of the main features of the Picacho-Eloy subsidence area. This fault exhibits a 0.5 m., west-side down, offset over a distance of 11 km. Post-interstate movement on the fault reflects subsidence in the Picacho basin due to ground water withdrawal for agricultural purposes. Steep gravitational contours in the area of the fault trace and its position astride the west boundary of the Picacho Mountain block suggest the recent activity might reflect the reactivated presence of a pre-existing basin and range fault. If so, the Picacho fault marks the structural boundary between the Picacho Mountain block and the Picacho basin.
- 1.3  
214 Superstition Mountains are in view in far distance from 2:00 to 3:00. Interstate 10 is now crossing the Picacho basin in which a thick, 1800 m thick evaporite section of anhydrite was penetrated by the Exxon State (74) - 1 well, about 5 km north of I-10. The anhydrite section contained only minor interbeds of shale, tuff, halite, and limestone nodules, according to Eberly and Stanley (1978). The well also encountered at 2765 m. an ultrapotassic trachyte flow dated at 14.9 m.y. by the K-Ar method. Overlying this flow are fanglomerates that grade upward into the Picacho basin evaporites, beneath the trachyte flow. This flow is contained in a volcanic section at a depth from 2765 to 2946 m. A basalt above the trachyte yielded an age of 17 m.y. Below the volcanic section, the well cut reddish conglomerate from 2946 to 3001 m and then entered a quartz diorite gneiss that yielded highly discordant ages of 25 m.y. (K-Ar on biotite) and 1275 to 1540 m.y. (Rb-Sr whole rock). The reduced age suggests this rock is related to the mylonitic gneisses of the Southern Picacho Mountains which have also yielded late Oligocene reduced K-Ar ages (see STOP 2 DISCUSSION). Hence, formation of the mylonitic gneisses predates Basin and Range faulting and the middle Miocene volcanism (which also pre-date the Basin and Range faulting because they have been downdropped at least 2700 m relative to analogues at Picacho Peak and the Samaniego Hills).
- 4.0  
210 Table Top Mountain in far distance at 11:30 is capped by a 21.4 m.y. basalt that dips about 25° WSW (Shafiquallah and others, 1980).
- 4.0  
206 Sawtooth Mountains at 10:30 are composed mostly of late Oligocene-early Miocene rhyolite, dacite, and trachyandesite volcanics (Bergquist and others, 1978). One of the rhyodacites from an insellberg 5 km south-east of the Sawtooth Mountains gave a biotite K-Ar age of 25.3 m.y. (Banks, and others, 1978).
- 0.5  
205.5 Battaglia Road overpass.
- 1.5  
204 Toltec Road overpass.
- 1.0  
203 Toltec Buttes (1:30) are composed of Precambrian 1.7 b.y. old Pinal Schist and migmatitic quartz-plagioclase-biotite gneiss that contains a northeast-striking, steeply southwest-dipping foliation. Casa Grande Mountains (10:30 - 11:30) are also largely composed of Pinal Schist

migmatitic gneisses with a general east-northeast foliation strike. The schist is cut by several northwest-striking, southwest-dipping medium-grained equigranular granodiorite dikes of "probable late Cretaceous or early Tertiary age", according to Bergquist and Blacet (1978).

The rock assemblage in the Casa Grande Mountains and Toltec Buttes probably represents upper plate crystalline rocks. Presumably, the tectonized basement terrane of the Picacho Mountains would rest at some unknown depth beneath this area (S.B. Keith's interpretation).

- 2.9  
200.1 Sunland Gin Road overpass.  
0.3  
199.8 Yuma Interstate 8 exit for Gila Bend and Yuma. Continue straight on I-10, northwest bound for Phoenix.  
0.6  
199.2 Interstate 8 overpass.  
1.0  
198.2 Bridge over Southern Pacific railroad tracks. Town of Casa Grande at 10:00. The East Sacaton Mountains are now in view at 12:00 to 12:30 with Pinal Peak, highest point in the Pinal Mountains (el. 7,848') in far distance at the 1:30 position.  
3.3  
194.9 State Highway 287 overpass.  
1.0  
193.9 Storey Road overpass.  
0.9  
193 According to the map by Bergquist and Blacet (1979), Burgess Peak @ 9:00 is composed of probably mid-Tertiary reddish-brown biotite rhyodacite agglomerate with abundant clast up to 50.5 m in diameter of Laramide-age medium to coarse-grained biotite hornblende quartz monzonite (The Three Peaks quartz monzonite of Balla, 1972). The low hills at 10:00 consist of Pinal Schist, intimately intruded and injected by Oracle Granite. Both are intruded by diabase dikes (Keith, unpub. mapping and Bergquist and Blacet, 1979).

Both of the aforementioned topographic outliers are expressions of an extensive bedrock bench that lies underneath a thin cover of alluvium 0 to about 600 feet thick between the Casa Grande Mountains (7:30) and the western extension of the Sacaton Mountains (10:30). From these observations, one can get a better impression of just how much pedimentation has occurred in this region since the Basin and Range topography was first blocked out. Indeed, pedimentation has occurred to such an extent that it is impossible on the basis of topography to closely identify the original position of the Basin and Range structural basins.

- 2.0  
192 The east Sacaton Mountains (12:00 - 2:30) are composed almost entirely of Laramide granitoid rocks. Balla (1972) divided this sequence into two major plutons. The ridge at 12:30 to 2:30 is composed of the Sacaton Peak granite, a medium-grained biotite quartz monzonite according to Balla (1972). Biotite from this rock gave a K-Ar age of about

62 m.y. Balla also recognized a core facies on the west side of the ridge at about 1:30 low that exhibited gradational contact with a porphyritic biotite granite core phase that locally contains abundant alternating bands of feldspar and biotite. Biotite from the core phase gave a K-Ar age of 50 m.y. which Balla interpreted as a reduced age due to reheating from a nearby aplite. Both phases of the Sacaton granite are cut by numerous northwest-striking aplite and pegmatite dikes that, in turn, are cut by numerous east-northeast striking lamprophyre dikes. Both dike sets have yet to be isotopically dated.

The 50 m.y. age on the porphyritic biotite granite core phase is intriguing in light of the recent discoveries of late Paleocene-early Eocene two-mica granitoids. Biotite-rich phases of these peraluminous granitoids are known (Haxel and others, 1980; Keith and Reynolds, 1980) and it is conceivable that the core facies of the Sacaton Peak granite might be a biotite-rich end-member of the two-mica clan. The age date and abundance of pegmatites in the area are consistent with this possibility. Obviously, this option must be tested by careful mapping, petrographic description, and isotopic analysis of the Sacaton Peak granitoid complex.

- 1.3  
190.7 McCartney Road overpass.
- 0.7  
190 Table Top Mountain is now at 9:00. See geologic comment at milepost 210.
- 1.0  
189 Small hill with water tower at 10:45 was the discovery outcrop for the Casa Grande or Sacaton porphyry copper deposit. Identification of pervasive quartz-sericite-pyrite alteration of Oracle Granite in the hill by ASARCO geologists in February of 1961 precipitated an extensive exploration drilling project. By 1968, ASARCO announced the existence of two ore deposits. One contained about 17 million tons of ore, averaging 0.8% Cu and was amenable to open pit mining (the current operation) and the other deposit contained about 12 million tons of ore averaging 1.5% Cu. This second deposit is now undergoing underground development. Sericite from drill core has yielded an age of about 65 m.y. and reflects the age of mineralization at the Casa Grande deposit (Pushkar and Damon, 1974). Production started in 1971, and through 1979 some 191 million pounds of copper, 654,000 ounces of silver and 5,500 ounces of gold have been recovered from 17.6 million tons of ore. The deposit is located near the southern margin of the Three Peaks monzonite at its contact with the Oracle Granite. The east-northeast elongate mineralized zone occurs in the Oracle Granite and an irregular-shaped monzonite stock centered near the southwest side of the deposit, and is intruded by post-mineral andesite dikes. The mineralized igneous rocks are unconformably overlain by a tilted conglomerate sequence that, in turn, is angularly truncated by a veneer of pediment alluvium. Like the San Manuel-Kalamazoo ore deposit in the southern Tortilla Mountains of Pinal County, the Casa Grande deposit and the tilted conglomerate sequence are cut by a major northwest-striking, northeast-dipping fault (the Sacaton fault) that has offset the eastern portion of the deposit down 1000 to 1800 feet to the east.

The Sacaton fault, like the San Manuel fault at San Manuel-Kalamazoo and the San Xavier fault at Twin Buttes, Mission-Pima-Palo Verde, and San Xavier deposits, is probably another example of a mid-Miocene-aged listric normal fault. These faults are common throughout central Arizona and locally have significantly offset in a normal fashion pre-existing Laramide age porphyry copper mineralization. Whether some or all of these structures root into some fundamental dislocation zone (see Rehrig and Reynolds, 1980, for use of this term) of regional extent and extensional origin is a matter of current lively debate. The Catalina fault of the Santa Catalina Mountains, the Guild Wash fault of the Tortolita Mountains, and the Rawhide-Buckskin-Whipple fault in west-central Arizona and southeast California could be examples of such a regional structure. If such a regional structure exists, it would lie at depth under the Sacaton Mountains (Sacaton Mountain are allocthonous in this model). If the structure exists, it is also possible (S.B. Keith's preference) that the structure formed in the early- to mid-Eocene as a regional compressionally-induced SW-directed thrust. This thrust then would have provided a regional planarity in the mid- to upper-crust that has subsequently localized and locally been overprinted the dislocational tectonism of mid-Miocene age. Other views (Davis and Coney, 1979; Davis, 1980; Rehrig and Reynolds, 1980; Reynolds and Rehrig, 1980) would emphasize mid-Tertiary timing and an extensional origin for such a structure and the underlying mylonites. Still other views (Drewes, 1976; 1978; 1980; Thorman, 1978) would ascribe an older formation age of early Laramide (80 to 70 m.y.) and a tectonic context of northeast-directed overthrusting to these structures and the underlying mylonitic basement. Davis and others (1980) and Shakelford (1980), in the Whipple and Rawhide Mountains infer a Laramide ancestry for the mylonite but a Miocene age for the Whipple-Buckskin-Rawhide low-angle fault. One can see, we still have a lot to learn and a lot to resolve! Whatever those phenomena are, they are extremely important to the unraveling of Arizona's tectonic and mineral deposit framework and history.

- 0.6  
188.2 Val Vista Road overpass.  
2.9  
185.3 Arizona State 387 overpass  
0.3  
185 Pediment on either side of interstate is underlain by Oracle Granite. Here the Oracle Granite occurs as a septum which separates the Laramide Sacaton Peak granitoid complex from the Laramide Three Peaks monzonite in the ridges ahead from 12:00 to 1:00.

About 2 km southwest of our position, in the pediment (9:00 low) is a low east-west trending ridge of recrystallized sedimentary rocks (south half of Sec. 7, T.5 S., R.6E). Here, a ridge about 2000 feet long and 200 feet wide contains a pure quartzite overlain by a few very small outcrops of carbonate. Wilson (1969) and Balla (1972) correlate the quartzite with the Cambrian age Bolsa Quartzite and the carbonate with the Devonian age Martin Formation. The outcrop is significant in that it is the only outcrop of Paleozoic rocks in the region. The nearest outcrop of similar rocks is in the Vaiva Hills over 25 miles to the southwest.

- 1.2  
183.8 Roadcuts here are in the Three Peaks monzonite pluton of Balla (1972). The Three Peaks monzonite underlies much of the southern part of the western Sacaton Mountains (8:00 - 10:00) where it intrudes Precambrian

Oracle Granite on the south and north and a muscovite granite at its western end. Balla (1972) describes the Three Peaks stock as compositely zoned northeast-elongate pluton. He recognized three major phases: a diorite border phase; an intermediate monzonite facies; and a central monzonite core facies. Biotite from the core facies yielded a 72 m.y. age. Several fine-grained granodiorite dikes intrude the stock as well as a set of lamprophyre dikes. Both sets strike N50E to E-W.

0.3

183.5

Exit for Roadside rest area. The northern portion of the western Sacaton Mountains (8:30 - 11:00) is underlain mostly by Oracle Granite which contains a few roof pendants of Pinal Schist in the northwesterly most pediment inselbergs (11:00). Biotite from the Oracle Granite gave an apparent K-Ar age of 1240 m.y. (Balla, 1972). This age is a reduced one and probably reflects resetting by numerous northwest-striking diabase dikes that intrude the Oracle Granite. The Oracle Granite is also intruded by numerous northwest and east-northeast striking dikes of aplite assigned a Precambrian age by Balla (1972).

In the southwestern part of the Sacaton Mountains the Oracle Granite is intruded by a muscovite granite named the Sacaton Granite by Balla. Muscovite from this rock gave a K-Ar apparent age of 860 m.y. Balla speculates that if this age is real, it could reflect a younger Precambrian event of muscovite granite magmatism in central Arizona. Balla's speculation is supported by roughly similar ages on muscovitic granites in the northern Pinal Mountains (a 619 m.y. K-Ar age on muscovite from the Solitude Granite reported by Creasey, 1980) and the Cimarron Mountains (Haxel and others, 1980; Haxel, Personal communication).

1.5

182

The western San Tan Mountains (2:00 - 3:00) are composed of more Precambrian crystalline rocks overlain by a late Oligocene-early Miocene volcanic section to the south. Balla (1972) has mapped an east-northeast elongate belt of Pinal Schist throughout much of the northern San Tan Mountains. This belt of schist is interleaved along its north and south borders with a foliated biotite quartz plutonic complex named the San Tan quartz monzonite by Balla (1972), diorite to granodiorite. A biotite concentrate from this rock gave an age of 1340 m.y. by the K-Ar method. In the north end of Table Top Mountains about 35 miles southwest of our present position, a similar rock is intruded by Oracle Granite equivalent, according to Balla. It has yielded a K-Ar age of 1330 m.y. on biotite. Balla considers the two rocks equivalents and correlates them with the Madera quartz diorite of Ransome (1903) further east in the Superior to Pinal Mountain region. The Madera quartz diorite has yielded numerous older ages ranging from 1695 m.y. to 1540 m.y. (Damon and others, 1962; Livingston, 1969; Banks and others, 1972). The 1330 and 1340 age probably reflect resetting by the 1.35 to 1.45 Oracle Granite which pervades much of the Precambrian basement throughout the region.

The Precambrian geology is overlain to the south by a typical section of mid-Tertiary rocks. These consist of a basal conglomerate overlain

by a series dark-colored basaltic andesites. These are, in turn, overlain by a welded tuff (conspicuous cliffs at 2:30). The tuff, named San Tan tuff by Balla, 1972, thins markedly from north to south and has yielded a 25.4 m.y. age on phlogopite (Balla, 1972). Balla considers the San Tan tuff to be the most southerly outcrop of the extensive ignimbrite volcanism present in the Superstition Mountains 25 miles to the north.

- 0.5  
181.5 Dirk Lay Road overpass.
- 1.5  
180 Directly ahead lie the South Mountains at 12:00, the object of our scrutiny for the next several hours. Astride the South Mountains to the southwest rest the Sierra Estrella (10:00 to 11:00), a spectacular northwest-trending jagged spine. The highest spine is Montezuma Peak (10:30) with an elevation of 4,337 feet.
- 0.5  
179.5 Seed Farm Road overpass.
- 1.1  
178.4 Gas Line Road overpass.
- 1.4  
177 Pima Butte at 10:00 low backed by Montezuma Peak in southern Sierra Estrella. The Sierra Estrella are mostly composed of northeast-striking steeply-inclined amphibolite-grade gneisses, intruded by a coarse-grained biotite quartz monzonite at the southern end of the range. A Rb-Sr model age reported by Pushkar and Damon (1974) for the granite is about 1.4 b.y. This age agrees with a 1380 m.y. K-Ar age on muscovite from a quartz-perthite-biotite-muscovite-garnet pegmatite that intrudes the gneisses just southwest of the pluton. K-Ar biotite ages on the granite are about 300 m.y. and are interpreted by Damon and Pushkar as hybrid ages that reflect partial resetting of the Precambrian granite, perhaps by subsequent Laramide or mid-Tertiary magmatism in the region. One candidate for such magmatism would be a two-mica, garnet-bearing granite at the extreme southernmost tip of the Sierra Estrella.
- Another provocative item in the Sierra Estrella is the occurrence of a carbonate section within the gneisses on the west side of the spine at about its mid-point (Ralph Rogers, personal communication). What those carbonates are and how they got into the gneisses is unknown. Clearly, much more geological work remains to be done in this range as its geology has largely evaded any detailed mapping and sampling to date. Pima Butte is mapped as Precambrian-aged schist and pegmatite of unknown affinity.
- 1.2  
175.8 Casa Blanca Road overpass.
- 0.8  
175 Four Peaks (el. 7657 feet) is the highest point in the southern Mazatzal Mountains (2:30) which form a backdrop for the Superstition Mountains at 3:00. The portion of the southern Mazatzal Mountains in view contains an assemblage of quartzites and shales of the Mazatzal group (about 1.7 b.y. old) intruded by another batholith of the widespread 1.4 b.y. granitoid group. These Precambrian rocks are unconformably overlain to

the south by the extensive Oligocene to mid-Miocene Superstition volcanic field. Stuckless and Sheridan (1973) have reported numerous fission-track and K-Ar ages ranging in age from about 29 m.y. to 15 m.y. in age. The San Tan Mountains (now at 3:00) are presumably the southernmost extent of the Superstition volcanic field.

- 0.4  
174.6 Nelson Road overpass. South Mountains remain at your 12:00 position.  
0.6  
174 Hill at 12:30 and roadcuts ahead are mapped on the 1969 Wilson and others Arizona geologic map as undivided schist and granite and assigned a Precambrian age. The roadcuts are mostly a coarse-grained biotite granite. No radiometric ages on these rocks have been reported in the literature.  
0.6  
173.4 Gila River bridge.  
0.4  
173 Roadcuts in coarse-grained biotite granite.  
3.1  
169.9 Goodyear Road overpass.  
1.2  
168.7 Maricopa County line.  
1.7  
167 Telegraph Pass is the conspicuous notch in the South Mountains at 11:30 with the T.V. tower complex to the east. South Mountains crystalline complex, another uparched plutonic and mylonite terrane is dead ahead.

By now, the scenario should be becoming fairly apparent. Between Tucson and Phoenix, two major packages of crystalline rocks are evident. The first package (Sierra Estrella, San Tan, Sacaton, Casa Grande Mountains, etc.) contains a heterogeneous assemblage of Precambrian crystalline rocks intruded by Laramide-age plutons, some attended by porphyry copper mineralization. North of the Tucson, Silver Bell and Vaiva Hills, this agglomeration of crystalline rocks is locally unconformably overlain by a non-metamorphosed sequence of Oligocene to mid-Miocene aged volcanics and predominantly clastic sedimentary rocks. In general, isotopic ages in these rocks are unperturbed and when disturbed or reduced can readily be attributed to a nearby younger magmatic event. Mylonitic phenomena in those rocks are generally absent.

In contrast, the second package (South Mountains, Picacho, Suizo, Tortolita, Santa Catalina, and Rincon Mountains) contains highly tectonized Precambrian crystalline rocks that are commonly intruded by Laramide through mid-Tertiary plutonic suites. Low-angle mylonitic phenomena are pervasive and all isotopic systems complicated to varying degrees. Inherited zircon problems plague the U-Pb zircon method while contamination effects are commonplace in Rb-Sr systems. With the exception of some coarse-grained muscovites and hornblendes, all K-Ar clocks have been reduced significantly; 28 to 24 m.y. cooling numbers are very common. Paleozoic rocks are sparingly present and are invariably tectonized. No former sedimentary contact has escaped at least some tectonic modification and formational protolith calls are difficult and sometimes impossible to make. Where the two packages are in contact, that contact is invariably a low-angle fault of some kind. The mylonitized

tectonic terranes invariably appear beneath these faults at a structurally lower level. In this context, the importance of the Anschutz-Buckhorn-Phillips drillhole cannot be underestimated, for the hole appeared to collar in the non-mylonitic, non-isotopically disturbed upper plate package and encounter lithologies consistent with "lower plate" package rocks. Hence, the reported extensive age dating by Phillips of numerous intervals in the drillhole is especially important. The Anschutz-Buckhorn-Phillips then could provide important verification of the existence of a lower tectonite basement terrane that may underlie much of the region.

3.0

164 Bridge over Queen Creek.

1.6

162.4 Maricopa Road Overpass. Immediately after passing under overpass, take Maricopa Road Exit 162 and turn right on Maricopa Road, which passes over the interstate. Proceed southwest for 0.5 miles and park in wide areas on either north or south side of road for STOP 3.

## STOP 3

## GEOLOGICAL OVERVIEW OF THE SOUTH MOUNTAINS, CENTRAL ARIZONA

by Stephen J. Reynolds

## Introduction:

The South Mountains are located immediately south of Phoenix in central Arizona. They are a northeast-trending range approximately 20 km long and 4 km wide with about 500 meters of topographic relief. The range is isolated from other bedrock exposures, being surrounded by a low-relief surface underlain by late Tertiary-Quaternary surficial deposits.

Although the South Mountains were briefly mentioned by several early geologists, they were first reconnaissance mapped by Wilson (in Wilson and others, 1957; Wilson, 1969). Avedisian (1966) studied petrology of selected rocks in the western half of the range. The first detailed map and discussion of the geology of the range was done by Reynolds and colleagues (Reynolds and others, 1978; Reynolds and Rehrig, 1980; Reynolds, in progress). They recognized that the South Mountains have many characteristics similar to metamorphic core complexes (see Reynolds and Rehrig, 1980). The following discussion of geology of the area is extracted from published and ongoing studies of Reynolds and others.

## General Geology: (Refer to figures 1 and 2)

Precambrian rocks exposed in the western half of the South Mountains consist of amphibolite-grade gneiss and schist with local intrusive masses. Almost the entire eastern half of the range is underlain by mid-Tertiary granodiorite which generally displays a weakly to strongly-developed mylonitic foliation. In the center of the range a locally foliated mid-Tertiary granite intrudes between the Precambrian amphibolite gneiss and the granodiorite. Throughout most of the area, Precambrian rocks and the two mid-Tertiary plutons are intruded by numerous north-north-west-trending mid-Tertiary dikes which are, in many places, mylonitically foliated. In the northeastern portion of the mountains, the mylonitic granodiorite becomes progressively jointed, brecciated, chloritic, and hematitic up structural section until it is converted into chloritic breccia. In the southern foothills of the mountains, the chloritic breccia is overlain by a low-angle dislocation surface above which lie Precambrian metamorphic rocks similar to those exposed further to the west.

## Structural Relationships: (Refer to figures 2 and 3)

Most rocks in the range exhibit a gently dipping mylonitic foliation which contains a pervasive N60E-trending lineation. The foliation is defined by planar mineral aggregates and thin bands of intensely granulated and recrystallized rock. Mylonitically foliated rocks contain joints, quartz-filled tension fractures, and "ductile normal faults"

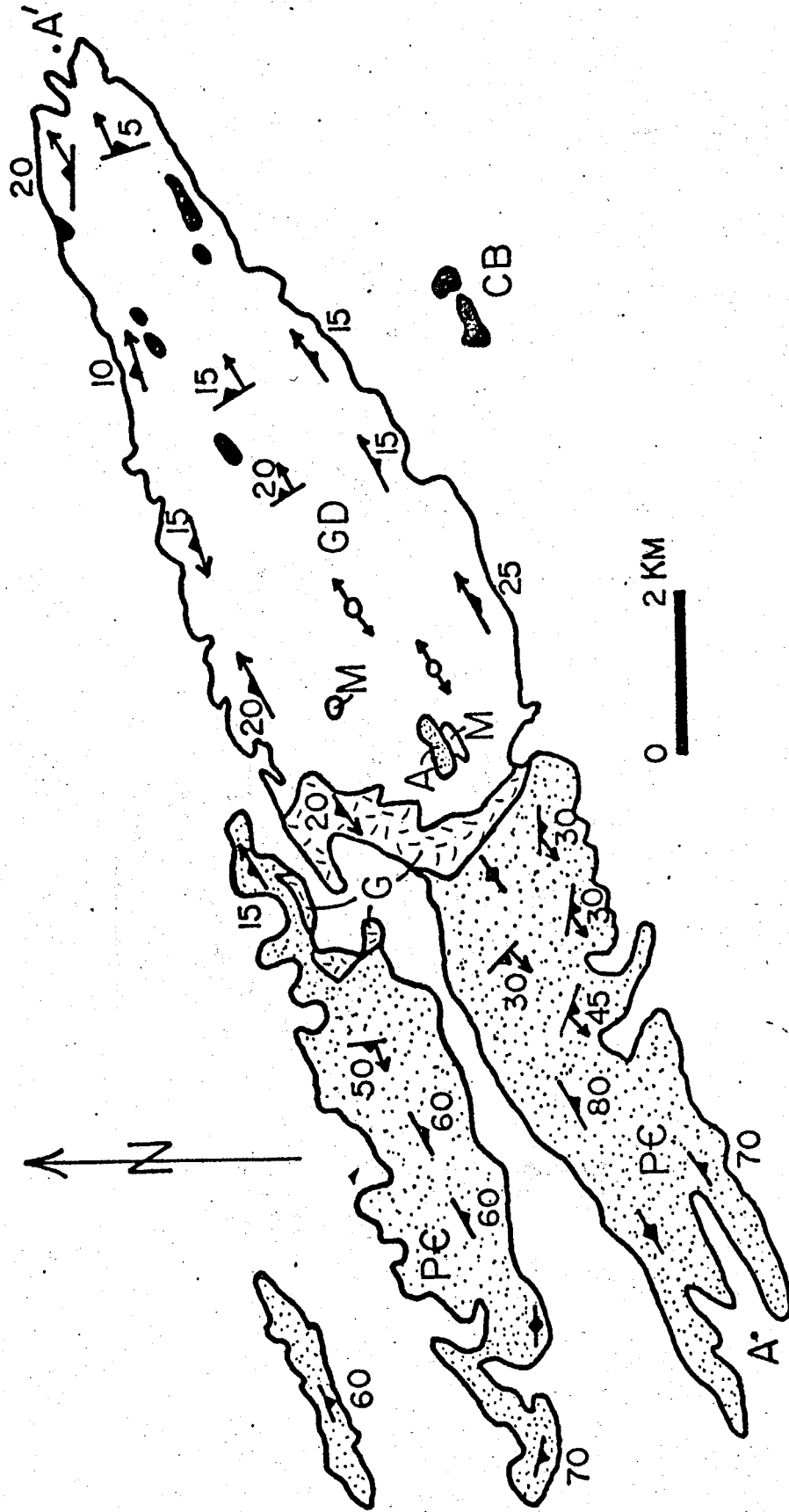


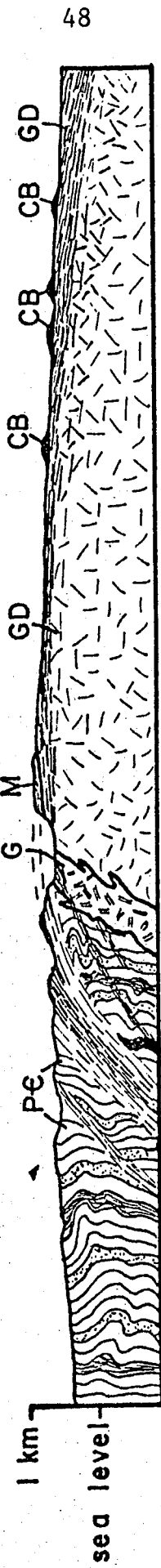
Figure 1. Generalized geologic map of the South Mountains, exclusive of the southern foothills. PG: Precambrian metamorphic and igneous rocks; GD: Oligocene granodiorite; G: Oligocene granodiorite; A: Oligocene alaskite; M: mylonitic rocks; CB: chloritic breccia.

S60W

N60E

A

A'



1 km

sea level

0 2 km

Figure 2. Cross-section of the South Mountains.

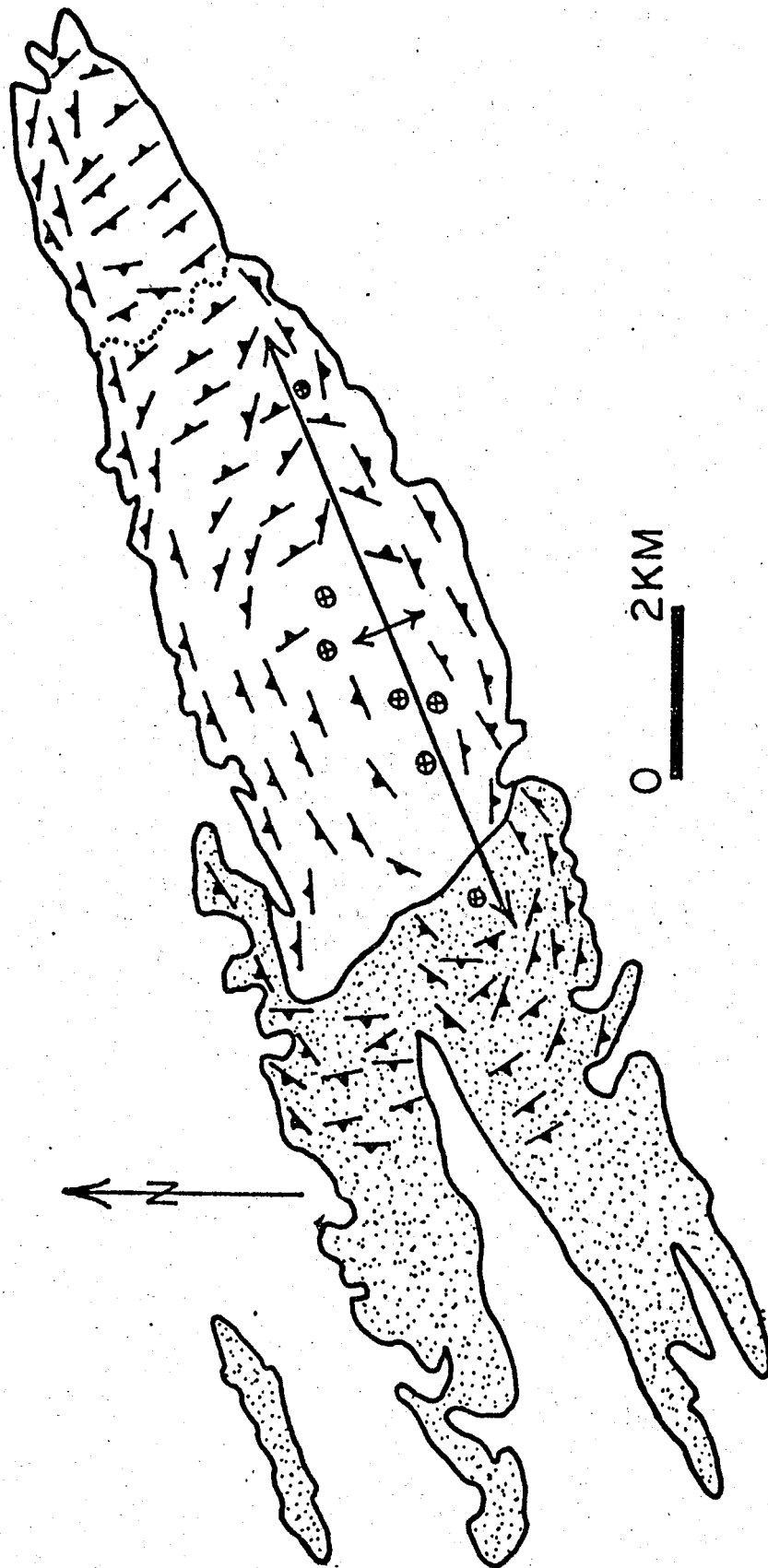


Figure 3. Orientation of mylonitic foliation where it is present in the South Mountains.

which mostly strike NNW, perpendicular to lineation. Inclusions in deformed plutonic rocks are elongated parallel to lineation and flattened perpendicular to foliation. Folds are rare in mylonitic plutonic rocks, but are more abundant in mylonitically deformed Precambrian amphibolite gneiss.

Gently dipping mylonitic foliation defines an asymmetrical northeast-trending, doubly-plunging arch or dome. The foliation generally dips less than  $20^{\circ}$  where it is contained within plutonic rocks, but is more steeply dipping where it affects Precambrian amphibolite gneiss. The simple pattern of the arch is interrupted on its northeast end where southwest-dipping foliation is present. This attitude of foliation is restricted to structurally high rocks which are chloritic, jointed, and brecciated.

Excellent exposures in the range display the three dimensional distribution of mylonitic fabric and variations in its intensity. Both the granite and granodiorite are undeformed in the core of the arch except for jointing and minor faulting. However, both plutons exhibit a gradual increase in intensity of mylonitic fabric toward the top and margins of the arch (up structural section). A similar distribution of mylonitic fabric is revealed where mylonitization affects Precambrian amphibolite gneiss. In the core of the range near the granite contact, the amphibolites possess a Precambrian foliation which is generally nonmylonitic, northeast-striking, and steeply dipping. The intensity of mylonitic deformation increases upward from the core to several 15 m-thick zones of northeast-lineated, mylonitic gneiss that cut equally thick zones of much less mylonitic amphibolite. Importantly, the mylonitic fabric also decreases in intensity upward from the main zones of mylonitic rock. At high structural levels in the western parts of the range, foliation in the amphibolite gneiss is again nonmylonitic, generally east- to northeast-striking, and steeply dipping.

NNW-striking dikes are likewise undeformed in the core of the arch. They are also generally undeformed where they intrude rocks with moderately well-developed mylonitic fabric. However, in structurally high parts of the range where adjacent rocks are intensely deformed, the dikes locally exhibit a gently inclined mylonitic foliation and ENE-trending lineation. Undeformed dikes are commonly near well-foliated dikes of similar lithology and strike.

Another important lithological and structural transition is exposed along the northeast end of the range where mylonitic granodiorite grades upward into chloritic breccia. Structurally lowest exposures of the granodiorite in this area are nonchloritic and well foliated. Up section, chlorite and anastomosing, curvi-planar joints are present in the granodiorite. The rocks are progressively more jointed and brecciated higher in the section where they ultimately grade into chloritic breccia. Remnants of mylonitic foliation in the granodiorite are preserved in the breccia. Relict mylonitic foliation in the breccia generally dips to the southwest, indicating that total disorientation

and random rotation of the foliation did not occur, except locally. Joints, breccia zones, and normal faults (northeast side down) have variable northwest strikes. Slicken sides in the breccia have scattered, but dominantly northeast trends. In the southern foothills of the range, the chloritic breccia is overlain by a dislocation surface which dips gently to the northeast. Upper plate rocks above the dislocation surface are Precambrian metamorphic rocks which locally have a mylonitic fabric.

### Geological Evolution:

Reynolds and Rehrig (1980) have discussed geological evolution of the South Mountains. Around 1.7 b.y. ago Precambrian sediments and volcanics were deposited and subsequently metamorphosed and deformed into a steep northeast-striking foliation. Granitic rocks in the westernmost parts of the range may be representatives of the 1.65 b.y. old suite of granites which are common in Arizona. There are no Paleozoic or Mesozoic rocks in the range. Around 25 m.y. ago, the Precambrian rocks were successively intruded by the granodiorite and granite. At this time, the plutons and the Precambrian metamorphics were subjected to deformation which formed a low-angle mylonitic foliation containing a northeast-trending lineation. NNW-striking dikes were intruded both during and after mylonitization. Strain indicators in the mylonitic rocks require that during mylonitization, the rocks were vertically flattened and extended parallel to the lineation. After mylonitization, the chloritic breccia was formed in the response to northeast movement of rocks above the dislocation surface. Normal, dip-slip movement is suggested by structures in the upper plate rocks and underlying chlorite breccia. Arching of the mylonitic foliation and chloritic breccia is probably one of the last events in the range. It was followed by the Basin and Range disturbance in which steep normal faults down-dropped the adjacent Phoenix basin around 14 to 8 m.y. ago. Since 8 m.y., the area has been tectonically quiet and geological developments have been dominated by erosion and deposition.

### Features in View From STOP 3:

The main features of the geology of the South Mountains to the north can be seen from this vantage point. The range has a broad arch-like profile with a prominent notch or saddle near the center of the range. West of the central notch are Precambrian metamorphic and igneous rocks. The rocks exhibit two distinct foliations: a northeast-striking, steeply dipping Precambrian foliation and a younger (middle-Tertiary) mylonitic foliation which dips moderately to the west.

The central notch is underlain by easily eroded, Oligocene granite. Along its western contact, the granite intrudes the Precambrian metamorphic rocks. Along its eastern contact, the granite grades into and locally intrudes an Oligocene granodiorite (25 m.y. old) which occupies most of the range east of the notch. The television and radio towers are built upon a subhorizontal tabular body of alaskite which overlies and intrudes the granodiorite. The pronounced gentle topographic profile

where the granodiorite has been brecciated in the northeastern end of the range. The topography of the range is controlled by an east-north-east-trending arch in the mylonitic foliation of all rock units.

The geology of the main range extends into the southern foothills which are composed of the same three major rock units (Precambrian metamorphics, Oligocene granodiorite, and Oligocene granite). The numerous man-made cuts in the southern foothills are part of an International Harvester proving grounds.

Turn around and head east on Maricopa Road for 0.5 miles. Return to the northbound lane of Interstate 10.

- 6.8
- 156 Road cut on west side of road exposes chloritic and brecciated Oligocene granodiorite.
- 1.0
- 157 EXIT 155 - Baseline Road. Exit and turn east (right) on Baseline Road.
- Begin  
Cumulative  
Mileage
- 0.2 56th St.--Turn right and proceed south through town of Guadalupe.  
56th Street becomes Avenida del Yaqui.
- 1.0
- 1.2 Calle Guadalupe--turn right and proceed west on road over Interstate.
- 0.8
- 2.0 Pavement ends--continue straight on main gravel road.
- 0.7
- 2.7 Parking area to right. Park and lock cars for short hike.

#### STOP 4

#### TRAVERSE THROUGH THE AHWATUCKEE CHLORITIC BRECCIA.

Walk approximately 0.4 miles up the road to the west and then slowly climb slopes of small ridge south of the road. In this slope is the upwards transition from nonchloritic, mylonitic, Oligocene granodiorite to Ahwatuckee chloritic breccia that was derived from the granodiorite. As one proceeds up the slope, the granodiorite becomes progressively more chloritic, brecciated and jointed. The cliffy exposures are composed of chloritic breccia. They are capped by a meter-thick ledge of microbreccia that was also derived from the granodiorite. The microbreccia weathers tan but exhibits a characteristically gray, flinty or resinous appearance on fresh surfaces. Although not preserved here, Precambrian metamorphic rocks overlie the microbreccia in low-angle fault contact in the southern foothills.

Structures within the Ahwatuckee chloritic breccia are upon first inspection, chaotic. However, hundreds of measurements of joints and

slickensides reveal the structures to be systematic. The predominant strike direction of joints is NNW and the modal trend of slickensides is ENE, perpendicular to the joints. Normal faults which dip gently to the northeast are locally present.

After inspecting the complete traverse, carefully return to the cars.

Turn around and proceed east on the gravel road upon which we entered the park.

- 1.3  
4.0 Avenida del Yaqui (56th St.), Turn left (north).
- 1.0  
5.0 Baseline Road--Turn left (west) and proceed west on Baseline Road.
- 0.2  
5.2 Underpass beneath Interstate 10.
- 0.8  
6.0 Note destruction of landscape of hills to the south by off-road vehicles.
- 2.0  
8.0 After 32nd St., note two hills on top of range at 10:00. They are composed of chloritic breccia. The rest of the rounded outcrops are Oligocene granodiorite which possesses a mylonitic foliation which dips gently to the north. The topography of this area mimics the north flank of a major foliation arch that parallels the range.
- 3.2  
11.2 Central Avenue--Turn left and proceed south on Central Avenue.
- 1.5  
12.7 Stay on Central Avenue, which curves to the right.
- 0.3  
13.0 Small hills to the right (north) are composed of Precambrian metamorphic and Oligocene granitic rocks.
- 0.5  
13.5 Park entrance--Granodiorite dikes have intruded Oligocene granodiorite to the right.
- 0.1  
13.6 Road junction after dip in road. Turn right toward Las Ramada picnic area.
- 0.4  
14.0 Lower ramadas--continue up road to west.
- 0.1  
14.1 Upper ramadas--park cars for lunch and an orientation talk.

#### STOP 5A

#### CONTACT BETWEEN LOMITAS GRANITE AND ESTRELLA GNEISS

After lunch and the talk, walk a short distance up trail west of the ramada. Exposed in this area is the contact between Oligocene Lomitas granite and Precambrian gneiss. The granite is medium-grained, light-colored and contains approximately 3 percent biotite (locally altered to sericite). In this hill, the granite is undeformed except

for some exposures near its contact with the Precambrian Estrella gneiss where the granite is mylonitic. A white, fine-grained aplitic phase is locally present along the contact. The Precambrian rocks are quartzo-feldspathic gneiss with some amphibolite and deformed porphyritic granite. The Precambrian rocks exhibit a steep, northeast-striking foliation which is cut by the younger mylonitic foliation. The mylonitic foliation dips gently to the north-northeast and contains a conspicuous east-northeast-trending lineation. This mylonitic fabric is also present within several Tertiary alaskitic dikes.

After inspecting the exposures, return to the cars. Proceed back to the road junction near park entrance.

- 0.5  
14.6 Road junction. Turn right towards Summit Lookout.
- 0.6  
15.2 Hill to left of road contains the contact between Precambrian metamorphic rocks and the Oligocene Lomas granite.
- 0.2  
15.4 Soap Box Derby track to left of road.
- 0.2  
15.6 Mile-post 1.
- 0.4  
16.0 Junction. Bear left towards Summit Lookout. Exposures along next mile are of Precambrian metamorphic rocks. Both the older (steep dipping) and younger (gently dipping) foliations are present. Ridge south of road is composed of Precambrian metamorphic rocks and Oligocene-Miocene dikes.
- 0.3  
16.3 Mylonitic, Oligocene-Miocene alaskite sill in Precambrian gneiss.
- 0.2  
16.5 Note steep foliation in Precambrian gneiss.
- 0.1  
16.6 Granite-Precambrian contact to right, small parking area to left, continue straight on road.
- 0.1  
16.7 Andesitic dikes have intruded into the Oligocene granite.
- 0.1  
16.8 North-northwest-striking fractures in granite contain limonite, sericite and very minor amounts of copper. Dark coloration to hill is due to a fairly recent grass fire.
- 0.5  
17.3 Switchback.
- 0.1  
17.4 Contact between Oligocene Lomas granite and South Mountains granodiorite.
- 0.3  
17.7 Microdioritic dikes in South Mountains granodiorite. Road curves to the left.
- 0.3  
18.0 Road junction. Turn left toward Holbert Lookout.
- 0.3  
18.3 Parking loop.

## STOP 5B

## CONTACT BETWEEN SOUTH MOUNTAINS GRANODIORITE AND LOMITAS GRANITE

Exposed in this area is the contact between Oligocene South Mountains granodiorite and Oligocene Lomitas granite. The contact here is mappable, but gradational. The granite is more leucocratic while the granodiorite has a higher percentage of biotite. Exposures of the gradational contact such as those present downstream (to the north) indicate that the granite and granodiorite are nearly contemporaneous and are phases of the same pluton. The contact between the two rocks is commonly gently to moderately inclined, with the granite on top. In some exposures, the granite clearly intrudes the granodiorite. Rb-Sr whole rock isochrons on both plutons indicate an emplacement age of approximately 25 m.y. ago.

Return to cars and proceed back to road junction.

- 0.3  
18.6 Road junction. Turn left. Road traverses through hills of foliated granodiorite. Radio and T.V. towers are built upon a subhorizontal, tabular exposure of alaskite. The alaskite is most likely a phase of the granite.
- 0.1  
18.7 Mile-post 4.
- 0.7  
19.4 Road Junction. Bear left to Dobbins Lookout.
- 0.3  
19.7 Parking area at Dobbins Lookout. Park and lock car.

## STOP 5C

## OVERVIEW OF THE SOUTH MOUNTAINS

The lookout provides a good view of the entire range. The lookout is built on a hill of mylonitically foliated alaskite sills that overlie mylonitic South Mountains granodiorite. Precambrian rocks are also locally present. Lineation in both rock types trends east-northeast. After examining both rock types and their contact relationships return to the cars.

- 0.3  
20.0 Road junction. Turn left toward Hidden Valley.
- 0.2  
20.2 Milepost 5. This area of the range is composed of a mylonitic South Mountains granodiorite and a swarm of north-northwest-trending dikes. The dikes are commonly mylonitic and exhibit the east-northeast lineation that characterizes mylonitic rocks throughout the range.
- 0.6  
20.8 Road junction. Turn right toward T.V. towers.
- 0.1  
20.9 Foliated dike north of road.
- 0.3  
21.2 Road cuts of alaskite injected into granodiorite. Both rock types are mylonitic.

21.4 0.2  
End of road: Park and lock car.

### STOP 5D

#### ROOF RELATIONS IN THE OLIGOCENE GRANITOID COMPLEX.

Exposed in this area are complex relationships between mylonitic Oligocene granodiorite, overlying Oligocene alaskite, and a small area of Precambrian metamorphic rocks that locally occurs as a subhorizontal pendant above the granodiorite and below the alaskite. All three rocks are extremely mylonitic. Exposures of all three rocks can be seen by walking west of the loop for approximately 0.3 miles. Be careful of the cliff that is formed by the granodiorite.

#### SUMMARY AND SOME SPECULATIONS ABOUT THE SOUTH MOUNTAINS CRYSTALLINE COMPLEX (from Reynolds and Rehrig, 1980).

##### Summary:

Some of the more important observations should be summarized before inferences and speculations can be discussed.

- (1) The complex is asymmetrical: gently dipping mylonitic granodiorite is overlain by chlorite breccia in the northeast half of the range, whereas no chlorite breccia is associated with moderately dipping mylonitic amphibolite gneiss on its southwest side.
- (2) Mylonitization in the amphibolite gneiss, plutons, and dikes increases in intensity upward from the nonmylonitic core of the arch.
- (3) Mylonitic fabric cuts a broad zone through the Precambrian amphibolite gneiss. Rocks above and below the zone are lithologically identical, and most retain their Precambrian structure.
- (4) Fabrics in all rock types indicate that mylonitization resulted from extension parallel to lineation and flattening perpendicular to foliation. Lineation contained within the foliation trends N60°E, orthogonal to dikes, joints, quartz veins, "ductile normal faults," and other extensional features in the mylonitic rocks. Dikes in particular are perpendicular to lineation, are essentially the same age as mylonitic deformation, and are almost totally confined to positions either within or below the zone of mylonitization. They presumably represent fillings of tensional features that formed as rocks extended parallel to lineation.
- (5) The chlorite breccia deforms and postdates the mylonitic fabric. Mylonitization took place under conditions of biotite stability. Mylonitization resulted in recrystallization and flow of quartz and formed a well-defined foliation and lineation. The deformation that formed the breccia occurred under chlorite-stable conditions

and was accompanied by very minor recrystallization of quartz. It destroyed the earlier mylonitic fabric and generally formed no foliation. The chlorite breccia is not present everywhere that mylonitic rocks are. The two clearly are drastically different in structural style and are at least partly different in relative age.

- (6) Mylonitization is of mid-Tertiary (late Oligocene to early Miocene) age and is exposed in a range characterized by abundant evidence of mid-Tertiary plutonism. Mylonitization is only slightly later in age than the plutonism and is not a protoclasic phenomenon from the fact that the mylonitic fabric is superimposed across cooling joints, dikes, aplites, and quartz veins which postdate solidification of the plutons.
- (7) Foliation in the Precambrian amphibolite gneiss was apparently little affected by Mesozoic and Laramide tectonics. It maintained its steep, northeast-striking orientation from its formation 1.7 b.y. ago until mid-Tertiary time, when the plutons were intruded discordantly across it.

#### Speculations:

Some speculations regarding origin of the complex can be made after considering the foregoing observations and inferences. The spatial and temporal association of mylonitization and the mid-Tertiary plutons implies a genetic relationship. However, because mylonitic fabric cuts through the amphibolite gneiss, the event is not strictly a case of "granite tectonics." Perhaps mylonitization was facilitated by heat that the pluton brought into upper levels of the crust. As the rocks were heated or while they were still hot, they extended parallel to the east-northeast-trending lineation and were flattened perpendicular to the subhorizontal foliation. This was possibly in response to the regional mid-Tertiary stress field of  $\sigma_1$  (maximum compression) vertical,  $\sigma_2$  north-northwest, and  $\sigma_3$  (minimum compression) east-northeast that was proposed by Rehrig and Heidrick (1976). Davis and others (1975) have documented similar orientations for strain and possible stress axes for mylonitic rocks in the Tortolita Mountains near Tucson, Arizona.

All evidence indicates that east-northeast-directed extension slightly predated, was synchronous with, and slightly postdated development of the mylonitic fabric. Hydrothermally altered and mineralized fractures in the mid-Tertiary plutons, when interpreted in the manner suggested by Rehrig and Heidrick (1972, 1976) indicate that  $\sigma_3$  was east-northeast during late magmatic to postmagmatic cooling and fracturing of the plutons. North-northwest-trending dikes the same age as mylonitization indicate east-northeast-west-southwest extension. Mid-Tertiary dikes outside the complex also trend north-northwest and thus indicate that this is a regional extension (Rehrig and Heidrick, 1976) and not one related to local strains accompanying mylonitization! Dikes that post-date mylonitization in the complex also strike north-northwest and imply that east-northeast-west-southwest extension existed after mylonitization. In addition, fabrics in the chloritic breccia imply that some form of northeast-southwest extension continued after mylonitization ceased.

It is important to emphasize that the mylonitization is not believed to be a part of classic Basin and Range deformation. Mylonitic rocks evidently occur both in the present-day ranges and the bottoms of the basins. Mylonitization clearly predates essentially all faulting within the past 14 m.y. which formed the present basins and ranges (Eberly and Stanley, 1978; Peirce, 1976; Shafiquallah and others, 1976). Therefore, mylonitization is believed to be a manifestation of a poorly understood Oligocene to early Miocene flattening and extensional event that took place along low-angle surfaces and zones. Mylonitic fabric of this type and orientation in southern Arizona is unrelated to Laramide thrusting, as has been hypothesized by some workers.

Exact temperatures of mylonitization are not known, but several observations provide some constraints. Temperature and fluid content must have been sufficient so that, for the strain rates involved, quartz and some biotite could recrystallize while plagioclase and most K-feldspar deformed brittlely. Silica must have been mobile because quartz veins are more abundant where the rock is mylonitic than in non-mylonitic rocks.

Confining pressure during deformation cannot have been excessive. Plutons slightly predating mylonitization are not deep-level stocks but are instead hydrothermally altered and fractured in a fashion suggestive of fairly low confining pressure. Dikes that are the same age as mylonitization are generally aphanitic; again this situation indicates fast cooling at shallow depths. These dikes and plutons appear to be the only satisfactory way to convey sufficient heat to these high crustal levels.

If the complex is analogous to similar complexes in southern and western Arizona, the chloritic breccia was formed in association with an overlying dislocation surface, above which would lie highly extended rocks as young as early to middle Miocene. In the South Mountains, slickensides, observed displacements of low-angle normal faults in the breccia, and antithetic rotation of mylonitic foliation in the granodiorite all indicate relative transport related to the chloritic breccia as being dominantly to the northeast. The chloritic breccia and overlying dislocation surface are well exposed in the southern foothills of the South Mountains. In this area, upper-plate rocks above the dislocation surface are faulted and brecciated amphibolite gneisses. Relict mylonitic foliation in the gneisses dips southwest and is cut by northeast-dipping normal faults. Additional possible upper-plate rocks are brecciated mid-Tertiary volcanic units, tilted and faulted mid-Tertiary sedimentary and volcanic units, and deformed Precambrian (?) granites locally exposed near Tempe (3 to 10 km northeast of the northeasternmost outcrops of mylonitic rocks in the South Mountains). The sedimentary and volcanic units dip moderately to the southwest; this is consistent with antithetic rotation that would have accompanied southwest-to-northeast transport along low-angle, listric normal faults.

Finally, I would like to emphasize that rocks with mylonitic fabrics nearly identical to those in the South Mountains compose large parts of

the metamorphic core complexes of Arizona (Davis, 1980; Rehrig and Reynolds, 1980). The majority of these ranges are depicted on the geologic map of Arizona gneiss, but several are shown as Tertiary-Cretaceous gneiss. However, studies on the South Mountains indicate that the mylonitic fabric in many of these ranges may largely be mid-Tertiary in age.

Return to the cars and exit the park the way we came in.

- 2.3  
23.7 Road junction. Turn left.  
0.8
- 24.5 Road junction. Turn left. Road to the right leads to Dobbins Lookout.  
0.8
- 25.3 Road junction. Bear left.  
2.4
- 27.7 Road junction. Bear right.  
1.4
- 29.1 Park entrance.  
2.3
- 31.4 Baseline Road intersection with Central Street. Continue straight on Central Street.  
1.0
- 32.4 Southern intersection with Central. Continue straight on Central Street.  
0.9
- 34.3 Central Street bridge over Salt River. During the Salt River floods of recent years, this and the Mill Street bridge were at times the only communication links between metropolitan Phoenix on either side of the Salt River. Traffic was literally backed up for hours during those times.  
0.5
- 34.8 Maricopa Street. Interstate 10 overpass is directly ahead. Proceed under bridge and take first left turn immediately after passing under bridge. Proceed west along frontage road.  
0.5
- 35.3 Stop sign.  
0.1
- 35.4 7th Street stoplight. Merge left onto Interstate 10 freeway onramp immediately after crossing 7th Street intersection.  
Return to Mile-  
post  
format.  
198 1.0  
Milepost 198  
0.8
- 198.8 Buckeye Road overpass.  
1.0
- 199.8 Van Buren Street overpass.  
2.0
- 201.8 Thomas Road exit. We are now on Interstate 17 northbound for Flagstaff.  
2.0
- 203.8 Camelback Road exit.  
0.2
- 204 Milepost 204  
0.5
- 204.5 Phoenix Mountains appear over houses at 3:00. The Phoenix Mountains are composed of older Precambrian aged schist, quartzite, slate and gneiss overlain unconformably by probably Miocene age, northeast tilted volcanics to the northwest.

- 205.6 Glendale Avenue exit.  
1.3
- 206.9 Northern Avenue overpass. After passing overpass notice well-developed steeply-dipping Precambrian age foliation in the Phoenix Mountains schists. Several small mercury deposits composed of cinnabar, metacinnabar, and quartz occur in pockets within quartz-sericite schist. These deposits were first noted in 1916 and have since had a production of less than 100 flasks of mercury (Bailey, 1968).  
2.1
- 209 Shaw Butte (2:30) is at the southern end of the Union Hills. North Mountain is at 3:00 with Lookout Mountain (3:30) is capped by probably Miocene-age volcanics.  
2.7
- 211.7 Bell Road exit.  
2.3
214. Hedgpeth Hills (9:30) and Deem Hills (11:30) are also composed of northwest-striking, northeast-dipping probably Miocene-age volcanics on strike with those at Lookout Mountain.  
1.0
- 215 Pyramid Peak at 10:30.  
1.0
- 216 Deer Valley Road overpass. Southeast end of Deem Hills are in near view (11:00).  
2.0
- 218 Happy Valley Road overpass. Union Hills (12:00 - 3:00) consist of Precambrian schist in the northern portions and Precambrian granite locally overlain by probably Miocene-age volcanics in the southern portions.  
2.0
- 220 New River Mountains on skyline at 1:00 are capped by thick flat lying basalts. Two of these basalt flows have K-Ar ages of 14.7 and 14.8 m.y. (Scarborough and Wilt, 1979). The flat lying basalt section unconformably overlies (locally discordantly) a sequence of basaltic flows, white tuffs, agglomerates, mudstones and some distinctive very bright red lithic tuffs. One of the tuffs yielded a 21.3 m.y. K-Ar age and was very near a Miocene oreodont fossil find (Gomez, 1978; Scarborough and Wilt, 1979). The Miocene volcanic and sedimentary sequence unconformably overlies older Precambrian schists metavolcanics and granitoid rocks.  
0.4
- 220.4 Interstate crosses aqueduct for Central Arizona Project (CAP) now under construction.  
0.6
- 221 Bradshaw Mountains dominate the skyline at 11:00-12:00 and are composed almost entirely of undivided pre 1.4 b.y. granitic rocks.  
2.6
- 223.6 Lake Pleasant-Carefree exit (Arizona State highway 74). Merge right onto offramp.  
0.4
- Turn left onto State highway 74 for Lake Pleasant and Wickenburg.  
0.1
- 30.8 Overpass over Interstate 17. Hieroglyphic Mountains on skyline at 12:00. Cuesta at 2:00 consists of a northeast tilted block of Miocene volcanics and sediments. The base of the cuesta contains poorly exposed sediments overlain in slight angular unconformity by a basaltic

ledge forming cap dated at 15.9 m.y. by the K-Ar methods (Scarborough and Wilt, 1979). The underlying predominantly clastic sediments contain a dolomitic unit that have anomalous radioactivity in cherty portions of the dolomite.

- 1.8  
29 Pyramid Peak at the northwest end of the Deem Hills is at 9:15.
- 4.3  
24.7 'T' Intersection and stop sign. Turn right and follow signs for Lake Pleasant where road curves left about 0.5 miles ahead.
- 1.7  
23 Road ahead drips off uppermost terrace surface (the one we have been traveling on for the last several miles) and descends onto lower terrace levels along the Agua Fria river.
- 0.7  
22.3 Stop sign. Turn left for Wickenburg.
- 0.3  
22 Lake Pleasant turnoff on right.
- 0.1  
21.2 Bridge over Agua Fria river. Roadcuts ahead are in generally flat-lying indurated conglomerates. To the west the conglomerate rests unconformably on probably Miocene age volcanics. To the north, on the west side of Lake Pleasant, the conglomerate rests in angular discordance on a tilted and folded sequence of tuffaceous sediments, minor fluvial fine-grained mudstones, locally interbedded with basaltic flows. One of the basaltic flows gave a K-Ar age of 16.6 m.y. (Scarborough and Wilt, 1979). The relationship of the dated sequence at Lake Pleasant to the volcanic rocks extensively exposed in the Hieroglyphic Mountains is unknown. The above relationships, however, suggest that the conglomerate exposed in the roadcuts on highway 74 represents older 'basin fill' in the sense of Scarborough and Peirce, 1978.
- 0.8  
20.4 Roadcuts here and for next mile are in probably Miocene age volcanics intercalated with conglomerates.
- 1.6  
18.8 Roadcut on left provides a good glimpse of structural and stratigraphic relationships within the Tertiary section. At the west end of the cut reworked waterlain sandy tuffs are intricately cut by small scale normal faults. The tuff sequence is overlain by a thin glassy ashflow and volcanoclastic rocks that are also cut by the normal faults. The entire sequence outlined above is juxtaposed against another section of waterlain tuffs by a southwest-dipping N50°W striking fault. These tuffs are also intricately laced with small-scale normal faults.
- At the east end of the cut the waterlain tuffs are overlain by a monolithologic andesitic breccia. The andesitic breccia appears to post-date the intricate normal faulting that cuts the underlying tuff because its base truncates the normal faults.
- Similar rocks and structural relationships are exposed in the next several roadcuts ahead.
- 0.8  
18 Saddleback Mountain composed of more mid-Tertiary volcanics is the most southerly and prominent of the prominent knobs south of the highway.
- 1.0  
17 You may have noticed several new appearing claim stacks along the road. These are part of the recent gold rush to the old Pikes Peak

district in the Heiroglyphic Mountains. In January 1980, Ranchers Mining Development Company announced a significant gold find in the Heiroglyphic Mountains with reported gold-rich intercepts in drill core that assayed as high as 3.46 oz./T. All of the excitement is currently centered on the Mystic claim group (N $\frac{1}{2}$ , SW $\frac{1}{4}$ , Sec. 12, T5N, R1W) about two miles south-southeast of Saddleback Mountain. The claims were originally located by Albert Harding, a retired Mining Engineer from Sun City who began prospecting in the area about 1973. Drilling financed by Mr. Harding has established an indicated 20,000 tons of ore averaging 0.7 oz. of gold per ton with slightly lower values of silver. The block is open on all sides and at depth (below 500 feet). Five foot drill sections assayed as high as 19.11 oz. of gold per ton (Harding report on file at Arizona Department of Mineral Resources in Phoenix). It is interesting that the present gold ore tonnage has been established entirely by drilling; there is no surface indication of high grade gold ore.

The mineralization appears to be localized along a fracture that cuts Precambrian schist. The fracture zone strikes N75°E, dips about 65 to 70° NW and is at least 1,200 feet long and three to five feet wide. A foliated andesite-like dike occupies much of the fracture. Apparently, very little to no quartz is present although calcite stringers and hematite are common. Ranchers now has several drill rigs operating at the property. The Mystic property is part of the old Pikes Peak district that to date has yielded a comparatively small amount of reported production (10,992 pounds of copper, 7,287 pounds of lead, 1,118 ounces of silver and 1,162 ounces of gold from 2,147 tons of ore). Obviously, the future of the district, is much more golden (sic).

1.4

15.6 Roadcuts on both sides of the road expose vertical to steeply southwest-dipping fragmental volcanics and volcanoclastics that have been deformed by several faults parallel to compositional layering.

0.5

15.1 Roadcut on right and most of the roadcuts in bedrock ahead are in Precambrian quartzitic schists that underlie the probably Miocene aged volcanic section in the eastern Heiroglyphics. In this area the volcanic section dies shallowly northeast. Foliation in the quartzitic schist here strikes N40°E and dips 65° SW.

3.1

12 A good view of the White Tanks Mountains, another presumed metamorphic core or crystalline complex, is seen at 9:00 to 9:30.

## GEOLOGY OF THE WHITE TANK CRYSTALLINE COMPLEX

by Stephen J. Reynolds

## Introduction:

The White Tank Mountains are an irregularly shaped range that is located west of Phoenix in central Arizona. The base of the range has an elevation near 1,500 feet above sea level while several of the highest peaks reach elevations of over 4,000 feet. The Tonopah Desert and ephemeral Hassayampa River valley bound the range on the west and the Gila River valley lies immediately to the south.

Geology of the range was mapped in reconnaissance fashion by Moore (in Wilson and others, 1957), but no written description of the range resulted from that study. Since that time, much of the range has been mapped in reconnaissance and detail by the author. Preliminary accounts of the geology of the range are contained in Rehrig and Reynolds (1980). The descriptions included below are from the ongoing research of Reynolds and others.

## General Geology:

The crystalline core of the White Tank Mountains is composed of Precambrian metamorphic rocks and a series of younger granitic rocks of Precambrian, Mesozoic, and Cenozoic age. The Precambrian metamorphic rocks consist of amphibolite-grade, quartzo-feldspathic gneiss and biotitic schist derived from sedimentary and igneous protoliths. They typically exhibit their original Precambrian foliation which strikes northeast and dips moderately to the southeast. In the southern foothills of the range, the metamorphics are intruded concordantly by a granodioritic to quartz dioritic pluton. The deformed granodiorite is probably Precambrian because it was evidently intruded during the Precambrian metamorphic-deformational event.

In the northeastern and western parts of the range, equigranular granodiorite, biotite granite, and muscovite-bearing slaskite, pegmatite and aplite intrude discordantly across the foliation of Precambrian rocks. These plutons are almost assuredly Cretaceous or Tertiary. These young plutons as well as their Precambrian host rocks have been subjected to an episode of mylonitization which has imported onto the rocks a gently to moderately inclined foliation which contains the familiar WSW- and WNW-trending dikes of microdiorite, granodiorite and more felsic lithologies. Intensely brecciated rocks similar to the chloritic breccia zone of other complexes are present on the northeast and southern extremities of the range, but no dislocation surface has yet been identified. Preliminary geochronologic data of Rehrig and Reynolds (1980 and unpublished) document Tertiary cooling in some parts of the complex.

## Geological History:

In the Precambrian, sedimentary and volcanic rocks were deposited, metamorphosed, and intruded by several generations of plutons. During the Paleozoic, the area was probably part of cratonic North America; thereby receiving a thin cover of sedimentary rocks. The Mesozoic

history of the region is uncertain, but some granodiorites in the range may be latest Mesozoic (Laramide). In the Tertiary, several types of granites were intruded and were subjected along with their wall rocks to an episode of mylonitization. Middle Tertiary (?) dikes in the range were intruded before, during and after mylonitization. Tertiary arching of the mylonitic foliation was followed by Basin and Range block faulting which resulted in the deposition of evaporitic and clastic rocks in the adjacent Phoenix Basin. The Gila and Hassayampa Rivers assisted in the sculpturing of the present landscape of the region.

## 2.0

- 10 Wickenburg Mountains (2:00) are underlain by Precambrian amphibolite-grade schists and metavolcanics extensively intruded by undated Precambrian granitoid rocks and pegmatites. Many of the pegmatites are complex nature and contain many mineral species, some 77 species have been documented (Jahns, 1952). Many of these occur in large enough amounts to warrant economic exploitation. Table 1 summarizes some of the production from the pegmatites and vein mineralization in the igneous and metamorphic rocks. The Precambrian crystalline rocks in the Wickenburg Mountains are unconformably overlain by another sequence of mid-Tertiary volcanic rocks. Studies of the volcanic sequence by Ward (1977) in the Castle Hot Springs area indicate the volcanics belong to an alkali-calcic magma series. Possibly, the volcanic series in the Heiroglyphic Mountains are age and geochemical equivalents.
- 2.0
- 8 Vulture Peak (11:55) the most distinctive landmark of the Vulture Mountains (11:30 - 12:00) is very close to Stop 6.
- 1.0
- 7 Arizona 74 is now crossing the highest geomorphic surface in the region. All major drainages (for example, the Agua Fria and Hassayampa rivers) have cut conspicuous incisions into this surface.
- 2.0
- 5 Big Horn Mountains at 10:30 consist of more mid-Tertiary volcanics resting unconformably on Precambrian amphibolite-grade gneisses and schists.
- 1.0
- 4 The Harquahala Mountains, object of Day 2, loom in the far distance to the left of Vulture Peak (11:30).
- 2.7
- 1.3 Junction with Castle Hot Springs road on right.
- 1.3
- 0 Termination of Arizona 74 at Junction with U. S. 60, U. S. 89, and Arizona 93. Turn right for Wickenburg. Road ahead traverses highly dissected topography cut into the high regional geomorphic surface we have been traveling on.
- 1.1
- 119 Vulture Mountains west of the Hassayampa River are now in good view from 9:00 to 12:00.
- 0.7
- 118.3 Roadcuts on both sides of the highway expose excellently the unconformable relationship between the veneer 'modern' alluviums and the underlying mid-Miocene age tuffaceous volcanics. Highway for next several miles will parallel the course of the Hassayampa River.
- 0.4
- 117.9 Roadcuts on left contain dramatic exposures of flow bonded rhyolites within the mid-Miocene volcanic series. We are now crossing a gravitational low

## MINERAL PRODUCTION FROM THE WHITE PICACHO DISTRICT\*

Commodity	Deposit	Quantity (tons)	Grade or Amount	Years
Feldspar	Picacho View Outpost Friction Midnight Owl	at least 2,000 tons	No. 1	1947-1952
Amblygonite	North Morning Star Midnight Owl	26 62	8.5 Li <sub>2</sub> O 7.4 Li <sub>2</sub> O	1947-1952
Spodumene	North Morning Star Lower Jumbo Midnight Owl	~20 55 none shipped	~5.0 Li <sub>2</sub> O 2.0-3.0 Li <sub>2</sub> O	1947-1952
Beryl	Midnight Owl	13	11-12 BeO	1947-1952
Bismutite	Outpost	12		1947-1952
Muscovite	Several deposits	~100		1947-1952
Columbite-tantalite	Midnight Owl	<1	not known	1947-1952
Scheelite	Scheelite Reef	6-7	37 lbs. of Conc. @ 62% WO <sub>3</sub>	
	Climax	11	1.1 WO <sub>3</sub>	1942
	Starlight (Buena Vista)	none shipped	0.3 WO <sub>3</sub> average <sup>3</sup>	
Copper	various	4,800	71,500 lbs.	1900-1979 reported production
Lead	various	4,800	343,000 lbs.	
Gold	various	4,800	610 ozs.	
Silver	various	4,800	41,000 ozs.	

\*Note: Pegmatite mineral production is from Jahns (1952); Scheelite data is from Dale (1961)  
Base and precious metal data is from BGMT file data.

in bedrock geology centered southeast of Wickenburg. Perhaps this low may reflect the presence of a caldera within the mid-Miocene volcanic field we are passing through.

- 0.9
- 119 Roadcuts on right for next several miles expose northeast tilted mid-Miocene rocks. The lower part of the sequence is an interbedded volcanic and clastic sedimentary section. Concordantly overlying this sequence is an indurated conglomerate section. Roadcuts for the next mile contain spectacular exposures of this conglomerate. The tilted volcanic sequence is angularly truncated by terrace gravel veneers related to earlier higher base levels of the Hassayampa River.
- 1.5
- 115.5 Bridge over Monarch Wash.
- 4.6
- 110.9 Tilted Tertiary volcanics cut by numerous low-angle faults are exposed in the roadcuts. The upper conglomerate section is juxtaposed against the older andesitic volcanics by a low-angle fault at the east end of the road cut on right. A K-Ar date near the top of the andesitic volcanics gave 16.5 m.y. (Scarborough and Wilt, 1979).
- 0.3
- 110.6 Bridge over Hassayampa River. Downtown Wickenburg is ahead.
- 0.3
- 110.3 Road Junction. U. S. 89 and Arizona 93 for Kingman on the right. Continue straight ahead on U. S. 60 for Salome.
- 0.1
- 110.2 Underpass.
- 1.2
- 109 Highway is crossing dissected alluviums on west side of Hassayampa River.
- 1.3
- 107.7 Vulture Mine Road intersection. Turn left onto Vulture Mine Road.
- Begin  
Cumulative  
Mileage
- 0.1
- 0.1 Mainly alluvial cover. To the southeast is the Vulture Mountain Guest Ranch, temporary home for many a Snow-bird. To the west, occupying the low ground and thinly mantled by alluvium, are rare exposures of the 68 m.y. Wickenburg batholith, which forms bedrock in this area and probably underlies the town of Wickenburg. A quarry several hundred feet west of road exposes unaltered granodiorite and evidence of weak copper mineralization.
- 1.6
- 1.6 Traversing poorly outcropping Wickenburg batholith cut by swarms of northerly-trending Miocene dikes of ultrapotassic rhyolite forming low, elongate hills. Higher hills straight ahead are Twin Peaks capped by 13-14 m.y. olivine basalt flows resting in marked angular discordance upon severely tilted 20-26 m.y. silicic tuffs and flows.
- 3.0
- 4.6 Here we cross the unexposed trace of the Vulture Peak listric fault, upon which lie the tilted volcanic sections of Vulture and Caballeros Peaks. The ridge immediately southwest of this mileage locality is composed of these volcanics which dip steeply eastward into the shallow, west-dipping Vulture Peak fault.
- 0.2
- 4.8 At low topographic pass, reddish colored ditch cuts expose conglomerate unit forming base of silicic, tuffaceous volcanic section.

From this point road proceeds south along trace of another NS-striking listric fault which places volcanics west of road against Laramide granodiorite east of road. To the east (left) the ridge exposes scattered outcrops of tilted red conglomerate (at base of ridge) and overlying volcanics.

0.8

- 5.6 To the left a short jeep trail leads to base of ridge east of Vulture mine road. Park vehicles along Vulture mine road and proceed eastward on foot.

## STOP 6

### GEOLOGY AND LISTRIC NORMAL FAULTING IN THE CENTRAL VULTURE MOUNTAINS

by William A. Rehrig

At stop 6 several key contacts are accessible: (1) partially covered by alluvial debris, a NE-trending intrusive contact between the Wickenburg batholith on the north and Precambrian (?) gneisses on the south; (2) At the base of the ridge, the Tertiary conglomerate unit unconformably overlaps both Laramide granodiorite and gneisses. Clasts in the conglomerate are mainly Precambrian (?) metamorphic rocks although granitic clasts of undetermined age are present; (3) The upper contact of the conglomerate is made with the overlying silicic volcanics, the lower units of which are well-stratified, thin, welded tuffs and/or base surge deposits. Volcanics farther up-section consist of more tuffs, a grey dacitic flow and, on the steep part of the west-facing ridge, a thick, massive obsidian flow which contains extensive devitrification and zeolitization. Potassium-argon dates of 26 m.y. (biotite) and 16 m.y. (whole rock) were analyzed from near the base of the volcanic section.

The section of volcanics and conglomerate dips up to 70° east toward the flat Vulture Peak normal fault. The lower part of the section with its unconformity and crystalline basement, is repeated just west of the Vulture mine road by another west-dipping listric fault.

Capping the ridge is a tectonic contact of special interest. A flat-lying listric fault and klippe of ultrapotassic rhyolite rest on the obsidian flow. Whole-rock K-Ar dates of 16 and 17 m.y. have come from the hanging wall rhyolite. The fault is beautifully exposed for detail study.

From the ridge top, a view northwest shows the faulted and tilted silicic volcanics overlain by relatively flat-lying basalt flows on Twin Peaks. Toward the south-southeast, the imposing Vulture Peak is seen with its tilted volcanic section rich in rhyolitic agglomerate and flows. This section dips 50-70° east. The Vulture Peak fault, along the eastern side of the peak is so flat that it outcrops on both east and west sides of the ridge, south of Vulture Peak.

GEOLOGY GEOCHRONOLOGY AND LISTRIC NORMAL  
 FAULTING OF THE VULTURE MOUNTAINS  
 MARICOPA COUNTY, ARIZONA

by William A. Rehrig,  
 Muhammad Sahafiqullah and Paul E. Damon

The Vulture Mountains, located near Wickenburg, about 50 miles northwest of Phoenix, consists principally of a faulted and tilted series of volcanic rocks surrounded and underlain by a plutonic and metamorphic basement. Intermittant geologic work during the past 10 years supported by chemical, isotopic and radiometric age analyses has led to a new appreciation of Miocene-Oligene volcanism and a fascinating period of extensional tectonism earlier and more profound than the traditional basin and range disturbance.

#### Regional Setting:

The Vulture Mountains are located in the Basin and Range Desert province within a north-northwest to northwest zone of severe normal faulting. Many of these faults are of the listric normal type. In the Vulture Mountains, tilting on these faults is toward the northeast. These rotations extend with progressively less effect to the northeast into the Bradshaw Mountains. This broad, northeast-tilted zone represents a major structural transition between the Mountain and Desert sub-provinces. Rotational normal faulting surrounds the Vulture Mountains on other sides as well. Taken collectively, the geometry and displacements of this fault system form an intriguing picture of northeast-directed crustal extension.

Two distinct volcanic sequences are found in the Vulture Mountains: an earlier silicious sequence of flows and tuffs and a later series of basalts. These same sequences crop out in surrounding mountain ranges across a broad, southwest-trending area from the Bradshaw Mountains to the Colorado River.

#### Rock Types:

Pre-Tertiary rocks in the Vulture Mountains consist of a Precambrian metamorphic-igneous basement intruded by a composite Laramide batholith. Tertiary rocks include hypabyssal intrusive and extrusive rocks (Figure 1).

Precambrian rock types exhibit a crude northeast-oriented outcrop pattern across the range (Figure 1). To the north (and between Vulture and Caballeros Peaks) a coarse-grained, porphyritic granite occurs which resembles 1400 or 1700 m.y. granites in adjacent areas. A 2-3 mile wide, northeast-striking zone of gneissic granite to granodiorite with minor amphibolite and pegmatite is found south of the porphyritic granite. Mafic schist lies south of the gneiss belt partly in fault contact with the gneiss (Figure 1).

A large, composite granodiorite pluton intrudes the core of the granitic gneiss belt. The pluton is dated at 68.4 m.y. It forms a highly elongate, dike-like mass extending well beyond the margins of the Vulture Quadrangle. The batholith is known as the Wickenburg batholith.

Postbatholith rocks include silicic and basic volcanic sequences--the former is tilted on listric faults. Above a reddish-colored basal conglomerate rest the silicic volcanics consisting of rhyolitic lava flows, welded tuffs and pyroclastic-volcaniclastic rocks interbedded with minor basaltic andesite to rhyodacitic lava flows. The basal volcanic unit is a buff to yellowish ash-flow which exhibits volcanoclastic and agglomeratic facies and commonly is intensely zeolitized. This unit is widespread in the Vulture Mountains and has been recognized (and dated) in the nearby Big Horn, Eagle Tail and Kofa Mountains. A biotite age of 26 m.y. and whole rock age of 16 m.y. has been established for this interval. The basal unit dates (biotite at about 23 m.y. in other ranges).

The silicic volcanic rocks display rapid, short-distance changes in thickness and character suggestive of nearby source areas. For example, the section on Vulture Peak consists largely of proximal vent facies of very coarse, tuffaceous, pumice-rich, agglomerate and thick rhyolite flows, whereas, the section near Highway 60 is rich in basaltic andesite flows and vitrophyres.

Chemically, the silicic volcanics are characterized by ultrapotassic rhyolite with  $\text{SiO}_2$ ,  $\text{Al}_2\text{O}_3$  and  $\text{K}_2\text{O} > 90\%$ . The  $\text{K}_2\text{O}$  content of these rocks is exceedingly high and for silicic samples averages 8.1 weight percent. Diagenetic or autoalteration potash metasomatism is suspected in part for the high  $\text{K}_2\text{O}$  contents. Some of the units are peralkaline with alkali- $\text{Al}_2\text{O}_3$  molecular ratios  $> 1$ . Some more basic flow rocks sandwiched between the rhyolites have  $< 60\% \text{SiO}_2$ , lower alkali contents and are basaltic andesites.

In contrast to the silicic sequence are the blocky basalt flows outcropping on Black Mountain and on Twin Peaks (Figure 1). Chemically this flow sequence is distinguished by relatively low-alkali content ( $\text{Na} > \text{K}$ ), high  $\text{CaO}$ ,  $\text{NaO}$  and low potash (~1%). Olivine occurs in the basalts. A K-Ar date of 13.5 m.y. was secured from a sample on Black Mountain.

#### Tectonic Considerations:

Certain geologic features in the Vulture Mountains exemplify important tectonic relationships in the southwestern U. S. These features are: (1) NE structural control of Laramide plutonism, (2) NNW control of mid-Tertiary plutonism, (3) listric normal faulting associated with mid-Tertiary silicic/potash-rich volcanic rocks, and (4) a fundamental change in tectonic style and volcanic petrology that took place between about 16 and 14 m.y. B.P.

Relationships (1) and (2) have been discussed by Rehrig and Heidrick (1976). In close association with the NNW aligned dike swarms of mid-Tertiary (~20-30 m.y. B.P.) age is the period of intense listric faulting which tilted shallow crustal rocks and extended them NE to E, in a direction approximately normal to the strike of the dike swarms. Silicic volcanics in the Vulture Mountains have been strongly affected by this style of deformation (Figure 1). The flat-lying Black Mountain and related basalts post-date the deformation, thus, bracketing the listric faulting event to the broad interval 26 to 13.5 m.y. Undeformed ultrapotassic rhyolite dikes intruding the flat listric faults and correlate with dated 16 m.y. dikes, further narrows the main extensional

faulting to the period from 26 to 16 m.y., or regionally from about 20 to 16 m.y. B.P.

From about 16 to 14 m.y. B.P. a fundamental tectonic change occurred which yielded the following results: (1) transition from low-angle to high-angle normal faulting (really a change from horizontal-to vertical-directed tectonics), (2) a major petrologic change from silicic, calc-alkaline volcanism ( $Sr^{87}/Sr^{86} \approx 0.708$ ) to more primitive basalt magmatism ( $Sr^{87}/Sr^{86} \approx 0.705$ ). These litho-tectonic changes show a similar timing regionally.

The regional setting of the Vulture Mountains on the northeast flank of a broad antiformal feature (Big Horn - Vulture Antiform) and presence of the adjacent Harcuvar Metamorphic Core Complex (see Figure 2) suggest a causal relationship between antiform (listric faulting) and core complex. The basic factor common to both is ductile or penetrative shallow crustal stretching below a relative thin, brittle, surficial layer (Figure 3). Stretching in the ductile layer (mylonite formation?) and listric fault extension in the brittle layer are colinear in an ENE-WSW direction.

During the 16 to 14 m.y. litho-tectonic transition, magmatism waned and changed from calc-alkaline to basaltic. Tectonics became vertically directed, faults penetrated deeper through a cooling and more rigid crust and allowed relatively uncontaminated sub-crustal melts access to the surface.

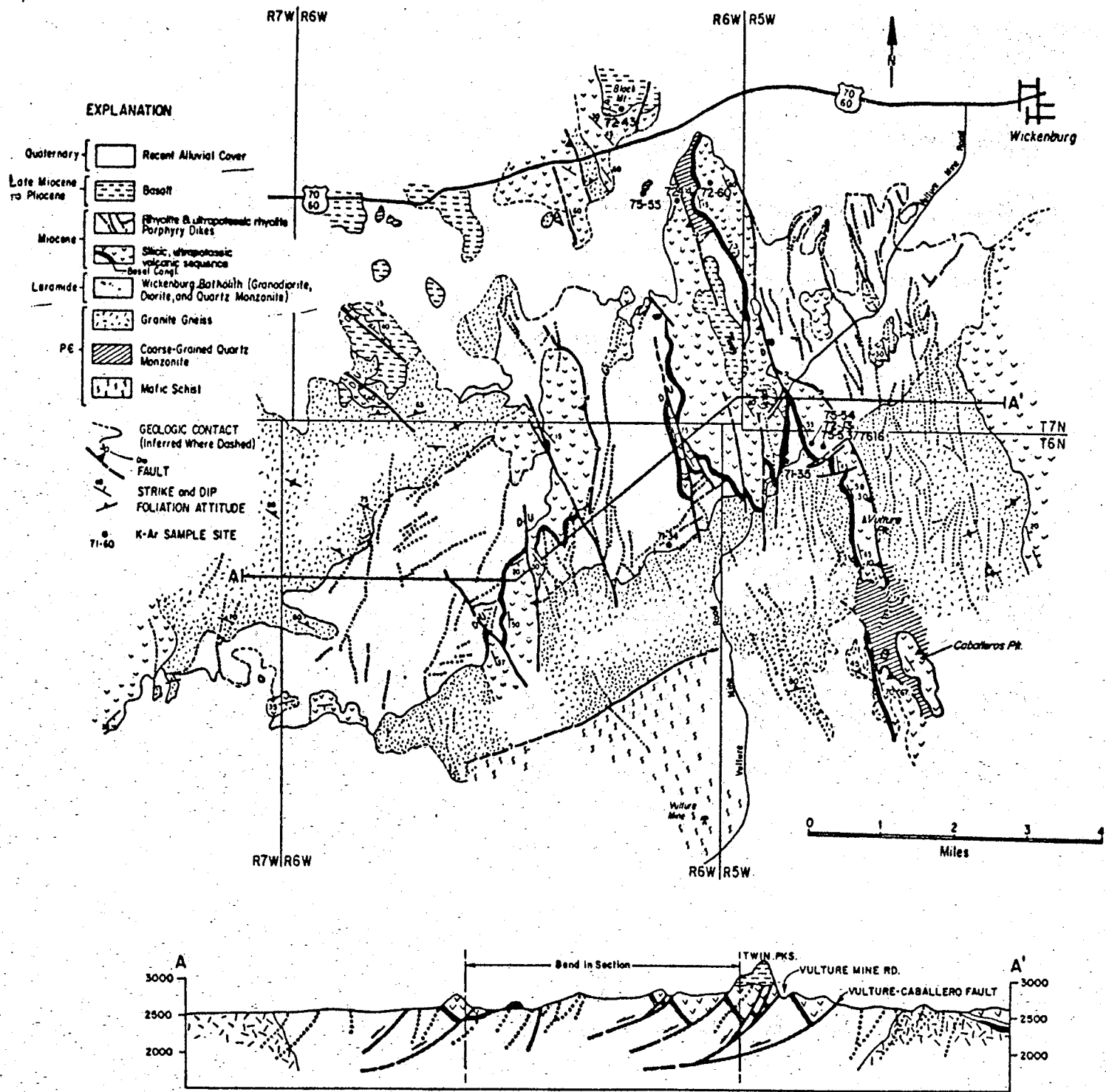


Fig. 1. Generalized geologic map and cross section of the Vulture Mountains. Note a crude northeast-oriented zonal pattern of Precambrian rocks. Mafic schists are common in the southern part. Silicic Tertiary rocks are intruded by a swarm of northerly trending dikes. Structural grain strikes north to northwest and is represented by dikes, normal faults, and tilted elongate fault wedges of silicic volcanic rocks. See explanation on facing page.

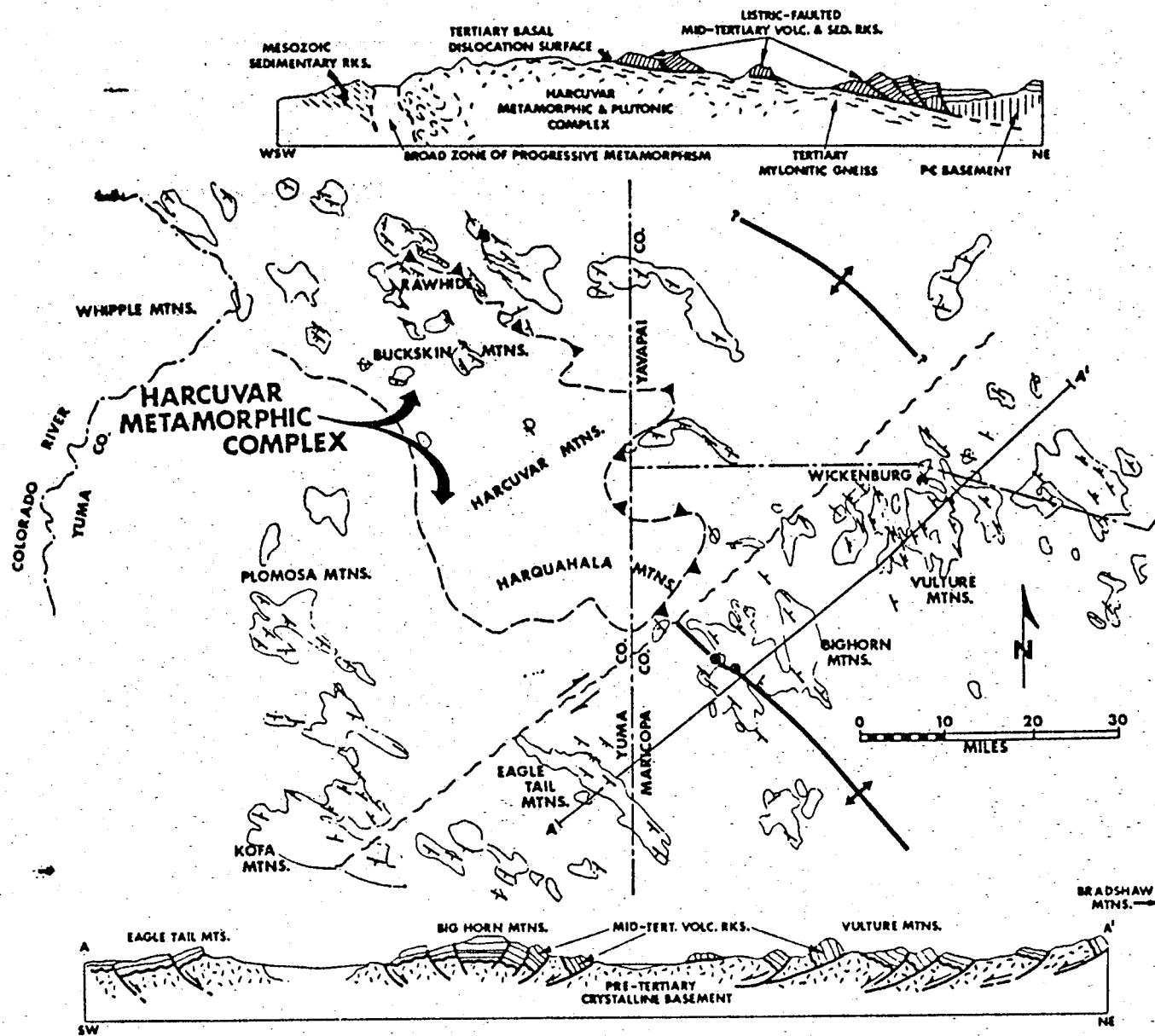


Fig. 2. Regional tectonic setting of the Vulture Mountains. Map shows outcropping areas of Oligocene-Miocene volcanic rocks (outlined areas) and their tilted attitudes. Double-bar dip symbols indicate dips  $> 45^\circ$ . Sources for structural data include: Arizona county geologic maps; unpublished tectonic map (Cooley and others, n.d.); Rehrig and Heidrick (1976, p. 218); and first author's more recent field observations. Information (map and section) on Harcuvar metamorphic complex is from Rehrig and Reynolds (n.d.). Barbs along eastern front of Harcuvar complex indicate general trace of northeast-dipping, Tertiary dislocation surface. Heavy-lined, anticlinal symbols indicate axial position of regional antiform (i.e., Big Horn-Vulture antiform) of Tertiary tilting. Wavy-lined, northeast-trending lineament may displace antiformal axis as shown (Stewart, n.d.). This transform(?) boundary possibly allowed differential northeast crustal expansion between the highly extended Harcuvar metamorphic complex (upper cross section) and the Big Horn-Vulture antiform (lower section).

Cross sections are highly schematic and not to scale. The Harcuvar section represents an idealized composite impression from the Granite Wash Mountains on the west through the Harcuvar Mountains.

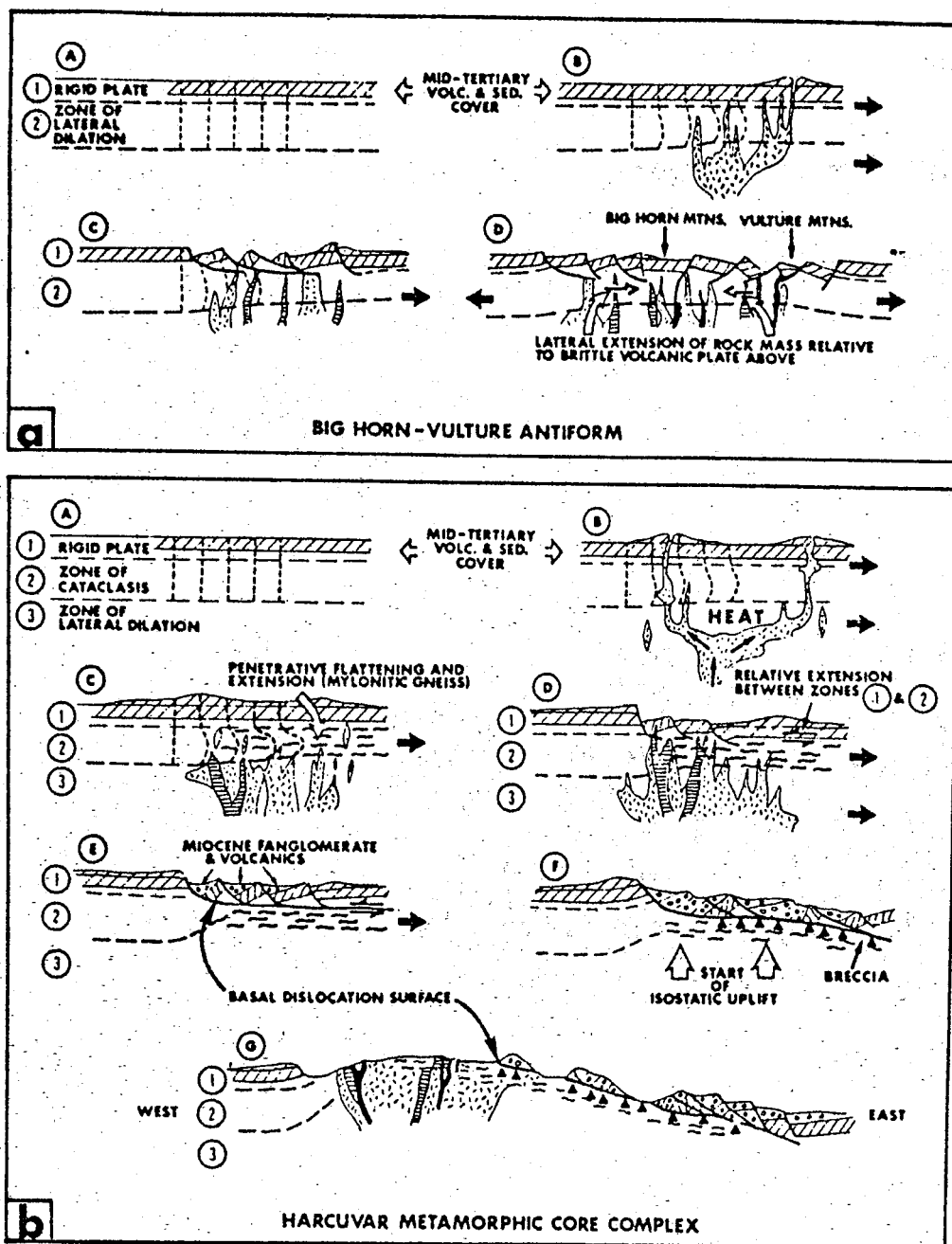
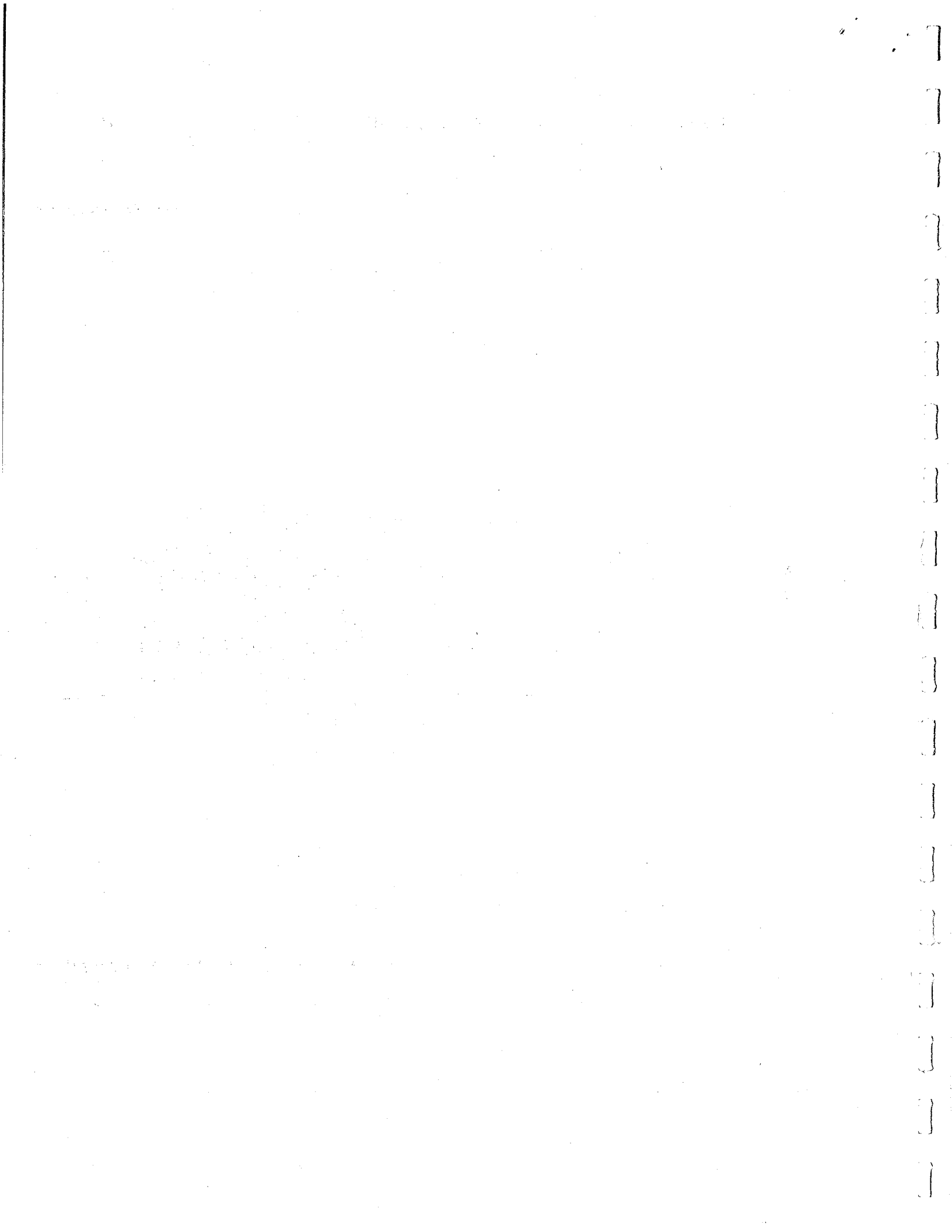


Fig. 3. Working hypothesis for development of listric faulting in the Big Horn-Vulture antiform (a) and Harcuvar metamorphic core complex (b). Large black arrows represent lateral extensional stress toward the northeast or southwest. Vertical dashed lines through plates 1 and 2 show extensional strain.

(a) Active lateral crustal extension combined with north-northwest-northwest-trending, mid-Tertiary dike swarms (B) allow zone 2 to expand past zone 1. This differential extensional strain is taken up by listric normal faults inclined in direction of greatest expansion below (C). Section (D) shows symmetrical bilateral development of stages (A) through (C) forming regional antiform.

(b) More intense intrusive activity (dikes, stocks, sills) and heat generation in active tensional stress field forms flattened and northeast-extended, mylonitic fabrics in subvolcanic, crystalline rocks (C). Continued stretching and dilation in zones 2 and 3 result in listric faulting and differential shear (dislocation surface) between ductile plate 2 and rigid plate 1 (D) (E). Severe thinning in plate 2 and tectonic removal of plate 1 initiate isostatic uplift (F) and lead to present configuration of metamorphic core complex (G). Figure 3b is based on text and figure 8 of Rehrig and Reynolds (n.d.).



## SECOND DAY

## ROAD LOG FROM WICKENBURG TO I-10-HOVATTER ROAD INTERSECTION VIA SALOME

Leaders: Stanley B. Keith, Stephen J. Reynolds and Stephen M. Richards

Sunday March 22, 1981

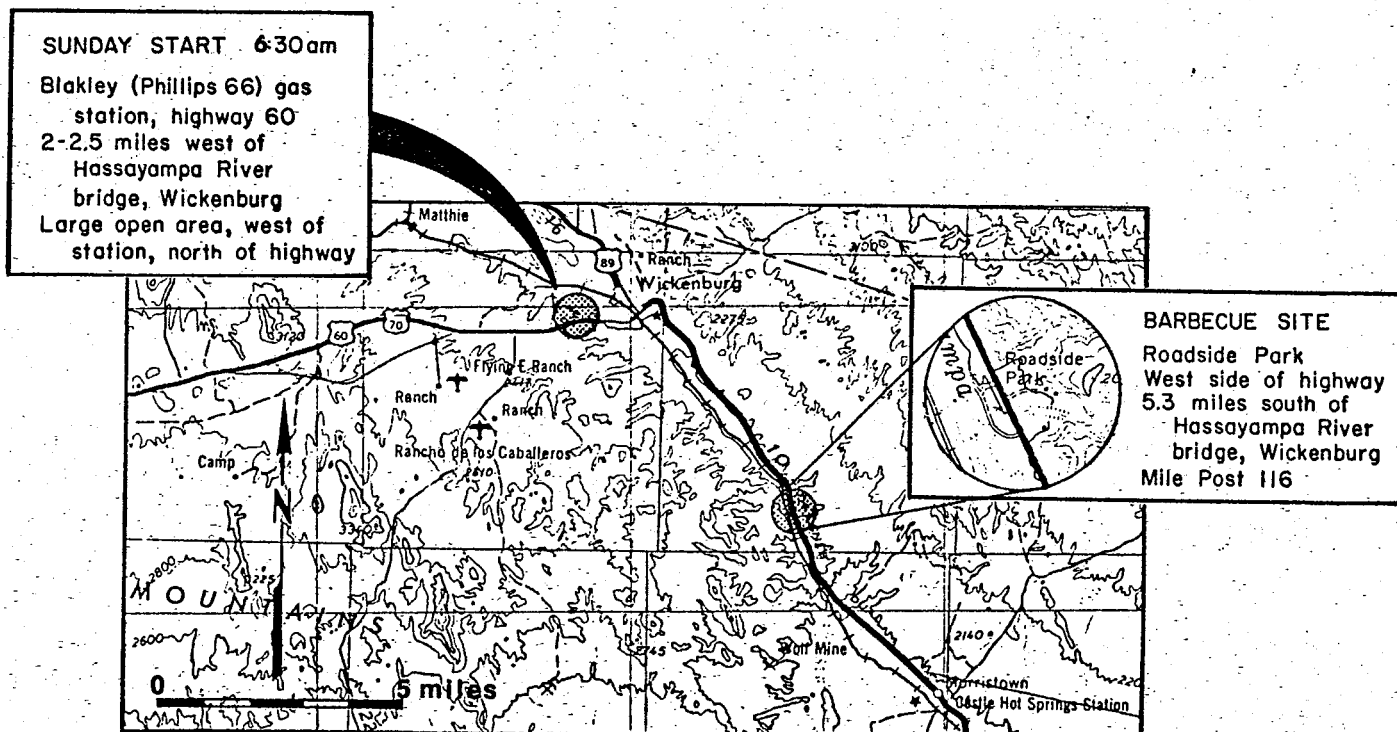
## Assembly

Point: Blakley (Phillips 66) gas station, U. S. highway 60, 2.2 miles west of Hassayampa River bridge, Wickenburg (in large open area, west of station on north side of highway).

Time: 6:30 a.m.

Stops: 4

Distance: Approximately 90 miles.



- 99 Middle Mountains are in middle distance at 2:00 to 3:00. The Weaver Mountains are in distance at 3:30. Inclined scar on south facing slope of Weaver Mountains is State High 71 to Prescott.  
0.5
- 98.5 Roadcuts on both sides of highway are in highly broken granite. Low hills to right are also underlain by the granite.  
0.3
- 98.2 Roadside rest on left.  
0.2
- 98 East end Harquahala Mountains now easily viewable to the left at 11:30.  
1.0
- 97 Black Butte in the west Vulture Mountains appear at 9:30. Black Mountain is capped by a dipping basalt dated at 15 m.y. (Scarborough and Wilt, 1979).  
1.0
- 96 Harcuvar Mountains pierce skyline at 12:00 to 1:30.  
3.0
- 93 East end of Harcuvar Mountains are at 1:30 and offer an excellent view of southwest-dipping volcanics that form well-developed hogback landforms. The volcanic pile is dominated by high potassium trachytes. One of these trachytes has been dated at 17 m.y. (Scarborough and Wilt, 1979).  
1.0
- 92 Small butes appear at 9:00 to 11:30.  
5.0
- 87 Eagle Eye Peak in probable mid-Miocene age volcanics appear at 10:00. Watch for the eagle eye which will become more obvious as you travel west. Eagle Eye Peak will be Day 2's first stop.  
1.0
- 86 Junction on right with Arizona State Highway 71 to Prescott, Arizona. Continue west on U. S. 60.  
1.0
- 85 Metropolis of Aguila ahead. Prepare to make left turn onto Eagle Eye Road in downtown Aguila.
- 84.4 Turn left onto Eagle Eye road.

Begin  
Cumulative  
Mileage

- 1.0 Eagle Roost suburban airport on left. Unnamed peak in eastern Harquahala Mountains is at 1:00. The eagle Eye is now at 11:45.

The unnamed peak (1:00) in the eastern Harquahala Mountains is probably underlain by equigranular banded leucocratic gneiss (ledge formers) interlayered with mafic, mesocratic, amphibolitic gneiss. These rocks are of probably Precambrian age. The foliation is generally non-mylonitic and no lineation was observed in exposures two miles east of the unnamed peak. The amphibolitic-grade rocks, on the unnamed peak and south facing slopes of the mountain, are separated from a mylonitically-foliated, biotite quartz monzonite by a zone of ultramylonite. This zone trends east-west and dips about 15 to 20° south. The ultramylonite zone is expressed as a slope former between the amphibolite-grade rocks and the underlying foliated biotite granite which forms rugged cliffs and bold outcrops below the ultramylonite zone.

Locally, a porphyritic mylonitic granite occurs between the amphibolite grade rocks and the biotite granite. All of the mylonitic rocks contain a pronounced N50 to 65E-trending lineation on foliation surfaces. The ultramylonite zone could be the eastern extension of the Harquahala Thrust, a regional thrust fault we have been mapping throughout the Harquahala Mountains. However, the northeast-trending lineation may be a younger lineation superimposed on thrust which normally contains a differently oriented, older fabric in the western Harquahala Mountains. We will see this fabric at the White Marble Mine later on (Stop 2).

- 3.1 Road to left. Continue straight.
- 3.5 Materials pit sign and road on left. Prepare to park for STOP 1 at Eagle Eye Peak.

### STOP 1

#### LOW-ANGLE TECTONIC PHENOMENA AT EAGLE EYE PEAK

Eagle Eye Peak contains the best exposures of the low-angle fault between the mylonitic basement of the Harquahala Mountains and an upper plate of tilted Tertiary sedimentary and volcanic rocks. A majority of mylonitic rocks in this area have been derived from a granitic protolith. Foliation is gently dipping and defines a broad N60E-trending arch. Eagle Eye Peak is slightly southeast of the axis of the arch. Dioritic rocks are exposed in the footwall of the fault where they are highly brecciated. The low-angle fault dips gently to the east and is immediately underlain by a chloritic breccia. Tertiary rocks above the fault include reddish sandstone-siltstone, conglomerate, sedimentary and volcanic breccia and volcanic units. The Tertiary rocks dip to the southwest.

#### GEOLOGIC OVERVIEW OF THE HARQUAHALA, HARCUVAR, BUCKSKIN AND RAWHIDE MOUNTAINS, WEST CENTRAL ARIZONA

by Stephen J. Reynolds

#### Introduction:

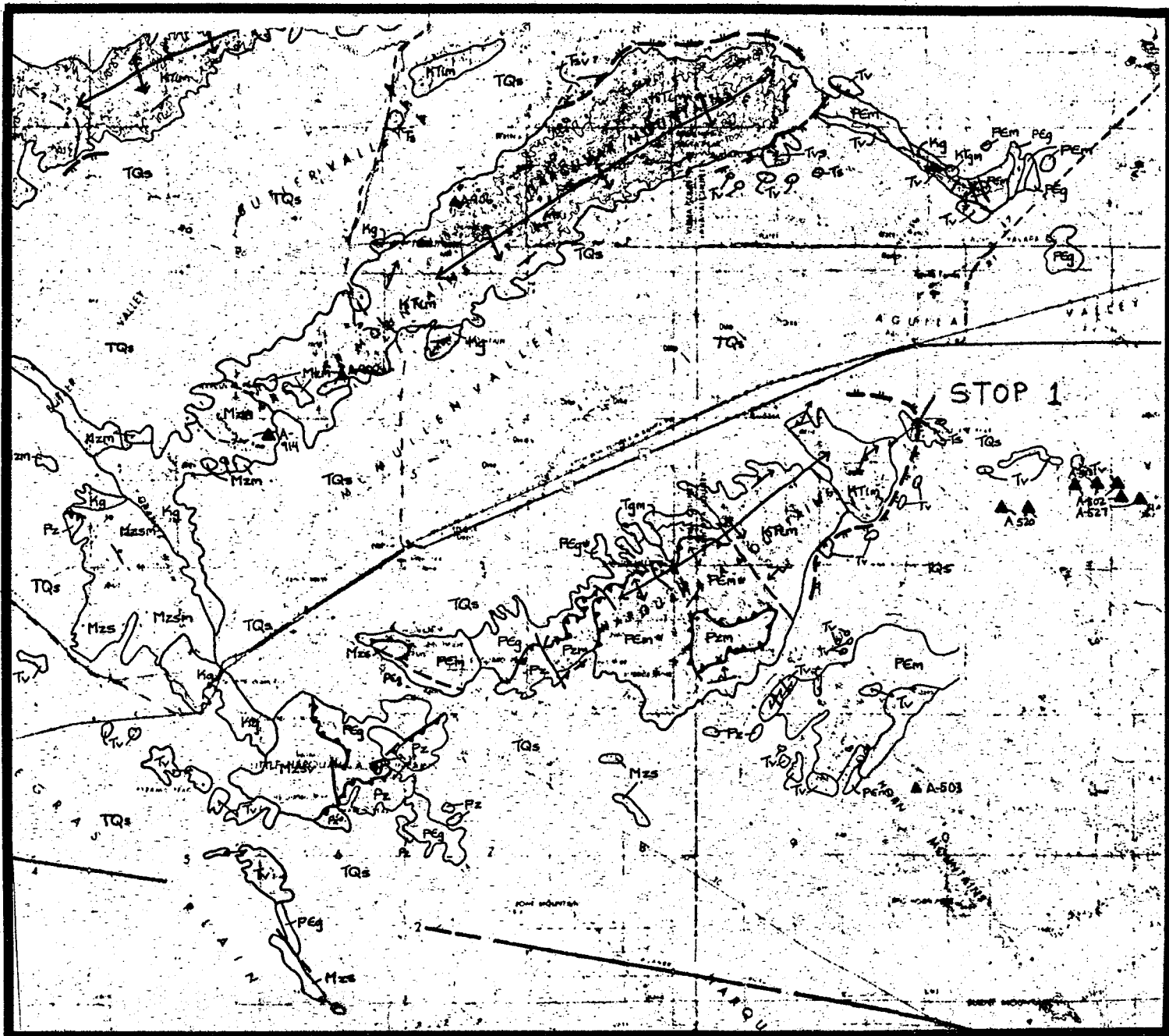
A northwest-trending zone of metamorphic core complexes in west-central Arizona is composed of (from southeast to northwest) the Harquahala, Harcuvar, Buckskin and Rawhide Mountains. These four ranges have a pronounced northeast trend or physiographic grain, in contrast to the north or northwest trends of most mountain ranges in western Arizona. The Harcuvar and Harquahala Mountains are especially prominent in the region because they are relatively high (elevations above sea level of over 5,000 feet compared to valley elevations of 2,000 feet), northeast-trending ranges. The large northeast-trending McMullen and Butler Valley bound the Harcuvar Mountains on the south and north sides, respectively. The Buckskin and Rawhide Mountains lie to the northwest and are parts of a single relatively low relief mountain range. They are separated by the Bill Williams River (the Rawhide Mountains are situated on the north side of the river).

Early geologic works in the area were of a reconnaissance nature or were concerned with the detailed geology of small mining areas (see

## MAP UNITS:

- TQs Late Tertiary-Quaternary surficial deposits
- Tb Late Tertiary basalt with interbedded sediments
- Tc Late Tertiary clastic rocks
- Ts Middle Tertiary sedimentary rocks
- Tv Tertiary volcanic rocks
- Tsv Tertiary sedimentary and volcanic rocks
- Tgm Tertiary muscovite-bearing granite
- KTim Cretaceous-Tertiary igneous and metamorphic rocks
- Kg Cretaceous granitic rocks
- Mzs Mesozoic sedimentary rocks (Mzsm where metamorphosed)
- Mzsv Mesozoic sedimentary and volcanic rocks
- Mzg Mesozoic granitic rocks
- Pz Paleozoic sedimentary rocks (Pzm where metamorphosed)
- PEg Precambrian granitic rocks (PEg\* where mylonitic)
- PEm Precambrian metamorphic rocks (PEm\* where mylonitic).
- PEu Precambrian metamorphic and granitic rocks undifferentiated

Figure 1. Generalized geologic map of the Harquahala and Harcuvar Mountains (from Reynolds and others, 1980a).



## SYMBOLS:

 Contact, dashed where approximately located

 Fault, dashed where approximately located

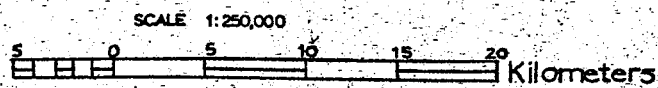
 Low-angle normal fault

 Low-angle thrust fault

 Dislocation surface

 tie leader

 Uranium occurrences



references cited by Stanton B. Keith, (1978) and Reynolds, (1980). Lasky and Webber (1947) mapped the geology of the Artillery Mountains (located immediately east of the Rawhide Mountains) and described two important Tertiary sedimentary units: the Artillery and Chapin Wash Formations. Wilson (1960; see also Wilson and Moore, 1959; Wilson and others, 1969) mapped the reconnaissance geology of the entire west-central Arizona region. Shackelford (1976, 1977, 1980) and Gassaway (1972) describe the geology of the Rawhide and Buckskin Mountains, respectively. Rehrig and Reynolds (1977, 1980) discuss results of their reconnaissance geologic and geochronologic studies of the region. They recognize that the Harquahala, Harcuvar, Buckskin and Rawhide Mountains are metamorphic core complexes. Davis and others (1977, 1979, 1980) integrated the geology of the Rawhide and Buckskin Mountains with that of adjacent areas. Suneson and Lucchitta (1979) determined the ages of volcanic units and tilting in rocks north of the Bill Williams River. Reynolds (1980) synthesized results of unpublished detailed and reconnaissance geologic mapping with that of previous workers, and presented a summary of the geologic framework of west-central Arizona. Reynolds and others (1980) documented major Laramide thrust faults in the Harquahala Mountains, adjacent to an area mapped by Varga (1976, 1977). Geologic research and mineral exploration in the area are continuing at an accelerated pace.

#### General Geology: (Refer to figure 1)

The Harquahala, Harcuvar, Buckskin and Rawhide Mountains have essentially all the characteristics that typify Cordilleran metamorphic core complexes. All four ranges are composed of a basement terrane of quartzo-feldspathic gneiss and micaceous schist interlayered with amphibolite, underformed to well-foliated granitic rocks, and local marble and quartzite. Foliation in the metamorphic rocks is gently dipping and defines large northeast-trending arches which parallel and control the topographic axis of each range. Field and isotopic studies define a major Late Cretaceous to early Tertiary metamorphic event which is probably spatially and temporally associated with plutons of the same age. The metamorphic rocks are most likely derived from Precambrian protoliths, although Paleozoic and Mesozoic sedimentary rocks are also locally incorporated into the basement terrane. Granitic rocks that are interlayered with the metamorphic rocks have Precambrian, Mesozoic and Cenozoic ages.

The metamorphic fabric and associated granites are overprinted by a gently inclined mylonitic foliation that contains a conspicuous northeast-to east-trending lineation. Mylonitic fabric is best developed in structurally high exposures and conforms to the arch defined by the non-mylonitic, metamorphic foliation. The mylonitic fabric is probably early to middle Tertiary in age because it clearly postdates Late Cretaceous - early Tertiary plutons and metamorphic fabric. In addition, mylonitic rocks in the ranges have so far yielded early and middle Tertiary K-Ar biotite and hornblende ages.

The metamorphic - plutonic basement of the Harquahala Mountains has additional structural complexities that have not been described for the other three ranges. For example, much of the range is composed of foliated, porphyritic Precambrian granite which is successively overlain by thrust slices of inverted Paleozoic rocks and Precambrian metamorphic

and granitic rocks (Reynolds and others, 1980). A mylonitic zone associated with one of the thrusts is disconcordantly intruded by early Tertiary muscovite-bearing pegmatites. Elsewhere, these pegmatites exhibit a younger mylonitic foliation that contains the familiar east-northeast-trending lineation. It is uncertain whether basement terranes of the other three ranges were also subjected to such complex structural histories.

In all four ranges, structurally high exposures of mylonitic rocks have been brecciated, jointed, faulted and affected by retrograde metamorphism or hydrothermal alteration which has formed chlorite, hematite, epidote, sulfides and copper minerals. This assemblage of rocks and minerals is best termed a chloritic breccia. The chloritic breccia is overlain by a thin (approximately one meter thick) ledge of microbreccia. A dislocation surface is well exposed above the microbreccia throughout much of the Rawhide and Buckskin Mountains and in more isolated exposures along the northeastern ends of the Harcuvar and Harquahala Mountains. The most common allochthonous rocks above the dislocation surface are Oligocene (?) - Miocene conglomerate, sandstone, siltstone and volcanic rocks. However, Precambrian metamorphic and granitic rocks, Paleozoic carbonate and clastic rocks, and Mesozoic igneous and sedimentary rocks are also locally exposed in upper plate positions. Upper plate rocks dip, on the average, moderately to the southwest and are cut by northwest-striking listric-normal faults. Relative tectonic transport of upper plate rocks is mostly to the northeast and is as young as 15 m.y. (Davis and others, 1980; Rehrig and Reynolds, 1980).

#### Geological Evolution:

In the Precambrian, west-central Arizona was the site of tectonic unrest, crustal construction and stabilization via a series of depositional, metamorphic and plutonic episodes. Deposition of clastic and volcanic rocks was closely followed by metamorphism, deformation, and plutonism around 1.6 to 1.7 b.y. Besides possible emplacement of diabasic intrusions in late Precambrian time, the next younger rocks in west-central Arizona are Paleozoic. Equivalents of younger Precambrian Apache Group rocks are evidently absent from the area. Paleozoic rocks are a relatively thin sequence of carbonate and clastic rocks that represent a cratonic platform environment.

After the Paleozoic interval of relative tectonic quiescence, the area experienced major mid-Mesozoic volcanism, plutonism and tectonism. The mid-Mesozoic plutons and volcanic rocks are parts of a subduction-related (?), northwest-trending magmatic arc. After the mid-Mesozoic arc swept or jumped westward, thick sequences of clastic rocks were deposited unconformably on the volcanic rocks. Clastic sedimentation was followed by plutonism and metamorphism in the Late Cretaceous and Early Tertiary as magmatism swept eastward across Arizona. Metamorphism was, in part, synchronous with plutonism, and formed high-grade gneissic and migmatitic terranes that are exposed in the metamorphic core complexes. This was successively followed by northward-vergent Laramide thrusting and intrusion of early Tertiary muscovite-bearing granites. Mylonitization in the core complexes postdates these events and is early or middle Tertiary in age.

A period of widespread early Tertiary erosion was followed by Deposition of middle Tertiary conglomerates, sandstone, siltstone, lacustrine units and volcanic rocks. Plutonism and extensive thermal disturbances accompanied the volcanism. Middle Tertiary rocks were tilted and rotated during dislocation and listric-normal faulting. Final cooling in the core complexes occurred at this time. Block-faulting formed the present-day basins and ranges between 14 and 5 m.y. Variably sized clastics were shed into the downdropped basins; evaporites were deposited in some closed basin. The region was moderately tectonically stable when the Pliocene Bouse Formation was deposited in a partly marine embayment accompanying development of the Gulf of California. Basins that had earlier been characterized by internal drainage became interconnected as part of the integrated Colorado-Gila River system.

Return to  
Mile Post  
Format

Leave Eagle Eye Peak Stop. Return to Aguila and Turn west (left) onto U. S. 60

2.3

- 82 Smith Peak at 2:34 is the highest point (el. 5,242') in the Harcuvar Mountains. At Smith Peak, amphibolite grade (Precambrian?) gneisses have been intruded by shallowly-inclined sheets of biotite granite which resembles the Tank Pass pluton at the west end of the Harcuvars. The biotite granite contains a penetrative mylonitic lineation that trends N60E - S60W.

2.0

- 80 Bullard Peak at low 3:00 backed by main mass of eastern Harcuvar Mountains. Dark rocks at Bullard Peak are 15 m.y. southwest to south-southwest dipping volcanics. The volcanics are intercalated with coarse conglomerates and megabreccias. One of the common clast in these megabreccias are pebble through boulder-sized class of volcanic-derived arkoses and graywackes that strongly resembles the Livingston Hills assemblage of Mid-Mesozoic age in the Plomosa Mountains. The closest exposure of these rocks to Bullard Peak is in the western Granite Wash Mountains 25 miles west-wouthwest of Bullard Peak. Also, no mylonitic clasts have been recognized in the Miocene conglomerates. The entire Bullard Peak sequence has been tilted southwest and rests as an allochton on a low-angle normal fault that strongly resembles the Buckskin dislocation surface summarized by Rehrig and Reynolds (1980) and Shakelford (1980). The map trace of the low-angle fault in the eastern Harcuvar Mountains suggests it has been deformed by the ENE trending fold that follows the crest of the Harcuvar Mountains.

1.0

- 79 Pioneer Mountain at 9:00. Pioneer Mountain is entirely underlain by a biotite granite which strongly resembles the Tank Pass granite in the western Harcuvar Mountains. The granite carries mylonitic foliation that strikes NW, dips NE, and contains a lineation that trends N60E.

1.2

- 77.8 Dirt road on left provides access to Dushey Canyon area at 9:00.

1.6

- 76.2 Berg of Gladden.

1.0

- 75.2 Medusa-like multiple-armed saguaro on left.

0.7

- 74.5 Yuma County Line.

2.5

- 72 Main physiographic features of the Harquahala Mountains are now in good view to the left. Harquahala Mountain caps the high cliffs at 9:00

and is the highest point in the Harquahala Mountains (el. 5,681'). Sunset Canyon and Pass are at 8:00 and provide the best example of a very common physiographic form within the Harquahala Mountains. As at Dushey Canyon, Sunset Canyon trends northwest (the Canyon displays a very sharp northwest-trending linear on aerial imagery of various kinds and scales). Also, as at Dushey Canyon, Sunset Pass is connected to a shallowly-inclined, east-sloping ridgeline to the west and steeply inclined west-sloping ridgeline to the east. This physiography is a clue to a major, northwest-striking, northeast-dipping fault zone that strikes through Sunset Pass and closely follows the stream bed in Sunset Canyon. This structure is only one of the better examples of a group of northwest-striking northeast-dipping group of faults spaced at 1 to 3 km intervals throughout the length of the Harquahala Mountains. Our mapping in the western Harquahala Mountains has disclosed that these faults offset the low-angle thrusts we will examine on this trip. Indeed, the thrust stratigraphy provides a datum to evaluate offset on these faults. Our mapping in the western Harquahala Mountains reveals that these faults have consistent, northeast dips and reverse and right lateral separation. The faults contain common, shallowly-inclined slickensides and less common dip-slip slickensides. A reverse slip and right slip movement history that post-dates thrusting seems to be required for these faults. It is interesting that the Sunset Canyon structure is virtually on strike with the Lincoln Ranch fault, a major northwest-trending fault with post-mid-Miocene reverse movement, in the Rawhide and Buckskin Mountains. The Lincoln Ranch fault offsets the Rawhide-Buckskin dislocation surface which itself has experienced a major 18 to 15 m.y. low-angle normal movement. If the northwest-striking structures in the Harquahala Mountains are correlative with the Lincoln Ranch fault and its kindred, then the entire Rawhide to Harquahala region has experienced post-mid-Miocene reverse faulting.

1.0

71 Harquahala Mountain massif now dominates the view to the left. The trace of the Harquahala thrust occurs near the top of the prominent cliffs. The country above the cliffs is one of low topographic relief and is underlain by amphibolitic grade metavolcanics and metasediments of probable Precambrian age within the Harquahala plate. The Harquahala thrust, the principal thrust within the main mass of the Harquahala Mountains, is structurally the highest fault of the regional thrust fault network (refer to Stop 2 discussion and for a summary of the regional thrust network). The bold cliffs below Harquahala Mountain are mostly underlain by mylonitically-deformed porphyritic Precambrian granite. In the lower slopes this granite is intruded by numerous dikes and masses of garnet-bearing muscovite granite and pegmatites (the light-colored outcroppings in the lower slopes of the mountain). Some of the muscovite pegmatites extend upwards and intrude through the Harquahala thrust into the overlying Harquahala plate. Thus, the muscovite-bearing pegmatites and granite post-date thrusting. A Rb-Sr mineral-whole rock isochron for samples of the muscovite granite collected just west of Sunset Canyon has yielded an Eocene age and provides a minimum age for the thrusting.

0.3

70.7 Rest area on left. Canyon to the west of Harquahala Mountain at 9:30 exposes about 2,500 feet of mylonitic granite below the Harquahala thrusts. We believe this mylonitization was imposed on the granite during an earlier episode of thrusting (see Stop 2).

0.8

69.9 Rest area on right.

0.9

69 Socorro Peak at 10:00.

1.0

68 Prepare to make left turn into Marble Stockpile area ahead on left for  
White Marble Mine traverse.

LARAMIDE THRUST-FAULT SANDWICH IN THE SALOME REGION, WEST-CENTRAL ARIZONA

by Stanley B. Keith, Stephen J. Reynolds,  
and Stephen M. Richards

Introduction:

As one drives southward on the dirt road leading to the White Marble Mine in the Harquahala Mountains, inspection of the slopes to the left and below the conspicuous conical peak on the skyline at 12:30 to 1:00 position, termed "the hat", reveals an inclined ledge (Figure 1). This ledge marks the trace of the Golden Eagle thrust (See below for definition and geographic distribution.).

Twenty kilometers southwest of the White Marble Mine one may observe the same thrust 1.5 km northeast of the Golden Eagle Mine. Here, vertically standing Paleozoic formations are spectacularly truncated by a flat fault that places the Paleozoic section on highly broken, but recognizable, porphyritic Precambrian granite.

The Golden Eagle thrust is one member of a major, regionally distributed series of low-angle thrust fault slices in the Harquahala and Little Harquahala Mountains (Figures 1, 2 & 3). Evidence of a former widespread Mesozoic event that completely inverted much of the Paleozoic section was severely overprinted and masked by the great thrust faults. In effect, the region consists of a vast thrust fault sandwich that was emplaced on a Mesozoic sedimentary and volcanic "basement" in the western Harquahala and Little Harquahala Mountains (Reynolds and others, 1980). As presently conceived, the thrust fault sandwich is composed of three major, regionally continuous plates (Refer to Figure 3 for nomenclature and location of the three plates.).

The lowermost plate is separated from the Mesozoic "basement" by the Hercules thrust, named for exposures near the Hercules Mine in the western Harquahala Mountains. The overlying plate is designated the Hercules plate which corresponds to the lowermost Precambrian sheet of Reynolds and others (1980). The Hercules plate, in the Little and western Harquahala Mountains, consists entirely of crystalline rocks of probable Precambrian age. The middle plate is separated from the underlying Hercules plate by the Golden Eagle fault, named for excellent exposures of the fault at the Golden Eagle Mine and vicinity in the Little Harquahala Mountains. The overlying plate is named the Golden Eagle plate which corresponds to the Paleozoic sheet of Reynolds and others (1980).

The Golden Eagle plate in the Harquahala and Little Harquahala Mountains consists almost entirely of Paleozoic rocks with local areas of Precambrian granite, beneath the lowermost Paleozoic unit, and local

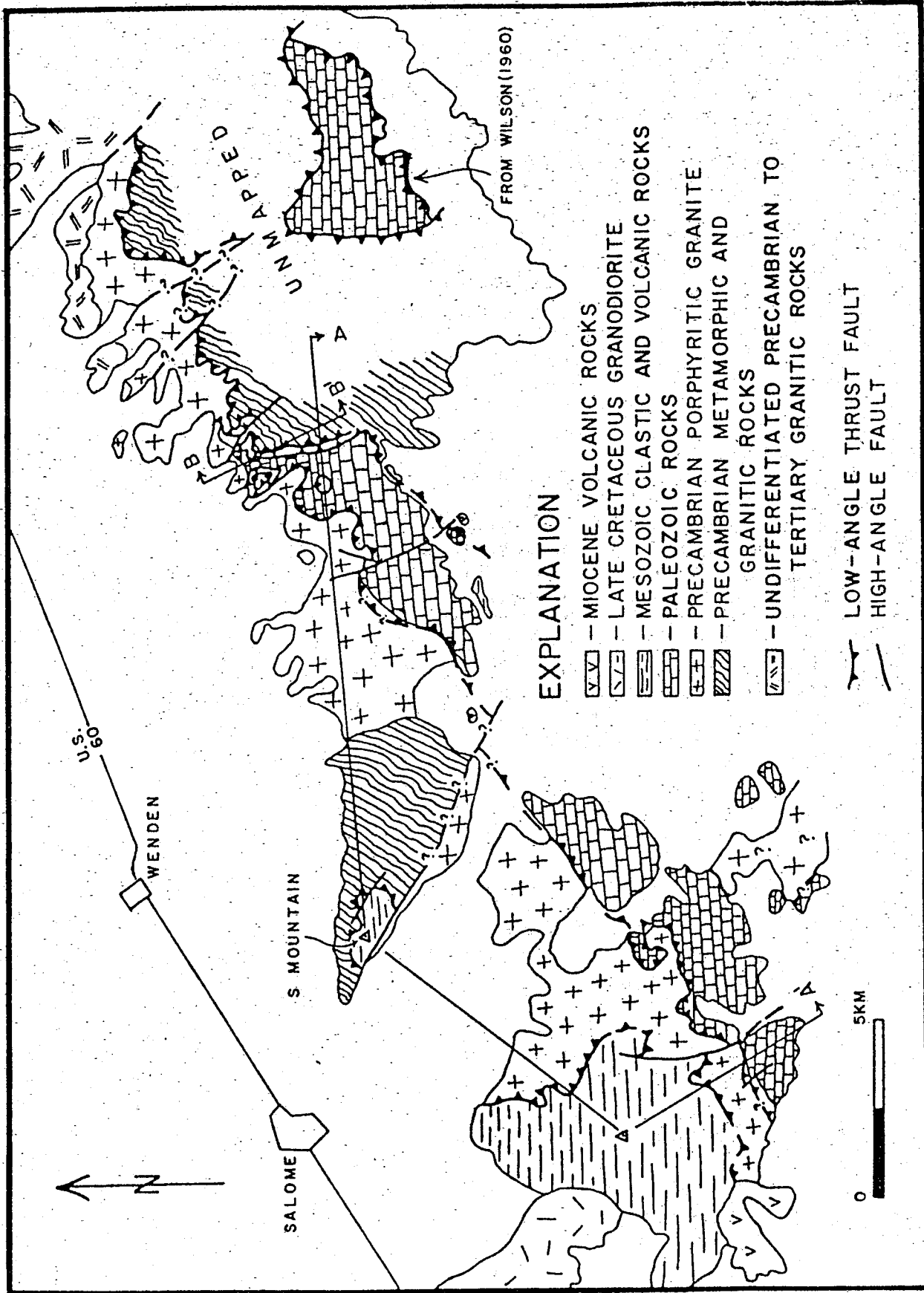


Fig. 1. Generalized geologic map of the western Harquahala Mountains and Little Harquahala Mountains. Includes data from Wilson (1960), Varga (1976, 1977), Rehrig and Reynolds (1980), and new geologic mapping by S. B. Keith and S. J. Reynolds.

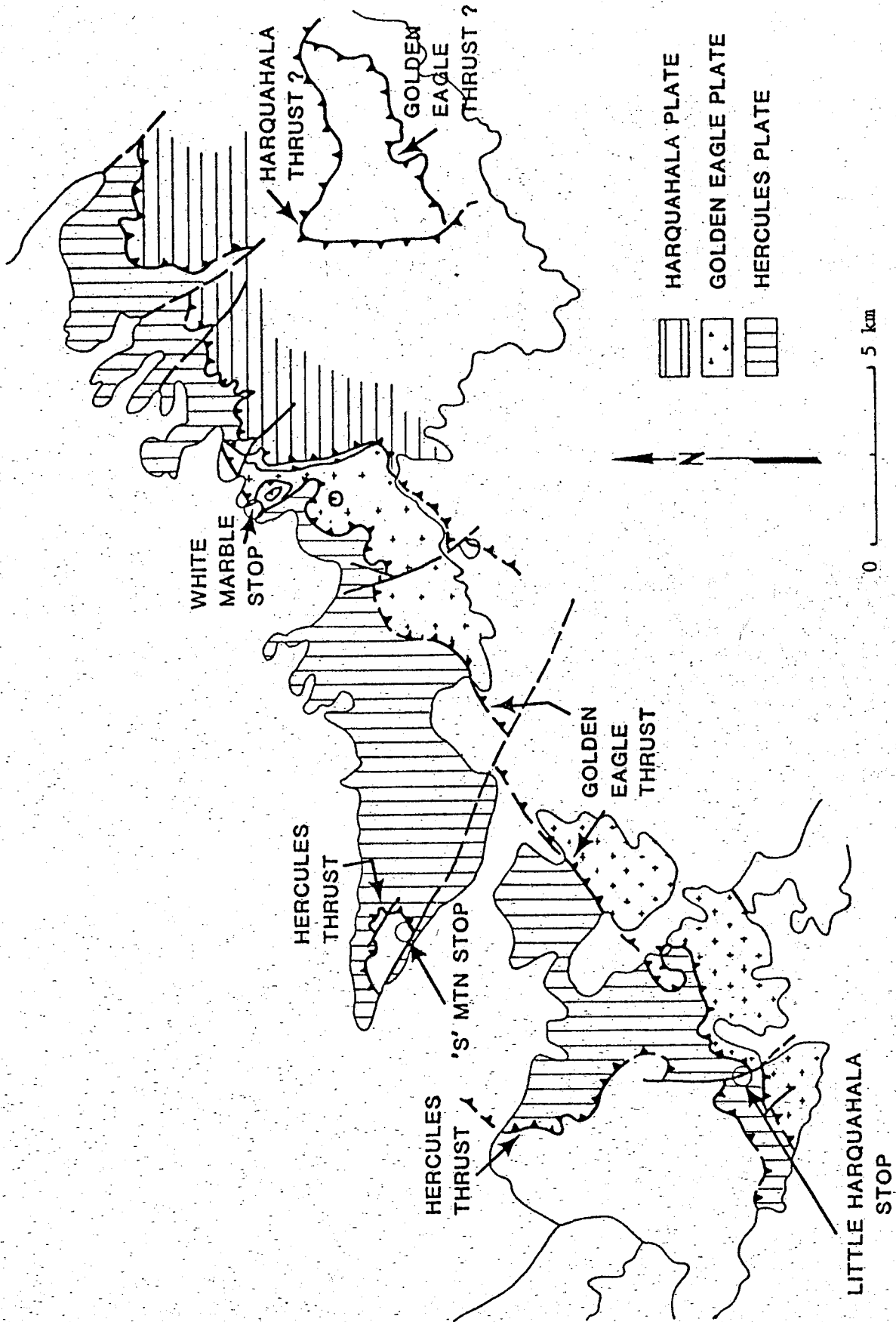


Figure 2. Proposed terminology for Laramide thrust plates in the Harquahala and Little Harquahala Mountains, west-central Arizona.

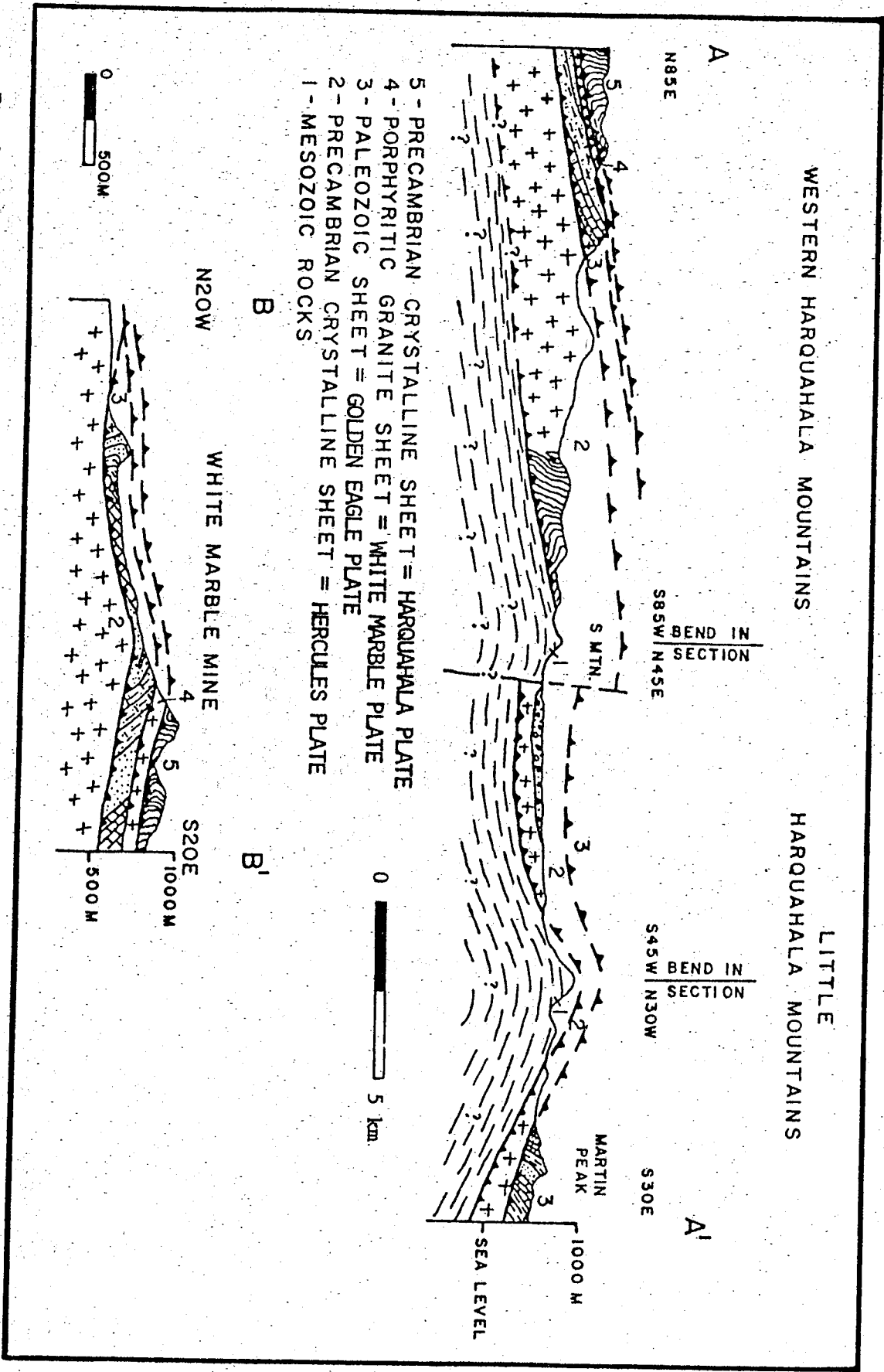


Fig. 3. Schematic cross sections A-A' and B-B'. See Figure 2 for location of cross sections. Note that A-A' is viewed to the south and east.

imbrications that contain granite of probable Precambrian age. The uppermost plate is separated from the underlying Golden Eagle plate by a fault designated as the Harquahala thrust because of its widespread distribution throughout the Harquahala Mountains.

In general, the Harquahala thrust has placed Precambrian(?) age amphibolite-grade metasedimentary, metavolcanic, and leucocratic plutonic rocks over Paleozoic rocks in the Golden Eagle plate. This uppermost plate is named the Harquahala plate and corresponds to the Precambrian crystalline sheet of Reynolds and others (1980).

Locally, the Harquahala plate rests directly on Precambrian crystalline rocks of the Hercules plate or it is separated from the Paleozoic rocks of the Golden Eagle plate by a thin thrust sheet of porphyritic granite in exposures within the Harquahala Mountains (the porphyritic granite sheet of Reynolds and others, 1980). This thrust is named the White Marble thrust for its conspicuous presence at the White Marble Mine and vicinity. For reasons discussed at Location D, the White Marble thrust is considered part of the Golden Eagle plate. (Fig. 2)

The White Marble Mine complex is situated virtually in the middle of the thrust fault pile. At the White Marble Mine, an upside-down Paleozoic section comprises a thin thrust sheet of carbonate rocks which are tectonically sandwiched between the White Marble and Golden Eye thrust sheets. A detailed look will be given to this thrust "stratigraphy."

#### WHITE MARBLE MINE ROAD LOG

Begin  
Cumulative  
Mileage From  
U.S. 60

- 0.0 Turn south from U.S. 60 at Milepost 66.7. Marble chip stockpile area and trailer mark the location of the exit. Road into marble stockpile area is gated. Once into marble stockpile area, bear slightly right through marble stockpiles following worn set of tracks. Once through the marble stockpiles, proceed down an excellent graded dirt road. (Cadillac grade, when mine is being operated.)
- 0.4
- 0.4 As you traverse south-southeast down the White Marble Mine road, the following features will be in view: Harquahala Mountain is on skyline at 10:30, while the Marble Mine (white scar not in full view yet) is at 12:05 low. Nipple-like feature on skyline ridge at 12:30 is referred to here as "the hat." "The hat" is in the vicinity of much of the more choice thrust fault action in the region. Socorro Peak is the prominent peak at 1:00 with Tenahatchapi Pass at low spot on the skyline in the 2:00 position.
- 1.7
- 2.1 Windmill and water tank on right. The Harquahala thrust forms a sub-horizontal ledge below the skyline ridge at 11 - 12:00. The ledge

separates ledgy layers of amphibolitic grade Precambrian rocks in the Harquahala plate (in upper third of skyline ridge) from more knobby outcrops of mylonitic granite in lower two-thirds of ridge. Prominent cliffs at 12:00 are Bolsa Quartzite within the Golden Eagle plate below the Harquahala plate.

0.5  
2.6 Twin saguaros on left. "The hat" is now at 1:00. Below "the hat" is a prominent inclined ledge that from this view, slopes to the right and passes beneath prominent cliffs (up and to right) composed of Bolsa Quartzite. The inclined ledge marks the trace of the Golden Eagle thrust. In this area, the Golden Eagle thrust truncates Bolsa Quartzite through Supai formation of the Paleozoic section.

0.4  
3.0 Inselberg hill on right is composed of mylonitically foliated Precambrian porphyritic granite in the Hercules plate. Foothills at 10:00 are mainly composed of the above granite plus other more equigranular, mylonitic, leucocratic, alaskitic granitoids of presumed Precambrian age. Mylonitic foliation in these rocks strikes northeast and dips northwest. Lination in the foliation planes plunges northwest. The mylonitic Precambrian rocks are intruded by a prominent microdiorite dike swarm of east-west to west-northwest strike, nearly vertical, that postdate the mylonitic deformation. Similar dikes elsewhere in the Harquahala Mountains have yielded K-Ar ages of 22.1 m.y. and 28.6 m.y. on biotite and hornblende respectively. (Shafiqullah and others, 1980).

1.0  
4.0 Road to right. This road leads around the ridge to the west and to the canyon northeast of "the hat" (a two-mile drive). Four-wheel drive is required. The road does provide good access to the thrust fault geology north of the hat. The White Marble Mine is at 11:45 low and is partially screened from view by a narrow canyon that is comprised of steep cliffs of Bolsa Quartzite on either side.

0.3  
4.3 Stream crossing. Hill and adjacent outcrops on right contain good exposures of the mylonitically foliated Precambrian granite. Foliation strikes northeast, dips northwest, and contains a northwest-plunging mineral lination. Structurally, one is in the upper part of the Hercules plate at this juncture.

In the foliation planes of mylonitic varieties of porphyritic granite within the Hercules plate north of the White Marble Mine, a streaky mineral lination is apparent and is composed of parallel alignments and trains of biotite and quartz. The mineral lination trends WNW to NW (see Figure 4). Linear structural elements within more mylonitic porphyritic granite, in the upper part of the Hercules plate, have a different orientation. At, or near, the Golden Eagle thrust the lination trends are more northerly to north-northeasterly and have a slickensided aspect (Fig. 5). This style and orientation of lination is also present in mylonitic granite immediately below the Harquahala thrust in the White Marble plate. It is our impression that these two lineations represent a difference in structural style of lination rather than a change in orientation of the same lination. We will inspect the north-trending linear structural elements in mylonitic granite of the White Marble Thrust sheet between Locations B and C.

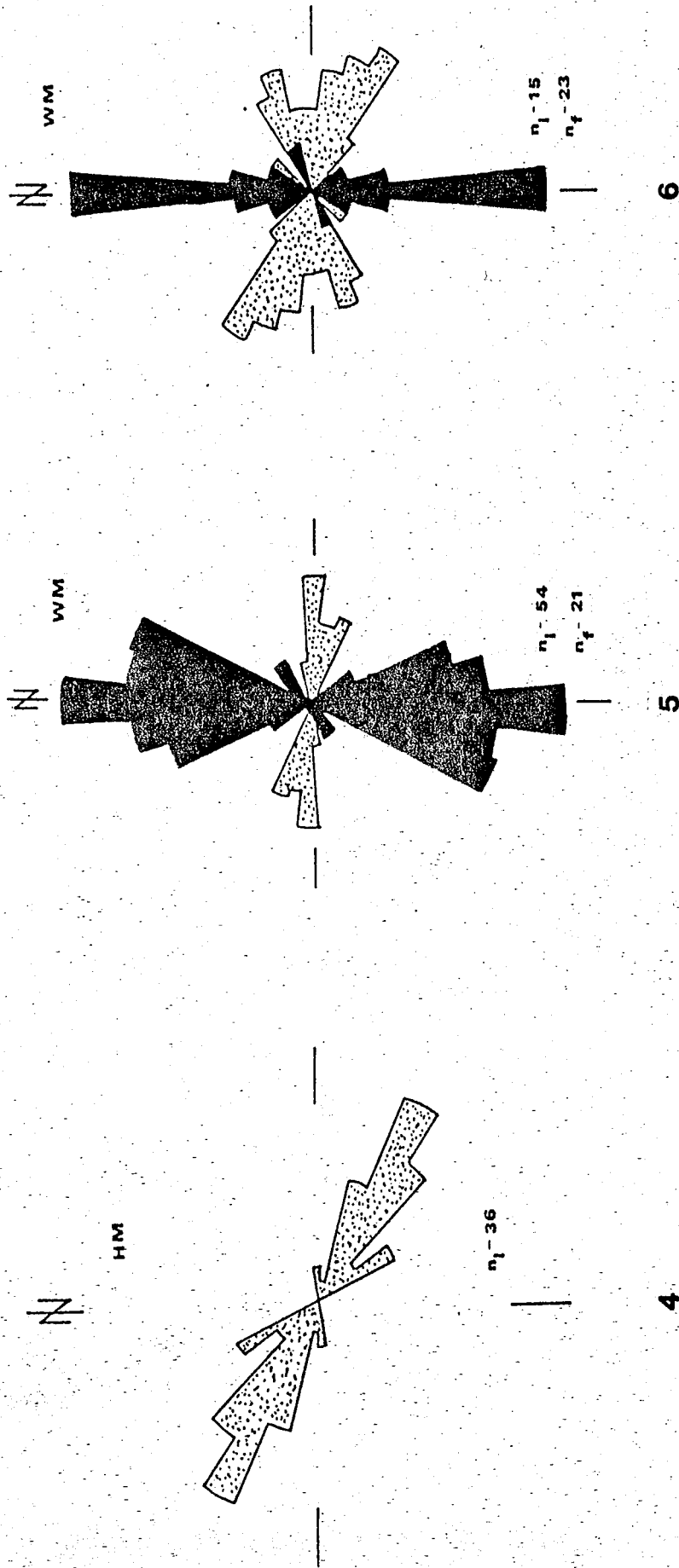


Figure 4. Trend rosette diagram for lineations in porphyritic granite within Hercules plate north of White Marble mine.  
 Figure 5. Trend rosette diagram for lineations in mylonitic granite within White Marble plate and uppermost Hercules plate and for folds near or at Harquahala thrust. Fold axes are represented by a stipple pattern.  
 Figure 6. Trend rosette diagram for linear elements and fold axes from Paleozoic rocks within Golden Eagle plate. Fold axes are represented by a stipple pattern.

Note:  $n_f$  equals fold axes;  $n_z$  equals mineral lineations on Figures 4 and 5 and slickensides mineral lineations, and stretched chert Tenses on Figure 7.

- 0.2  
4.5 Parking area on right. The road ahead is usually blocked by a locked cable. The Field Trip Stop will begin here. The full traverse will take about 2 hours so take the usual precautions. From here, navigation will be according to the geologic map provided. Participants will continue 100 m up the dirt road to Location A, which is a roadcut exposure of the Bolsa/granite contact.

#### WHITE MARBLE MINE TRAVERSE (Refer to figure 7)

##### Location A. Bolsa Quartzite/Porphyritic Granite Contact.

The contact between the Bolsa Quartzite and porphyritic granite dips 25 degrees to the south at Location A. The granite beneath this contact is weakly sheared but not to the degree expected at a major thrust surface. The Bolsa Quartzite here consists of coarse-grained arkose with the feldspar detritus identical to that in the underlying granite. The basal arkose rapidly grades upward into a well-sorted, medium- to fine-grained, feldspathic quartzite. From these facts, we interpret that this is a deformed depositional contact which is similar to other exposures in the Harquahala and Little Harquahala Mountains.

We have now passed into the Golden Eagle plate. The Golden Eagle thrust is concealed by surficial gravel veneer but occurs between Location A and the parking area.

##### Location A to Location B

From the Bolsa Quartzite-porphyritic granite contact, continue southeast, up the road, towards the White Marble Mine. While walking, note that the Bolsa Quartzite steepens in dip to a nearly vertical position. Also, notice that a flat-dipping, locally penetrative, fracture cleavage is present in the quartzite. We interpret that this fracture cleavage formed during thrusting because of its parallel alignment with the major thrusts; here, the Golden Eagle thrust occurs about 50 meters beneath the road. Prior to leaving the quartzite and entering the White Marble Mine area, note that the Bolsa Quartzite is overturned in the wash that is west of the road.

The bulldozer cuts, seen upon entering the White Marble Mine area, are in metamorphosed, fine-grained dolomites of the Martin Formation. Walk 100 yards into the mine area and look west. Climb the hill with the prominent subhorizontal ledge of Bolsa Quartzite; Location B is at the top of this ledge.

During your climb, look for purplish, slaty fragments and outcrops of phyllitic shale between the light-colored dolomitic marble; these rocks are metamorphosed Abrigo lithologies. By the time you have reached the quartzite ledge, it should be apparent that you have traversed an overturned, lower Paleozoic section.

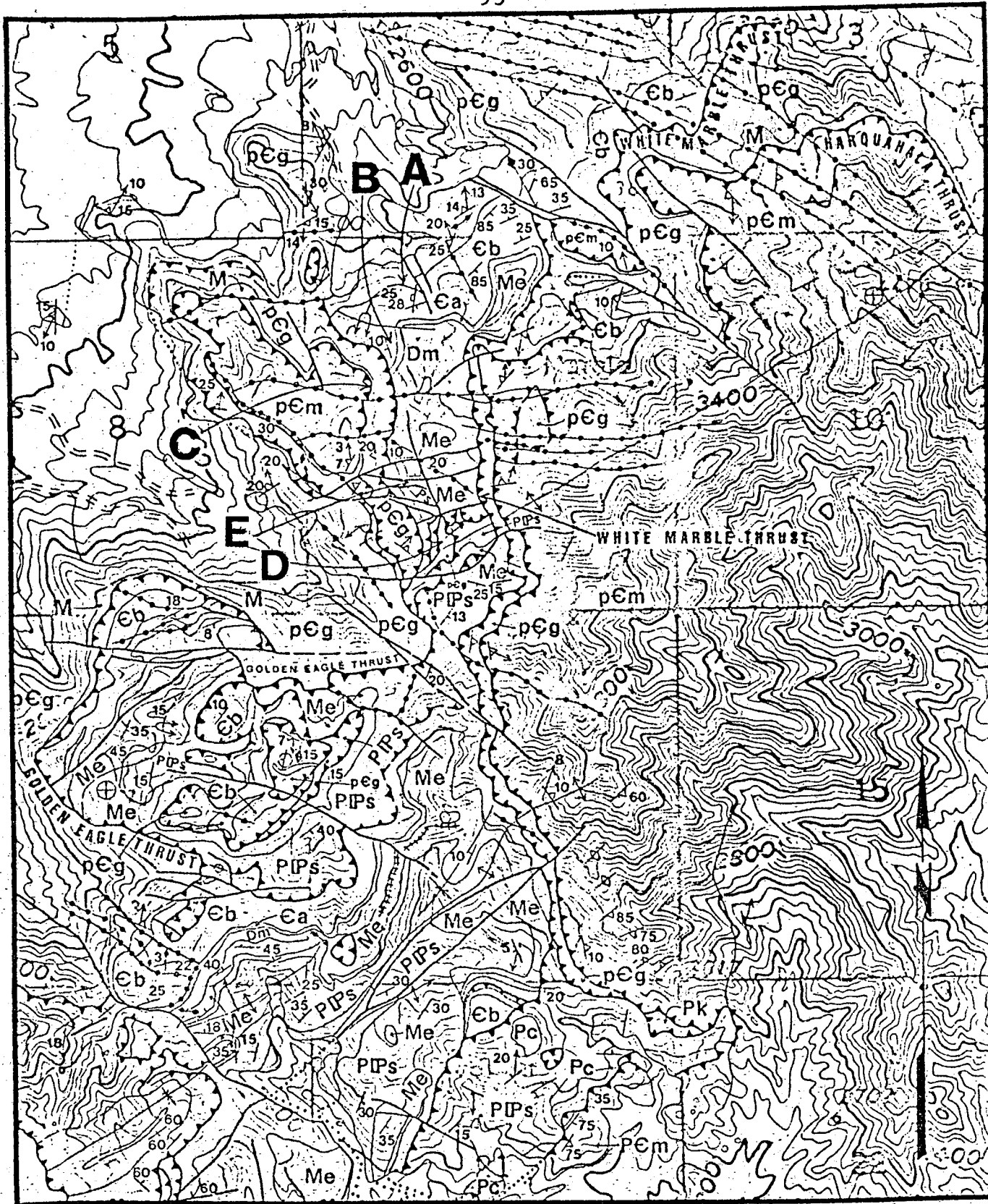


Figure 7. Geological map of White Marble mine and vicinity. Symbols are as follows: pEg = mylonitic porphyritic granite (protolith equals probable 1400 m.y. biotite granite) and minor amounts of probable Precambrian alaskitic granitoids; Eb = Cambrian Bolsa Quartzite; Ca = Cambrian Abrigo Formation; Dm = Devonian Martin Formation; Me = Mississippian Escabrosa Limestone; PPs = Permian-Pennsylvanian Supai Formation; Pc = Permian Coconino Sandstone; Pk = Permian Kaibab Formation; M = ultramylonite at Harquahala thrust. Diamond-shaped arrows are slickensides; arrows are lineation on foliation surfaces. PĒm = Precambrian age amphibolite grade metavolcanic and metasedimentary rocks locally intruded by probably Precambrian age alaskitic rocks.

## Location B. Recumbant Fold and Harquahala Thrust Overview.

From the top of the ledge, look northeast and observe the reason for the overturned Paleozoic section you just saw. Although a fold is not immediately obvious, the following evidence indicates its presence. First, focus on the overturned Bolsa Quartzite that you observed west of the road upon entry into the White Marble Mine. You will notice a slope-forming unit between the quartzite exposure and the bulldozer scars cut in dolomitic marble of the Martin Formation. There, the Abrigo Quartzite dips about  $60^{\circ}$  NNW in lower parts of the hill and flattens near the top of the low ridge. The quartzite/Abrigo contact can be traced northeast up the low ridge. Near the top of the ridge, the contact flattens, as marked by a southeastward deflection in the Bolsa Quartzite/Abrigo contact on the geologic map.

Dozer cuts occur in metamorphosed Martin at the north end of the White Marble Mine. There, the Martin is overlain by overturned, flat-lying Bolsa Quartzite and metamorphosed Abrigo that form the low ridge above the cuts. This relationship is identical to the inverted Bolsa Quartzite that you are standing on.

We have mapped a fold hinge where the flat-lying, inverted Bolsa/Abrigo section gives way to the steeply overturned Abrigo/Bolsa section. The trace of the fold hinge crosses the top of the low ridge west of the White Marble Mine and follows the small, southwest drainage located between the cuts in the marble and the northeast-trending Bolsa Quartzite ridge. The fold hinge then continues southwestward up the ridge we are now on and crosses the ridge about 100 m north of Location B. The axial plane of the fold dips about  $30^{\circ}$  south-southeast. As mapped, this fold represents a recumbant synclinal fold. Because the fold opens southeastward, it can be interpreted that the fold represents the lower half of a giant, nappe-sized, recumbant fold that is overturned towards the southeast. As such, the structure indicates tectonic transport from northwest to southeast or southeastward vergence. This fold exposure represents the best locality we have found thus far for the southeast vergent folding formed during the pre-Laramide, Mesozoic deformation. The top half of the fold was completely decapitated by the Harquahala thrust in the White Marble Mine area.

The Harquahala thrust is present on the ridge west of the White Marble Mine. The position of this thrust occurs just above the road near the top of the ridge and above the light-colored outcrops of Paleozoic carbonate rocks. The road is cut in slope-forming, mylonitic, porphyritic granitoid rocks of the White Marble sheet.

The base of White Marble sheet is the White Marble thrust which occurs at the contact between the brownish slope-former and more irregular, light-colored, cliffy knobs of the metamorphosed Martin and Escabrosa Formations. A similar relationship occurs west of the White Marble Mine, (southwest of Location A) and will now be the object of our scrutiny.

Just before you leave Location B and walk southwestwards (Fig. 7), the following observations will provide perspective for what you are about to walk through. Location B is on a flat, table-like bench at the top of an inverted Bolsa Quartzite section. The grass-covered slopes, immediately southwest of this bench, are underlain by mylonitic granitoid rocks of the White Marble sheet. Hence, the break in slope between the quartzite bench and the granite represents the White Marble thrust. It should now be clear that Location A is located virtually at the White Marble thrust surface. A careful search of the quartzite will reveal numerous north-south-trending slickensides (Fig. 5) that reveal the transport direction of the White Marble thrust.

Above Location B, a conspicuous 5 to 10 m thick, dark-green ledge, seen above the grass-covered slopes, is ultramylonitic granite which directly underlies the Harquahala thrust. Here, the White Marble thrust sheet is about 50 to 75 m thick. The alternating slopes and ledges above the ultramylonitic ledge are transposed amphibolite-grade rocks of the Harquahala plate.

With this framework in mind, you can make sense of some of the ledges in the distant main ridge of the Harquahala Mountains located about a km northeast of the White Marble Mine. The dark brownish-green ledges occur at several intervals on the middle slopes of the north-facing side of the main ridge. All of the conspicuous ledges are exposures of ultramylonitic, porphyritic granite that are immediately beneath the Harquahala thrust.

Subsequent offset of the Harquahala thrust by northwest-trending faults has caused the ledges to be at different elevations (Fig. 7). The first of the more subdued ledges, above the prominent ultramylonite ledge, contain locally abundant 'S' and 'Z' fold structures. We will see a good exposure of these folds in the Harquahala plate above the ultramylonite ledge, on the east side of the ridge we are now on at Location C.

#### Location B to Location C

As you leave Location B and climb the grass-covered slopes, you will encounter poor exposures of the mylonitic granite. A careful search will reveal the presence of relict feldspar augen. If luck prevails, a few "box car" feldspars can be found, especially near the middle of the White Marble sheet.

As you climb towards the ultramylonite ledge, note how the grain size and distance between foliation planes lessens until, at the mylonite ledge, all that remains of the original feldspars are a few strung-out, faint, light-colored wisps. Lineations trend northerly, within the shallow, inclined, mylonitic foliation planes, and are parallel to slickensides developed in the Bolsa Quartzite, near Location B, that were formed on the White Marble thrust. The mylonite ledge marks the position of the Harquahala thrust zone located near, or at the top of, the ledge.

Careful inspection of some of the ultramylonitic exposures in the ledge will reveal two sets of fabric. One fabric is composed of micro-crenulations with east-west axes. If one inspects this fabric from an end-on position, he will notice subcircular cross sections of quartz rods that are elongate in an east-west direction. We interpret the crenulation lineation as a 'b' lineation approximately perpendicular to the line of tectonic transport. If one observes the foliation planes that contain the crenulation lineation, he may see a second somewhat more subtle lineation that resembles faint slickensides. This lineation is oriented about N-S, perpendicular to the crenulation lineation. This lineation is parallel to the lineation in the mylonitic granite of the White Marble sheet and the slickensides in the Bolsa Quartzite at the White Marble thrust, now about 75 m structurally below our present position. We interpret this lineation as an 'a' lineation that parallels the direction of tectonic transport.

Once on top of the ultramylonite ledge, you are at the base of the Harquahala plate. This plate is widespread throughout the higher elevations of the main mass of the Harquahalas for several kilometers east and northeast of the White Marble Mine.

From the top of the ultramylonite ledge, one can climb up a slope-covered interval to examine the subhorizontal ledges in the lower part of the Harquahala plate. The original Precambrian fabric was thoroughly obliterated and transposed by foliation that is subparallel with, and probably related to, the Harquahala thrust. Locally, this foliation is folded. The rock here is an amphibolite-grade, aphanitic felsite (possibly a silicic metavolcanic) inter-foliated with darker quartz-feldspar-mica schistose rocks (possibly a metasediment). Quartz veins and segregations are common and, indeed, characterize many exposures in the lower part of the Harquahala plate.

Once the amphibolite grade rocks have been perused, contour around the ridge to the east staying in the Harquahala plate about 10 m above the Harquahala thrust. A study of the more cliffy ledges, at Location C, will quickly reveal numerous folds that deformed the subhorizontal foliation and are thought to be related to thrusting.

#### Location C. Folds Related to the Harquahala Thrust.

The folds exposed in the cliffy ledge are typical of many of the folds found at, or just above, the Harquahala thrust. Twenty-one fold axes, measured from various localities at this structural level, show a preference for an east-west direction. These axes are nearly orthogonal to slickensides in quartzite at the base of the White Marble thrust and to lineation directions in mylonitic granite within the White Marble plate (Fig. 5).

Asymmetry of 'S' and 'Z' folds is overwhelmingly northerly with middle limbs dipping southerly. However, as you can see at this outcrop, a few folds exhibit southerly asymmetry. The middle limbs of those folds are commonly detached from upper and lower hinges by small

reverse faults and, locally, 'S' and 'Z' fold pairs are present which exhibit opposing asymmetries (double vergence) and display conjugate 'box' fold geometries. The box folds suggest north-south shortening associated with the thrusting, whereas the preferred northward asymmetry, or vergence, suggests northward transport for the thrusting.

After viewing those folds, move upslope to the ridgeline.

#### Location C to Location D.

Once on the ridgeline, ascend the ridge until you have reached the top of the main north-northwest trending ridge west of the White Marble Mine. On the climb--you will notice that the low-angle mylonitic foliation that we associate with the Harquahala thrust becomes less intense. As it does, you will start to notice a higher angle northeast-trending foliation that we believe is a relic Precambrian age foliation associated with the Precambrian metamorphic rocks of the Harquahala plate.

Once on top of the ridge, walk south for about 0.5 km. As you do so, you will have an excellent panorama of the complex thrust fault sandwich underneath 'the hat' across the canyon to your south. The tip of 'the hat' is composed of carbonate (meta-Devonian Martin Formation?) in tectonic contact with a mylonitic porphyritic granite (slope former immediately beneath 'the hat'). The granite, in turn, rests tectonically on a cherty carbonate cliff-former (meta-Mississippian Escabrosa Formation?) which we believe is upside down. The granite sheet closely resembles that in the White Marble sheet and we tentatively correlate the underlying thrust beneath this granite with the White Marble thrust. As such, the hat represents an isolated klippe of the White Marble sheet. Beneath the Escabrosa (?) cliff is a slope former of probable meta-Supai (also upside down.) This assemblage rests tectonically via the Golden Eagle thrust on porphyritic granite in the Hercules plate in the lower slopes. The Golden Eagle thrust can be tracked to the northwest into the lower slopes where it forms a prominent dark-colored, northwest-dipping ledge beneath a right-side-up Paleozoic section. Between the upright Paleozoic section and the overturned Paleozoic just north of the hat, we have mapped a fold axis for a large overturned syncline within the Golden Eagle plate. We believe this fold is a continuation of the overturned southeast vergent fold we observed at location B.

It is important to realize how the Golden Eagle thrust juxtaposes Paleozoic section of the Golden Eagle plate with porphyritic granite in the Hercules plate without any regard for the layering within the Paleozoic section. This is best seen along the northwest-dipping segment of the Golden Eagle thrust where upright southwest-dipping Paleozoic section (Bolsa Quartzite through Escabrosa formation) dips down into the here northwest-dipping Golden Eagle thrust and is completely truncated by the thrust. This dramatically illustrates the distinctive non-decollement style of thrusting in the Salome region. Stratigraphic control simply was not a factor in the mechanics of this thrusting. Rather, the Paleozoic section is only one sliver within several slivers of relatively thin predominantly Precambrian crystalline rocks of various kinds.

As you continue southward along the ridgeline, you will cross back into the deformed porphyritic granite of the White Marble sheet. The Harquahala thrust is obscured here because of subsequent offset by east-west trending faults and intrusion by probably early Miocene microdiorite dikes (refer to Figure 7). West of the ridge, the Golden Eagle plate carbonate section is only a few meters thick and about 0.8 km to the northwest on the western slopes of the ridge is absent entirely. Hence, in a real way, the Paleozoic section of the Golden Eagle plate is noticeably boudined between the Harquahala and Golden Eagle thrusts and in some cases is not present at all.

About 100 m before the ridge starts to climb again (just south of Location D on the map), turn east and descend into the ravine on the east side of the ridge. As you do so, you will notice that here the mylonitic granite in the White Marble sheet rests directly on meta-Escabrosa carbonates (rather than Bolsa at Location B). You will also encounter a sliver of meta-Supai formation (upside down) beneath the meta-Escabrosa carbonate rocks. By the time you are in the ravine, a brownish-gray, slope-forming unit will be seen beneath the prominent ledges of Supai. This rock, and its relationship to the overlying, upside-down Supai Formation will be the object of our scrutiny at Location D.

#### Location D. Golden Eagle Thrust.

By the time you reach Location D you probably guessed that the punky, brownish-gray rock you are walking on is mylonitic granite. Comparatively undeformed 'box car' feldspar relicts are common in exposures on the west side of the stream at Location D. The mylonitic Precambrian granite rests in the Hercules plate which here is tectonically overlain by overturned Supai Formation which rests in the Golden Eagle plate.

The Golden Eagle thrust separates the cliff-forming, reddish-brown Supai Formation from the lower, slope-forming mylonitic granite. Here, this thrust dips gently to the north. Paleozoic units that comprise the Golden Eagle plate, west of Location E, total 100 m thick. Upstream from Location E, at the White Marble Mine, the plate measures 200 m thick between the Golden Eagle and White Marble thrust faults. The Paleozoic thrust sheet becomes progressively attenuated until it thins to a few meters thick near the ridge crest that is west of Location D. A good view of this tectonic thinning is available from the ridge west of Location D.

The Paleozoic thrust sheet is absent 1 km northwest of Location D. There, mylonitic Precambrian granite, of the White Marble plate, is separated from mylonitic Precambrian granite, of the Golden Eagle plate, by a 30 m thick zone of ultramylonite. It is interesting that the ultramylonite zones, associated with the Golden Eagle thrust, are thin or absent when that thrust involves Paleozoic rocks, as at Location D, while these zones are 10 to 30 m thick when the thrust occurs entirely within granite, as seen 1 km northwest of the hat.

The ridge top we traversed west of Location D is composed of mylonitic Precambrian granite of the White Marble plate. Although this plate is present throughout the White Marble mine area, we consider that the White Marble plate is an imbrication within the Golden Eagle plate because of relationships seen at the Silver Queen Mine and at the hat which are located  $1\frac{1}{2}$  to 2 km south and southwest of the White Marble Mine.

Recent mapping between the Silver Queen and Hidden Treasure Mines (Fig. 7) disclosed that the Harquahala plate rests directly on the Golden Eagle plate with no intervening porphyritic granite sheet. Hence, the White Marble thrust cannot be traced regionally. Also, as pointed out earlier, the geographic feature termed 'the hat' is capped by a small outcrop of Paleozoic carbonate (possibly metamorphosed Martin Formation) which rests, tectonically, on a thin, 50-75 m thick thrust sheet of mylonitic granite that is similar in structural position, thickness, and lithology to the foliated granite found in the porphyritic granite sheet by Reynolds and others (1980) in an area 0.5 km east of the hat. The presence of a Paleozoic carbonate section above the foliated granite suggests that small pods of Paleozoic rock might be present locally between the granite sheet and the Harquahala plate.

#### Location D to Location E

From Location D proceed down the ravine northward until the Supai cliffs on the west side of the ravine give way. Here you will find a track that ascends out of the ravine onto its western side. Contour along the slopes until you encounter a bulldozer road. When you reach this road, you will be at Location E.

The geology between Locations D and E consists of overturned and metamorphosed units of the Escabrosa Limestone and the Supai Formation. Numerous east-west-trending, post-thrust normal faults formed small horst and graben structures in the Paleozoic units. The Supai Formation, west of the stream is juxtaposed against strata of the upper Escabrosa Limestone by a north-striking fault mapped in the ravine (Fig. 7).

While the metamorphosed Supai lithologies here contain siltstones, quartzites and abundant phyllites, much carbonate material is present; much more than is typical of the Supai stratigraphy present along the southern edge of the Colorado Plateau. Carbonate-rich areas in many of the siltstone units have been dissolved by surface erosion and contain a distinctive texture that resembles termite holes in rotten wood. This 'termite effect' is diagnostic of Supai and metamorphosed equivalents throughout the Harquahala and Little Harquahala Mountains.

#### Location E. Overturned Contact Between the Escabrosa Limestone and Supai Formation

The abandoned road you have reached was cut along the contact between Escabrosa Limestone and Supai Formation. Because the older Escabrosa Limestone rests on top of the Supai, you have traveled through an

overtured Paleozoic section. This reaffirms our interpretation that the Paleozoic section at the White Marble Mine is inverted.

In these road cut exposures, the contact between the Escabrosa and Supai is placed where cherty, thin-bedded carbonate rocks of the upper Escabrosa Limestone overlie phyllitic schists of the lowest Supai Formation. Small pods and lenses of chert-pebble conglomerate and breccia occur at the base of the Supai Formation in an area 100 m south of Location E (West Peirce, 1980, oral communication). These rocks strongly resemble similar lithologies present in basal Supai units from less metamorphosed exposures in the Little Harquahala Mountains. Although the basal contact of the Supai Formation is tectonized at Location E, we are confident that only minor tectonic transport occurred (Fig. 7).

At the White Marble Mine, at least 1 km of overturned section was confirmed along a line that is perpendicular to the fold hinge described at Location B. This inversion involves units of Bolsa Quartzite through the Supai Formation. Thus, a feeling for the dimension of this large, nappe-sized fold can be obtained.

An even more impressive section of overturned Paleozoic strata was mapped 2 km south of the White Marble Mine in the vicinity of the Silver Queen Mine. Map relationships here and near the Silver Queen Mine suggest that the length of the middle limb of the southeast overturned nappe is between 1 and 2 km.

The knob of Escabrosa Limestone, located above the bulldozed road, contains a rather picturesque 'Z' fold in the carbonate rocks. This fold is a good example of inconspicuous, but significant, folding that locally pervades the carbonate section. Twenty-three fold axes, measured from folds with definite asymmetry within Paleozoic rocks of the Golden Eagle plate, cluster in two populations around an east-west axis (Fig. 6).

Linear fabrics from foliation surfaces in Paleozoic strata strongly show a preference for north-south bearings. The phyllitic lithologies of the metamorphosed Supai Formation commonly display these lineations. We interpret that the lineation represents the line of tectonic transport.

Asymmetry of the folds shows an overwhelming preference for northward overturning (look again at the knob). It is instructive to note that an impressive geometric similarity exists between structures in the Paleozoic rocks of the Golden Eagle plate and structures at, or just above, the Harquahala thrust in the Harquahala plate (compare Figs. 5 and 6).

#### Location E to Parking Area.

After inspecting the bulldozer cuts, follow the dirt road back to the White Marble Mine proper.

As you start away from Location E, you will notice a prominent knob of meta-Escabrosa to the north that is juxtaposed against overturned

Supai by one of the more prominent east-northeast-striking, post-thrust normal faults in the White Marble Mine area. Once past the knob, the road will contour for a short distance along the White Marble thrust and then drop down into the main mine area where dolomitic marble is being mined in upside down meta-Martin and Escabrosa Formations. Marble mined here is generally used for decorative purposes (rooftops, etc.) in the Phoenix area.

Follow the main road back down to the parking area and return to U. S. 60 westbound for Wenden and Salome.

## WHITE MARBLE MINE TO 'S' MOUNTAIN

Return to  
mile post  
format

After returning to U.S. 60 turn left (west) onto U.S. 60 for Wenden and Salome.  
0.7

66 Cunningham Pass in the western Harcuvar Mountains is at 3:00. The Harcuvar Mountains west of Cunningham Pass are mainly composed of Tank Pass granite, abundant roof pendants of amphibolite-grade gneiss, and numerous northwest-striking dikes of garnetiferous pegmatite-aplite, rhyolite, andesite, and microdiorite. The Tank Pass biotite granite is undeformed in its southwest exposures near Tank Pass (1:00), but becomes progressively foliated and deformed toward the northeast near Cunningham Pass. The foliation and its attendant northwest-trending lineation are different in style from the mylonitic fabrics that pervade the Harcuvar Mountains east of Cunningham Pass. Northwest-trending hornblende grains from one of the amphibolite roof pendants just north of Cunningham Pass gave a K-Ar age of 70.3 m.y. Biotite from foliated Tank Pass granite that contained the northwest-trending lineation gave a 51 m.y. apparent age (Rehrig and Reynolds, 1980; Shafiqullah and others, 1980).

In Cunningham Pass foliated Tank Pass granite is intruded discordantly by numerous leucocratic garnetiferous pegmatites and aplites. Both rocks are in turn cut by a younger mylonitic fabric that contains an ENE-WSW trending lineation. It is this fabric that pervades the eastern one-half of the Harcuvar Mountains and the eastern one-third of the Harquahala Mountains. A K-Ar biotite age on one of these mylonitic gneisses is 25.3 m.y. (Rehrig and Reynolds, 1980). It is interesting that in the Buckskin, Harcuvar, and Harquahala Mountains, the younger mylonitic foliation occurs in the eastern one-half to one-third of the mountain ranges. Relationships in the Harcuvar and Harquahala ranges suggest that as one passes westward, he descends structurally into foliation and structures associated with the north to northeast vergent thrusting (STOPS 2, 3, and 4A). The younger mylonitic fabric is discordantly cut by microdiorite, rhyolite, and andesite dikes of probable early to middle Miocene age. One of the microdiorite dikes in the Harquahala Mountains yielded K-Ar ages of 28.6 and 22.1 m.y. on hornblende and biotite respectively.

2.8

63.2 Yuma County dump road on left.

2.0

61.2 Bridge over Centennial Wash

0.3

60.9 Wenden town limit sign.

0.4

60.5 Road to Cunningham Pass, the Buckskin Mountains, and Alamo Dam and lake intersects from the right.

0.5

60.0 Tank Pass (2:00) is the type area for the Tank Pass biotite granite. Granite Wash Mountains (12:00 to 2:00) contain early Cretaceous ? clastic sedimentary rocks (Livingston Hills equivalent ?) intruded to the east by a calc-alkalic granodiorite pluton referred to as the Granite Wash Pass granodiorite by Rehrig and Reynolds, 1980. This pluton has yielded K-Ar biotite ages of 65 m.y. (Damon, 1968) and 69 m.y. (Eberly and Stanley, 1978). To the north (1:30) quartz diorite border phases of the Granite Wash Pass granodiorite intrude the Tank Pass granite.

2.4

- 57.6 International Inn in the metropolitan Salome area is on the left. The International Inn was our main staging area for field work in the area.
- 0.9
- 56.7 Salome town limit sign. Cross a short bridge just ahead and make a left turn onto Buckeye Road one block beyond the bridge.

Begin  
cumulative  
mileage

- 0.3 Y intersection with Harquahala Mine road on right. We will return to this intersection after the 'S' Mountain window stop (STOP 3).
- 1.7
- 2.0 Cross Centennial Wash. Centennial Wash, from here for the next several miles downstream, crosses a bedrock sill (largely Precambrian granite within the Hercules thrust plate) between the Harquahala and Little Harquahala Mountains. This sill is largely a pediment surface that separates the ground water basin in McMullen Valley from that under the Harquahala Plain south and southwest of the Harquahala and Big Horn Mountains.
- 0.1
- 2.1 Intersection on left. Well graded dirt road leads to Centennial Park which provides camping facilities and to Wenden and U. S. 60.
- 1.8
- 3.9 House with trees on right. Look for dirt road on left.
- 0.1
- 4.0 Turn left onto dirt road for 'S' Mountain stop. Prominent ledge-former on top of and south of 'S' Mountain is a quartzite marker ledge in a structural window of clastic-dominated Mesozoic-aged sedimentary rocks. Poorly preserved cross-bedding in the quartzite marker ledge on 'S' Mountain indicates that the Mesozoic sedimentary section is right side up.

## STOP 3

## THE 'S' MOUNTAIN "WINDOW"

An approximately one square mile area of Mesozoic sedimentary 'basement' crops out at 'S' Mountain. The Mesozoic sequence is structurally overlain on its north, east and southern sides by the Hercules thrust, a major low angle fault that places Precambrian crystalline rocks within the Hercules plate over somewhat metamorphosed Mesozoic sedimentary rocks. To the west the Mesozoic strata are juxtaposed against porphyritic granite (probably in the Hercules Plate) by a high-angle northwest-trending fault that nearly follows the present-day course of Centennial Wash (refer to figure 3 of Stop 2). Hence, 'S' Mountain is in effect a window into the underlying Mesozoic basement terrane that we infer may underlie a large portion of the western 'big' Harquahala and Little Harquahala mountains (see figure 3, Stop 2). The basement terrane is much more extensively exposed in the Little Harquahala Mountains, 8 km to the southwest.

Intriguingly, the Mesozoic rocks at 'S' Mountain are the structurally lowest package that we have mapped to date. Miller (1970) has also mapped Mesozoic strata that occur beneath several thrust sheets in the southern Plomosa Mountains. Hence, it is possible that a major Mesozoic basin of late Jurassic to mid Cretaceous age in west central Arizona has been structurally buried beneath subsequent Laramide age thrust sheets.

Mesozoic rocks below the Hercules thrust at 'S' Mountain consist of (in order of increasing stratigraphic level): 1) feldspathic sandstone and gritty arkose; 2) calc-silicate beds interbedded with quartzitic and argillitic units; 3) a ledge-forming quartzite that is capped by a stretched quartz-pebble conglomerate; and 4) quartzitic and argillitic strata. Probably Precambrian age rocks in the overlying Hercules Plate at 'S' Mountain include foliated quartz diorite, dioritic gneiss, amphibolite, quartzo-feldspathic gneiss, and a foliated leucocratic granitic rock that locally immediately overlies the Hercules thrust.

The Mesozoic rocks are locally highly deformed and exhibit a northerly trending lineation. Pebbles in the conglomerate are elongate parallel to the lineation. Precambrian rocks immediately above the thrust fault share the same lineation direction. Minor fold structures indicate that the direction of tectonic transport is parallel to the lineation. This transport direction is consistent with that documented for thrusts in the White Marble Mine area (Stop 2).

The Hercules thrust is easily observed by climbing up to the conspicuous ledge that is visible on a number of small hills. This ledge is composed of the resistant quartzite and quartz-pebble conglomerate that immediately underlies the Hercules thrust. After examining the thrust, return to the cars and drive back to the intersection of the Buckeye-Salome Road and the road to the Harquahala Mine. At this intersection, bear hard to the left onto the Harquahala Mine Road and begin new cumulative mileage.

Begin new  
Cumulative  
Mileage 'S' MOUNTAIN TO GOLDEN EAGLE MINE

- 0.0 Intersection of the Buckeye-Salome Road and the Harquahala Mine road. Facing south-southwest parallel to the road, Harquar Peak is the prominent peak at 12:00. It is underlain by an assortment of Mesozoic sedimentary and volcanic rocks. The Granite Wash Mountains are located at 3:00. They are composed of a similar Mesozoic sequence and two late Cretaceous plutons (the older Tank Pass Granite and the younger Granite Wash Granodiorite). These rock units are intruded by an impressive north-northwest-trending swarm of middle Tertiary dikes.
- 3.0
- 3.0 Entering the Little Harquahala Mountains. Small hills to the right at 3:00 are Precambrian crystalline rocks that occur in the upper plate of the Hercules thrust. In these hills, locally deformed biotite-rich granite is the predominant rock unit.
- 0.5
- 3.5 Road to right. Continue straight. Hills to left and right are in Hercules thrust plate.
- 0.9
- 4.4 Low ridge on the right contains the Hercules thrust on its west side. Rocks visible from the road consist of Precambrian granite that overlies the thrust.
- 0.2
- 4.6 Cross wash. Road in wash leads to exposures of the Hercules thrust. Road to left leads to the Rio Del Monte Mine area. The Rio Del Monte Mine consists of workings within quartz veins that cut the upper-plate rocks.
- 0.6
- 5.2 Trailers on right side of road. Rocks in this area consist of altered Precambrian granite that occupies the upper plate of the Hercules thrust. The Hercules thrust is exposed along the break in slope along the east side of Harquar Peak. The peak itself is underlain by coarse- to fine-grained clastic rocks of Mesozoic age along with fewer exposures of Mesozoic volcanic rocks. Both series of Mesozoic rocks occur in the lower plate of the Hercules thrust.
- 0.3
- 5.5 The Hercules thrust crosses the road but is very poorly exposed and difficult to trace due to alteration of both upper and lower plate rocks. Mesozoic rocks occur along the road for the next mile and consist of dark, intermediate volcanics which are locally highly altered.
- 1.0
- 6.5 Road crosses the trace of a north-trending, east-dipping, high-angle fault which has undergone normal and possible strike-slip movement. This fault offsets the Hercules thrust and juxtaposes upper and lower plate rocks (lower-plate Mesozoic rocks lie to the west of the fault).
- 0.5
- 7.0 Prospect on the right of the road is located along the high-angle fault.
- 0.4
- 7.4 Park cars for traverse to Hercules thrust and upper and lower plate rocks (Stop 4A).

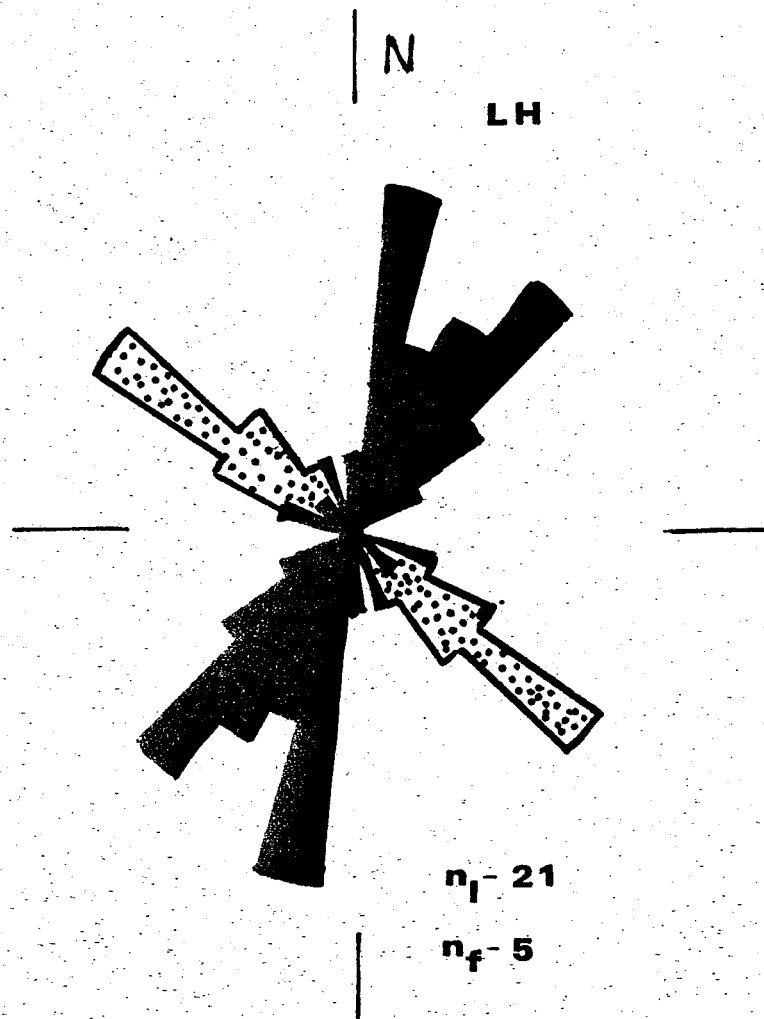


Figure 1. Trend rosette diagram for lineations in Mesozoic strata below Hercules thrust. Fold axes are represented by a stipple pattern.  $n_l$  equals slickensides lineation;  $n_f$  equals fold axes.

## STOP 4A

## HERCULES THRUST

At this stop, we will examine the Hercules thrust and lithologies of the upper and lower plates. Lower-plate rocks consist of Mesozoic clastic rocks that range from conglomerate to siltstone. Volcanic-derived detritus is locally very abundant. Volcanic rocks are also present below the Hercules thrust, but few volcanic rocks will be observed along this traverse. In this area the Hercules thrust dips very gently to the SSE and projects over the top of Harquar Peak. Above the fault are Precambrian granitic rocks which are commonly altered. In a few exposures, Precambrian metamorphic rocks accompany the granitic rocks in the upper plate of the thrust. Slivers of Paleozoic rocks occur in some exposures of the thrust. Minor structures in Mesozoic rocks about 30 m below the thrust indicate that transport was to the north-northeast (Figure 1). Primary sedimentary structures (curled mud chips, cross-bedding, ripple marks, and graded bedding) within the Mesozoic strata indicate that the Mesozoic strata at Stop 4A are right side up beneath the Hercules thrust. These structures also indicate the lower state of metamorphism and deformation of the Mesozoic section at Stop 4A compared to that at 'S' Mountain.

Return to the cars and continue south.

0.4

- 7.8 Crossroads. Make a sharp left turn onto road heading northeast. Proceed about 0.3 miles northeast and park at triangular road intersection for Stop 4B.

## STOP 4B

COPPER-GOLD MINERALIZATION ALONG  
THE GOLDEN EAGLE THRUST

As you leave the cars, you will notice that you are standing on coarse-grained porphyritic granite in the Hercules plate. The Hercules thrust is at least several hundred meters below you. Immediately east of the parking area are several conspicuous ridges that contain steeply-inclined Paleozoic strata (Bolsa Quartzite through Supai formations) which are dramatically truncated at right angles by the Golden Eagle thrust which contours around the base of the ridges. A particularly spectacular exposure of the truncation relationship may be observed in the peak two km northeast of Stop 4B.

The Golden Eagle thrust at Stop 4B is highly mineralized as the numerous prospects and tunnels near and along its trace attest. Particularly, high grade gold with minor copper mineralization was mined from shattered Bolsa Quartzite above the Golden Eagle thrust at the Golden Eagle (0.2 mile east of the parking area) and Harquahala (1 mile south-southwest of the parking area) mines. Minor copper and lead sulfide mineralization occurs in the granite underneath the Golden Eagle thrust according to Keith (1978). The Harquahala-Golden Eagle mine group is one of Arizona's larger gold mines. Recorded production is some 150,000 tons of ore averaging about 0.85 oz. of

gold per ton and 0.53 oz. of silver per ton. The Harquahala Mine is also one of the premier collecting localities in Arizona for the secondary copper silicate mineral diopside and plancheitz. Similar thrust-controlled mineralization may occur at the Socorro Mine, about seven miles to the northeast.

In addition to thrust-related occurrences, gold-copper mineralization occurs at several localities in high-angle north-striking and northwest-striking to east-west striking fissure veins. Some of these contain mid-Tertiary microdiorite dikes that predate mineralization. The north-south striking mineralized fault west of Stop 4A (see note at mileages 6.5 and 7.0) is one example of this structural style. Table 1 (from Keith, 1978) lists some of the more productive occurrences in the 'big' and Little Harquahala Mountains. Total reported and estimated production from the Harquahala district through 1974 is some 160,000 short tons of ore containing 90,000 pounds of copper, 121,000 pounds of lead, 131,063 ounces of gold and 89,500 ounces of silver valued at an estimated 4.8 million dollars.

Most of the mineralization in the Harquahala district is probably mid-Tertiary in age and associated in some way with the numerous mid-Tertiary dike swarms that lace the region. Perhaps the high-angle fractures associated with the dikes acted as conduits for the mineralization. Where these fractures intersect the low-angle faults of the region (for example the Laramide thrusts in the Harquahala or the Whipple-Buckskin-Rawhide detachment fault 30 miles north of Salome, Arizona, mineralization from the high-angle fractures may have moved laterally along the thrusts. Where it encountered reactive or permeable rocks (carbonates or fractured quartzites) relatively large amounts of mineralization may have formed.

From the cars we will walk to the thrust zone and inspect the phenomena outlined above. After inspecting the Golden Eagle thrust, overlying Paleozoic rocks and mineralization return to the cars and return to the cross roads at mileage 7.8. Cross straight through the intersection. Harquahala (Bonanza) Mine will be at 2:00 behind Martin Peak.

#### GOLDEN EAGLE MINE TO INTERSTATE 10 - HOVATTER ROAD INTERSECTION

- 0.3
- 8.1 Cemetary on right. We are structurally still within the Hercules plate. Paleozoic section on Martin Peak is upside down and in the Golden Eagle plate.
- 0.4
- 8.5 Road on right provides access to Cyanide leaching plant. Tailings from the Harquahala mine are being reprocessed for gold.
- 0.4
- 8.9 Road climbs a small hill and bends to the right. On the hill to the left a steeply dipping quartz vein about three feet wide stretches south into the contact with the Bolsa Quartzite. A boulder conglomerate at the base of the Bolsa Quartzite above the vein contains pieces of the full quartz. Thus the Bolsa is conformable on the granite in the lower part of the hill. The contact dips steeply to the south. The Silver Queen thrust which places Paleozoic rock directly on the Hercules plate further to the

TABLE 1: SUMMARY OF GOLD-COPPER OCCURRENCES  
IN THE 'BIG' AND LITTLE HARQUAHALA MOUNTAINS WITH  
REPORTED PRODUCTION (from Keith, 1978)

MINING DISTRICT AND MINES	LOCATION T R. Sec.	MINERAL PRODUCTS	GEOLOGY	TYPE OF OPERATION AND PRODUCTION	REFERENCES
Blue Eagle, Bunker Hill, and Four Winds mine group. (Bunker, Stehle, Campbell)	5N 12W SW <sup>1</sup> / <sub>8</sub> NE <sup>1</sup> / <sub>4</sub> W Cen 20	Au, Ag, W, Fe, Cu-	1. Pockety and irregular deposits of siliceous gold-silver ore in brecciated quartz lenses and veins, usually associated with iron oxides, in fissure zones cutting Precambrian metamorphic schist, gneiss and quartzite. Minor associated copper. 2. Stringers, blebs, and narrow discontinuous seams of scheelite along cleavage or fissure zones, with quartz, in Precambrian metamorphics.	Shaft, adit, and open cut operations. Worked intermittently from the early 1900s through 1956. Production of precious metals, mainly as high silica-gold flux ore, would be some 430 tons averaging about 0.4 oz. Au/T and 0.6 oz. Ag/T. Some 1100 short ton units of 80% WO <sub>3</sub> produced in the 1950s.	Dale, 1959, p. 6-7 ABM file data
Bonanza (Harquahala) and Golden Eagle mine group (Hubbard & Bowers, Bonanza Mg. Co., Harqua Hala Gold Mg. Co., Yuma Warrior Mg. Co., Harquahala Operating Co., Bonanza & Golden Eagle Mg. Co., Jones, Oberstine)	4N 13W SW <sup>1</sup> / <sub>2</sub> NW <sup>1</sup> / <sub>4</sub> NE <sup>1</sup> / <sub>4</sub> 22 Protracted	Au, Ag, Pb, Cu, Zn-	Rich, pockety shoots of gold with minor silver in a gangue of iron oxides, shattered quartz, calcite, and gypsum in oxidized zone, above about 300-foot depth, in shear zones and shattered quartzite in strongly folded and faulted Paleozoic sedimentary beds intruded by Laramide quartz monzonite. In depth, gold values mainly in auriferous pyrite with some copper and lead sulfide mineralization, in fracture veins in underlying crushed and fractured quartz monzonite. Veins often flat dipping with larger and richer deposits in the shattered quartzite.	Shaft, tunnel, and open cut operations. Extensive stoping in oxidized zone. Discovered in 1888 and worked intermittently on large scale to 1918. Subsequently on small scale, largely by reworking dumps and tailings, to 1964. Total estimated and recorded production would be some 150,000 tons of ore averaging about 0.85 oz. Au/T, 0.53 oz. Ag/T and minor lead and copper.	Bancroft, 1911, p. 105-109 Wilson, 1934 (rev. 1967), p. 128-131 ABM file data
Gold Leaf, Rattlesnake; and Rosebud mine group. (Hadgens, Worcester)	5N 12W NW <sup>1</sup> / <sub>4</sub> 13 13	Au, Ag, Fe, Cu-	Spotty, high-grade gold values with minor copper oxides in lensing quartz, brecciated wall rock, and iron oxides in a shear zone cutting Precambrian granitic gneiss.	Shaft and tunnel workings. Protracted in late 1800's but worked mainly from 1930 through 1941, producing some 400 tons of ore averaging about 0.6 oz. Au/T, 0.2 oz. Ag/T and minor copper.	ABM file data
Hercules mine (Hercules Gold Mg. Co., Shanley, McDonald, Rogers & Farrington; Cline & Hartz, Sharp)	5N 12W 8 Cen 18	Au, Ag, Cu, Fe	Gold and silver mineralization, with local copper, in brecciated, discontinuous, banded, quartz-jasper fissure veins cemented by limonite from oxidation of auriferous pyrite and chalcocopyrite. Wall rock is a Precambrian quartz diorite gneiss intruded by quartz diorite dikes and overlain by Precambrian calcareous schist.	Incline shaft, adits, and open cut operations. Worked prior to 1900 and sporadically from 1934 through 1950, producing a total of some 2670 tons of ore and siliceous gold flux averaging about 0.25 oz. Au/T, 0.27 oz. Ag/T, and 1 1/2 tons of copper.	Bancroft, 1911, p. 109-110 Wilson, 1934 (rev. 1967), p. 132 ABM file data
Hidden Treasure mine (Majic group; Myers & Lazare, Johnson, Nohlebeck & Hummel, Powell, Kast & Johnson, Howell, Seely & Johnson, Warren, Wilkinson & Walsh, Tulsa Minerals Corp.)	5N 11W N Cen & NW <sup>1</sup> / <sub>4</sub> 29	Au, Ag, Cu-, Pb-, Zn-, Mn-, Fe-	Fine gold particles with silver in irregular cellular masses of limonite and calcite, local chrysocolla, oxidized lead and zinc minerals and manganese oxides in seams and tabular replacements along a fault or shear zone in Paleozoic or Mesozoic quartzite and silicified limestone. Wall rock intensely silicified with some sericitization.	Shaft, tunnel, and open cut workings. Located in 1932 and mined somewhat sporadically through 1967, producing some 1775 tons of ore averaging about 0.95 oz. Au/T, 3.9 oz. Ag/T and minor Cu, Pb, and Zn. In 1953-1954, several small lots of 20% Mn shipped to Wendon stockpile.	Wilson, 1934 (rev. 1967), p. 133 Farnham & Stewart, 1958, p. 83 ABM file data
Mars & Mescal mine group (Old Noel; Nuevo Mundo Mountain Mines, Jerome Wenden Copper Co.)	5N 11W NW <sup>1</sup> / <sub>4</sub> 19	Cu, Au, Ag, Fe	Irregular lenses of oxidized copper mineralization with silver and gold, in brecciated diorite, cherty limestone and heavy batches of iron oxides, along a fissure zone bordering a diorite dike in a complex Precambrian granite-schist alternating with altered distorted Paleozoic or Mesozoic limestone. Series of northwest-striking diorite dikes along fissure zone.	Tunnel operations, mainly in 1916 through 1918, producing some 110 tons of ore averaging about 1 1/2% Cu, 0.15 oz. Au/T and 0.3 oz. Ag/T.	ABM file data
Rio del Monte mine (Rio del Monte Mg. Co., McCauley & Orberg, Rio del Monte Mines Inc.)	4N 13W SE <sup>1</sup> / <sub>4</sub> 4 Protracted	Au, Ag, Cu, Pb, Zn, Fe	Lenticular shoots of quartz and limonite containing oxidized copper minerals and gold, and lenses and pods of partly oxidized lead and zinc mineralization in vuggy quartz, in irregular veins cutting Precambrian granitic-gneiss capped by some volcanic flows.	Shaft operations. Known as early as 1899 but worked mainly, intermittently, from 1913 through 1949, producing some 350 tons of ore averaging about 0.23 oz. Au/T, 0.7 oz. Ag/T, 0.3% Cu and 0.2% Pb. Zn not recovered.	ABM file data
San Marcos mine group (Pittsburg Harquahala, Wilson; Salome Development Co., Pittsburg Harquahala Gold Mg. Co., Smith, Sibley, Worcester)	5N 12W N Cen 14	Au, Ag, Fe, Cu-	Spotty high-grade gold, with minor silver and copper mineralization, in oxidized zone with quartz, brecciated wall rock and abundant iron oxides. Lenses of gold-bearing quartz and minor sulfides in depth, in lensing veins along shear zone in Precambrian granitic rock intruded by basic dikes and aplites. Strongly sheared zone.	Shaft workings. Located in late 1890's and worked intermittently through 1934, producing some 300 tons of ore from mine and dumps averaging about .2 oz. Au/T, 0.3 oz. Ag/T and minor copper.	Bancroft, 1911, p. 113-115 Wilson, 1934 (rev. 1967), p. 132 ABM file data
Socorro mine (Socorro Gold Mg. Co., Death Valley Araciveda Consol. Mines Co., Gilbert & Schmidt, Klix)	5N 12W SW <sup>1</sup> / <sub>4</sub> 25	Au, Ag, Fe, Pb-, Cu-	Mostly oxidized, gold-bearing pyrite in quartz and iron oxides above the 250 foot level and scattered pyrite in quartz and wall rock, pockets of galena, and minor oxidized copper minerals below, in an irregular, lensing fissure vein in Paleozoic or Mesozoic quartzite, limestone and shale intruded by Laramide granite and related dikes. Vein is vuggy, brecciated, and cemented by silica and jasper.	Shaft, tunnel, and open cut operations. Worked intermittently from early 1900's through 1960, producing some 4800 tons of ore averaging about 0.2 oz. Au/T, 0.1 oz. Ag/T and a small amount of Pb.	Pratt, 1902 Smith, 1907 Bancroft, 1911, p. 111-113 Wilson, 1934 (rev. 1967), p. 131 ABM file data
Why Not, Clipper, and Gold mine groups (Salome Gold Co., Carper et alia; Hutton & Earp; Johnson; Smith, Long & Gilbert)	5N 11W Cen & E Cen 30	Au, Ag, Cu, Fe	Spotty gold with silver and copper mineralization and iron oxides, quartz, and calcite, in irregular fissure veins in Paleozoic-Mesozoic metamorphosed sediments intruded by dikes.	Tunnel and open cut operations. Worked mainly from 1932 through 1939, producing some 370 tons of ore averaging about 3.3 oz. Au/T, 1.8 oz. Ag/T and 1.8% Cu.	ABM file data

- 205.6 1.1  
Glendale Avenue exit.  
1.3  
Northern Avenue overpass. After passing overpass notice well-developed steeply-dipping Precambrian age foliation in the Phoenix Mountains schists. Several small mercury deposits composed of cinnabar, metacinnabar and quartz occur in pockets within quartz-sericite schist. These deposits were first noted in 1916 and have since had a production of less than 100 flasks of mercury (Bailey, 1968).  
2.1
- 209 2.1  
Shaw Butte (2:30) is at the southern end of the Union Hills. North Mountain is at 3:00 with Lookout Mountain (3:30) is capped by probably Miocene-age volcanics.  
2.7
- 211.7 2.7  
Bell Road exit.  
2.3
- 214 2.3  
Hedgpeth Hills (9:30) and Deem Hills (11:30) are also composed of northwest-striking, northeast-dipping probably Miocene-age volcanics on strike with those at Lookout Mountain.  
1.0
- 215 1.0  
Pyramid Peak at 10:30.  
1.0
- 216 1.0  
Deer Valley Road overpass. Southeast end of Deem Hills are in near view (11:00).  
2.0
- 218 2.0  
Happy Valley Road overpass. Union Hills (12:00-3:00) consist of Precambrian schist in the northern portions and Precambrian granite locally overlain by probably Miocene-age volcanics in the southern portions.  
2.0
- 220 2.0  
New River Mountains on skyline at 1:00 are capped by thick flat lying basalts. Two of these basalts flows have K-Ar ages of 14.7 and 14.8 m.y. (Scarborough and Wilt, 1979). The flat lying basalt section unconformably overlies (locally discordantly) a sequence of basaltic flows, white tuffs, agglomerates, mudstones and some distinctive very bright red lithic tuffs. One of the tuffs yielded a 21.3 m.y. K-Ar age and was very near a Miocene oreodont fossil find (Gomez, 1978; Scarborough and Wilt, 1979). The Miocene volcanic and sedimentary sequence unconformably overlies older Precambrian schists, metavolcanics and granitoid rocks.  
0.4
- 220.4 0.4  
Interstate crosses aqueduct for Central Arizona Project (CAP) now under construction.  
0.6
- 221 0.6  
Bradshaw Mountains dominate the skyline at 11:00-12:00 and are composed of almost entirely undivided pre-1.4 b.y. granitic rocks.  
2.6
- 223.6 2.6  
Lake Pleasant-Carefree exit (Arizona State highway 74). Merge right onto offramp.  
0.4  
Turn left onto State highway 74 for Lake Pleasant and Wickenburg.  
0.1
- 30.8 0.1  
Overpass over Interstate 17. Hieroglyphic Mountains on skyline at 12:00. Cuesta at 2:00 consists of a northeast tilted block of Miocene volcanics and sediments. The base of the cuesta contains poorly exposed sediments overlain in slight angular unconformity by a basaltic

northeast here places granite on granite. Above the Bolsa, dips steepen and become overturned to the southwest.

0.1

- 9.0 Harquar Peak at 3:30. The sedimented area below the peak is in crystalline rocks of the Hercules plate. The Hercules thrust approximately follows the sediment-mountain slope break. The low hills at 11:30 to 12:30 are underlain by Paleozoic rocks resting (probably unconformably) on Precambrian granite.

0.3

- 9.3 The low hill immediately west of the road is underlain by Devonian Martin Formation. Upside down Mississippian Escabrosa Limestone is visible on Martin Peak to the left.

0.3

- 9.6 Courthouse rock is visible on the skyline in the Eagletail Mountains at 9:00. Courthouse rock and nearly all the terrane visible to the south is underlain by mid-Tertiary volcanic and volcanoclastic rocks.

0.4

- 10.0 Spectacular view of upside down section on Martin Peak. (7:00). The low ridge extending south from Martin Peak and the dark reddish-brown ribbed outcrops on Martin Peak are Supai Formation. The Supai Formation is underlain in the lower slopes by upside down Coconino quartzites. Bold, light tan and grey carbonate outcrops along ridges extending southwest from Martin Peak are Escabrosa Formation. The Martin Formation occupies the dark brown drainage area north of the Escabrosa ridges with no outcrops. The northern most ridge contains reddish ledges of Bolsa quartzite overlain by a thin slope-forming upside down Abrigo section in the southerly slopes.

0.5

- 10.5 Black Rock hills (12:00 - 2:30) are composed of Tertiary volcanics.

0.5

- 11.0 Road on right, leads to Hope and U. S. 60.

2.0

- 13.0 Pavement starts. Hills south of I-10 are the southeast extension of the Black Hills. Mesozoic sediments in low ridges at 1:00 are in low-angle tectonic contact with porphyritic granite to the north. The contact lies at about 1:30 as you cross the I-10 overpass. The hills north of I-10 are underlain by granite and Tertiary volcanics. Cross the overpass and turn left onto I-10 heading east for Phoenix and Tucson.

End of road log.

- Avedisian, G. E., 1966, Geology of the Phoenix South Mountain Park, Arizona: M. S. Thesis, Arizona State University, 54 p.
- Banks, N. G., 1980, Geology of a zone of metamorphic core complexes in southeastern Arizona: Geological Society of America Memoir 153, in press.
- Briscoe, J. A., 1967, The general geology of the Picacho Peak area: Masters Thesis, University of Arizona, Tucson, 52 p.
- Davis, G. H., 1980, Structural characteristics of metamorphic core complexes, southern Arizona: Geological Society of America Memoir 153, in press.
- Keith, Stanley B., Reynolds, S. J., Damon, P. E., Shafiqullah, M., Livingston, D. E., and Pushkar, P. D., 1980, Evidence for multiple intrusion and deformation within the Santa Catalina-Rincon-Tortolita metamorphic core complex: Geological Society of America Memoir 153, in press.
- , 1979, The great southwestern Arizona oil and gas play: Arizona Bureau of Geology and Mineral Technology Fieldnotes, v. 9, no. 1, p. 10-15.
- , 1980, The great southwestern Arizona oil and gas play: Drilling commences: Arizona Bureau of Geology and Mineral Technology Fieldnotes, v. 10, no. 1, p. 1-3, 6-8.
- Keith, Stanton, B., 1978, Index of mining properties in Yuma County, Arizona: Arizona Bureau of Geology and Mineral Technology Bulletin 192, 185 p.
- Rehrig, W. A., Shafiqullah, M., and Damon, P. E., 1980, Geochronology, geology, and listric normal faulting of the Vulture Mountains, Maricopa County, Arizona: Arizona Geological Society Digest 12, p. 89-110.
- and Reynolds, S. J., 1980 Geologic and geochronologic reconnaissance of a northwest-trending zone of metamorphic complexes in southern and western Arizona: Geological Society of America Memoir 153, in press.
- Reynolds, S. J., 1980, Geologic framework of west-central Arizona: Arizona Geological Society Digest, v. 12, p. 1-16.
- and Rehrig, W. A., 1980, Mid-Tertiary plutonism and mylonitization, South Mountains, central Arizona: Geological Society of America Memoir 153, in press.
- , Keith, S. B. and Coney, P. J., 1980, Stacked overthrusts of Precambrian crystalline basement and inverted Paleozoic sections emplaced over Mesozoic strata, west-central Arizona: Arizona Geological Society Digest, v. 12, p. 45-51.
- Varga, R. J., 1976, Stratigraphy and superposed deformation of a Paleozoic and Mesozoic sedimentary sequence in the Harquahala Mountains, Arizona: M. S. Thesis, University of Arizona, Tucson, 61 p.
- Wilson, E. D., 1960, Geologic map of Yuma County, Arizona: Tucson, Arizona Bureau of Mines; scale 1:375,000.
- , Moore, T. R. and Peirce, H. W., 1957, Geologic map of Maricopa County, Arizona: Arizona Bureau of Geology and Mineral Technology County Map Series.
- , Moore, R. T. and Cooper, J. R., 1969, Geologic Map of Arizona: Washington, DC, Arizona Bureau of Mines and U. S. Geological Survey Map, scale 1:500,000.
- Yeend, W., 1976, Reconnaissance geologic map of the Picacho Mountains, Arizona: U. S. Geological Survey map MF-778, scale 1:62,500.